CORROSION-FATIGUE IN FERROUS ALLOYS

A THESIS

PRESENTED TO THE UNIVERSITY OF GLASGOW

FOR THE DEGREE OF

DOCTOR OF PHILOSOPHY

By

WILLIAM MacFARLANE, B.Sc., A.R.C.S.T.

January, 1959.

ACKNOWLEDGEMENTS

The experimental work presented in the thesis was carried out in the laboratories of the Departments of Metallurgy, and Mechanical, Civil and Chemical Engineering, Royal College of Science and Technology, Glasgow.

The author wishes to record his gratitude to Professor Robert Hay of the Metallurgy Department, his supervisor, for the constant interest and encouragement, and to Professor Adam S. T. Thomson and Professor Alexander W. Scott of the Mechanical, Civil and Chemical Engineering Department for their helpful advice and the facilities provided. The author would also like to express his thanks to Dr. P. T. Carter of the Metallurgy Department for his constructive criticism, to Mr. J. W. Sharpe of the Natural Philosophy Department for assistance in the use of the electron microscope, and to the British Shipbuilders Research Association and the Trustees of Sir James Caird's Travelling Scholarships for the financial assistance which made the research possible.

CORROSION-FATIGUE IN FERROUS METALS

CONTENTS

CORROSION-FATIGUE IN FERROUS ALLOYS

INTRODUCTION

The object of the present work is an endeavour to assess the controlling factors that initiate corrosion-fatigue. With this end in view a study was made of the effect of certain factors on corrosion-fatigue and how they were influenced by the presence of inhibitors. The factors chosen were surface finish and temperature in addition to various concentrations of the corrosion environment and of various types of inhibitor. It was hoped that a comprehensive examination of the resulting data would help in elucidating some aspects of crack propagation. To this end an extensive metallographic examination of the cracks was carried out.

It was necessary that the work should be so ordered that the results of one series of experiments could be used to control the next series. Thus in order to determine the amount of damage caused by the additions of chlorides to the corrosive environment, it was first necessary to determine the fatigue limit in air and the endurance limit in distilled water. These two limits having been determined additions of synthetic sea water varying from 0.1 per cent to 10 per cent were/

were added to a distilled water environment, and the endurance limits of mild steel in these solutions determined. From these tests it should be possible to determine the effect of a small addition of sea water and the increasing effects of further additions.

The maximum temperature chosen for tests was 88 °C. This temperature was chosen for two reasons. These are that very little is known about the corrosion-fatigue behaviour of ferrous metals in hot solutions, and that at this particular temperature the solubility of oxygen is at a minimum.

Sea water additions decrease the endurance limit of ferrous metals but inhibitor additions increase the endurance limit. There are two different ways in which an inhibitor can act, namely by reacting with the surface atoms of the metal undergoing test, and by forming an adsorbed film on the surface.

A number of inhibitors from each of the types was chosen. The anodic inhibitors (those which react with the surface atoms of the metal) selected were sodium chromate sodium nitrite, potassium dichromate and sodium benzoate. These particular inhibitors were chosen because they permit a range of pH from 5.5 to about 9. This allowed a measurement of the effects/

effects of pH on corrosion-fatigue damage.

Adsorption inhibitors were chosen because they alter the properties of corrosive environments such as surface tension and wettability. These influence the rate of reaction between the inhibitor and the metal, since adsorbed films are dependent on such factors as the wettability of the liquid and the interfacial tension between the liquid and the metal. Thus it was decided to choose six "soluble" oils which would permit a range of environments from opaque and clear emulsions to truly soluble oils. The oils forming opaque emulsions are Solubriol SL, Soluble K4, and Dromus B, which will be respectively known as Oils A, B and C. Those forming clear emulsions are Clear Dixol and Dromus D, and these will be called Oils D and E respectively. The only truly soluble oil is Dromus E and it will be known as Oil F. These six oils gave the complete range of solutions necessary for the study of adsorbed oil films.

The best inhibitors were determined by running tests at a constant stress, namely 12 tons per square inch. The best inhibitor having been determined S/N curves were then run for this inhibitor to find the nature of the corrosion-fatigue curve, with special attention being paid to the occurrence of an endurance limit.

Since corrosion-fatigue is associated with corrosion pitting/

pitting which itself is related to the surface topography, surface finish would appear to be of prime importance. Experiments were carried out at constant stress, and the surface finish varied between 2½ μ and 120 μ.

Although most of the tests were carried out at 88°C, it would be very difficult to assess the value of these unless the effect of temperature variation was investigated. Since the apparatus to be described was easily adapted for experiments at varying temperatures, experiments were carried out at temperatures varying from room temperature to 88°C to determine the effects on the endurance limit.

These tests could be correlated one with the other and the performances of the inhibitors compared with the electro-chemical data for the inhibitors.

An attempt was made to follow the process of protective film breakdown during a test, by measuring the change in the specimen potential during the progress of a test. The result obtained in this series of tests enabled inhibitors to be compared on an electro-chemical basis.

A metallographic study was made of the corrosion-fatigue cracks, and an attempt made to show whether corrosion precedes or succeeds the fatigue crack. The observations were then correlated with the experimental results on inhibitors.

SECTION ONE

CHAPTER ONE

FATIGUE OF METALS.

When metals are subjected to repeated cyclic loading they may, under certain circumstances, undergo failure due to what is termed 'fatigue'.

Some metals, notably ferrous, have safe ranges of stress in air and in vacuo, below which the metals can be subjected to an unlimited number of stress cycles, without failure, as shown by curve A, in Fig. 1.

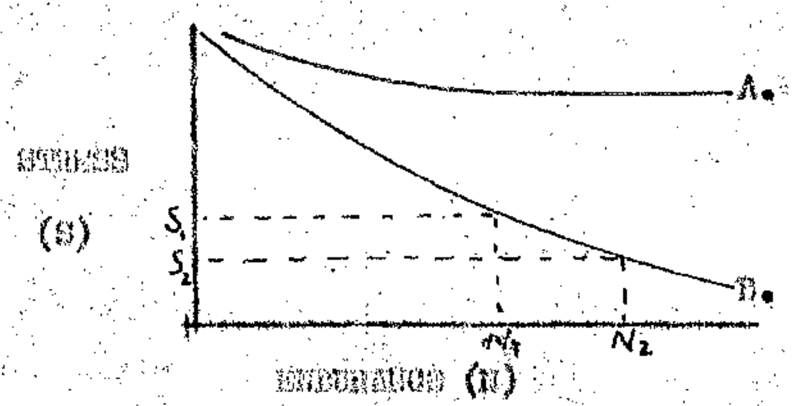

Fig. 1

The limit of this range is known as the fatigue limit of the material, and in the case of mild steel may be as low as half the ultimate tensile strength. However, other alloys, when tested in air and in vacuo, and all metals in aqueous environments will eventually fail even at very low stresses, as shown by Curve B in Fig. 1. In these cases the resistance of the metal to fatigue is usually/

usually defined by its 'Endurance Limit' which is the maximum stress that the metal can withstand without failing after a specified number of cycles. For example Curve B shows an endurance limit of S_1 after N_1 cycles of stress, and S_2 after N_2 cycles of stress.

The main method of approach to the study of fatigue has been the investigation of the general effects of a number of important variables. The results obtained are normally plotted in terms of S/N curves, as in Fig. 1 and these data are used by the engineers in the designing of components and structures. This has been the main method of investigation since the time of Fairbairn (1) and Wöhler (2). The work done in this field has been reviewed in a number of well-known text books for example Battelle 1956 (3); Moore and Kommers 1927 (4), and Gough 1926 (5).

A fair proportion of the work on fatigue has been devoted to the basic mechanism. The studies have been mainly carried out using metallographic methods, such as optical and electron microscopes and X-ray techniques. The use of these techniques has enables many theories of fatigue to be put forward.

The attrition theory was proposed by Ewing and Humfrey

(6)/

(6) in 1903. This stated that repeated slip within the crystals wore away the slipping faces and built up debris on each side. This progressed until the slip bands were so broad that a crack started and spread to similarly affected areas in the close vicinity. Ewing and Humfrey stated that they were able to detect the build up on each side of the crack, but the evidence obtained was not conclusive.

The amorphous layer Theory proposed by Beilby (7) in 1907 and developed by Rosenhain and Ewen (8) in 1912, closely resembles that of Ewing and Humfrey. During repeated slip, portions of the metal were assumed to become amorphous and these amorphous layers were then assumed to alternate with crystalline layers. Where two amorphous layers met, a crack was initiated. Unfortunately it was not possible to obtain sufficient experimental support for the existence of amorphous layers.

In 1923, Gough and Hanson (9) proposed a mechanism which undoubtedly forms the nucleus of present ideas on the subject. Plastic deformation was assumed to take place in certain regions of the metal. With an increasing number of stress reversals the deformation was assumed to increase, but/

but at a decreasing rate, due to the action of strain hardening. If the stress is under the fatigue limit for the material, plastic deformation will finally cease, leaving the crystal hardened, while for stresses above the safe range, local strain hardening was considered to exceed the amount which the metal could withstand without forming a crack. Hence, if the stress is greater than the fatigue limit, a crack will be initiated and propagate until fracture occurs.

Further work was carried out by Gough and Wood (10) using single crystals and X-ray techniques, but little further progress was made into the problem of the mechanism of fatigue failure till 1939. In that year Orowan (11) introduced the additional factor of inhomogeneous stress distribution into the theory of Gough and Hanson (9). The effect of strain hardening, due to plastic deformation on the local highly stressed regions, which Orowan stated were present, was assumed to be sufficient to enable the yield point to be reached and for cracked to be initiated.

Experimental evidence in support of Orowan has been obtained by Thompson (12) and Wood (13). Thompson describted/

ed the surface examination of single and poly crystals of nickel and copper. Thompson's objective was to detect the stage at which the fatigue crack forms and to follow its progress to fracture. Although the tests were productive of results, Thompson was very cautious of concluding at what stage a crack was initiated. The results were discussed in terms of 'dislocation theory' concepts, and the initiation of the crack is pictured as the effect of intersecting 'screw dislocations', creating permanent and cumulative vacant lattice sites within slipbands; when a sufficient concentration is obtained, the resulting lattice distortion may be so great that a process akin to recrystallisation may take place at ordinary temperatures, resulting in a loss of coherence of the structure, possibly assisted by a change in density on recrystallisation. Presumably, the crack propagates by a similar process, but no definite view was expressed.

Wood (13) conducted research on the same topic using optical observations; X-ray diffraction supplying confirmatory and definite evidence that the breadth of coarse slip was about 10^{-4} or 10^{-5} cm and of fine slip about 10^{-7} cm.

The/

The former occurs by a relatively small number of coarse movements. Massed slipbands which are peculiar to fatigue, are attributed to a build up of subsidiary slip movements multiplying within the fine slip bands, fatigue cracks forming by the opening up of a massed slip band. He considers the dislocation theory to be consistent with his observations. Hempel (14) describes metallographic observations on the deformation characteristics of mild steel. In general the formation and early growth of slip bands due to ranges of stress both above and below the fatigue limit were essentially similar. Cracks always started in areas of heavy slip. Electron microscopy showed that slip bands were in relief to their background, showing that mass movement had occurred. Fine dark lines or sub-microscopic fissures were also clearly revealed within some slip bands. These fissures, Hempel concluded, "give some limits" of the mechanism of fatigue failure, but it is generally accepted that the discovery of these fissures represents an outstanding contribution to the basic knowledge of fatigue failure.

Mott (15), who has presented much data towards the basic/

basic study of fatigue, suggested a process of extrusion that involves the to and fro movement of a screw dislocation which jumps cyclically from one plane to another by means of the occurrence of cross-slip at the end of its path. This caused material to be squeezed out of the crystal, leaving voids in the region of slip. The reverse of this process would presumably create an intrusion. Hull (16) observed that slip consisted of these intrusions and extrusions, and noted their early formation (one per cent of estimated life).

The subsequent modifications of the theories of Gough and Hanson (9) and Orowan (11) have not met with universal support. In 1936, Moore (17) put forward the crystallite theory in which small crystals were supposed to break off the main crystals, when slip occurred. It was assumed that this process allowed the initiation of cracks to take place. This theory bears a close resemblance to that of Ewing and Humfrey (6) and Beilby (7). The former did not specify the nature of the debris formed during the slip process while the latter assumed it to be amorphous. Moore regarded it as crystalline in nature and this has received support from Forsyth (18) who from an examination of age-hardening alloys concluded that the crystallites measured/

measured 10 μ across. However, he was using age-hardening alloys electron microscopy may prove the crystallites to be crystalline precipitates produced by strain, because the crystallites were not obtained with other types of alloys.

CHAPTER TWO

REVIEW OF PREVIOUS WORK ON CORROSION-FATIGUE

The fatigue strength of a metal may be reduced to an extremely low value when corrosive action occurs simultaneously with the application of fatigue stresses. This phenomenon is called 'Corrosion-fatigue'.

Haigh (19) showed that by separating the two processes the action is a conjoint one associated simultaneously with corrosion and fatigue. He first subjected specimens to corrosion, and then after cleaning and drying, to fatigue. Although the prior corrosion caused pitting on the surface, the severity of the fatigue was only slightly enhanced. The action was much more intense when the two processes were applied simultaneously. Evans and Whitwham (20) reversed the procedure of Haigh, and subjected specimens first to fatigue and then to corrosion. They observed no decrease in the expected life, and indeed, if the initial period of fatiguing in air was carried out at stresses below the fatigue limit, a slight increase in life was obtained during corrosion-fatigue testing. Their results verified the conclusions of Haigh (19) that corrosion-fatigue is associated with the simultaneous action/

action of corrosion and fatigue, although Gough (21) considered the main factor to be corrosion, and considered it very doubtful whether stress, as such, played an important part in corrosion-fatigue.

Metallography of Corrosion-Fatigue Cracks and Factures

Corrosion-fatigue fractures are 'brittle' in nature and exhibit no ductility. They resemble normal fatigue fractures, the essential difference being a characteristic discoloration at the fracture face, which is dark at the area of initiation and becoming gradually lighter as the distance from this area increases. Fig. 2 illustrates the salient differences between a corrosion-fatigue fracture and a fatigue fracture.

Another characteristic of corrosion-fatigue is that there are many areas of attack and a specimen may have corrosion-fatigue cracks in more than one area. In ordinary fatigue it is normal for only one crack to form.

It has been shown (21) that except in the case of the duralumin type of alloys, the cracks brought about by corrosion-fatigue are transcrystalline. The cracks tend to align themselves with slip planes, along which slip has already occurred

and/

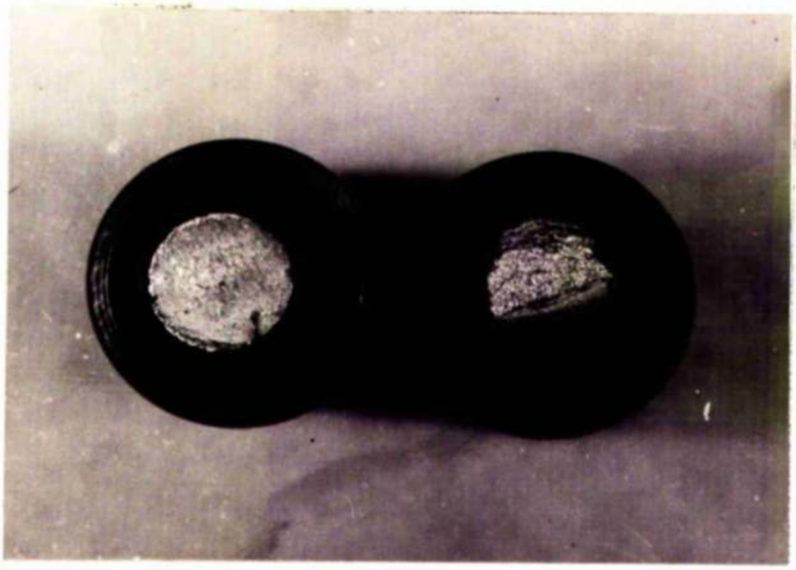

FIG 2

and Gough and Sopwith (22) suggested this as a possible reason for the cracks being transcrystalline. From their observations on the behaviour of single and bi-crystals of aluminium in tap water, Gough and Sopwith (23) suggested that the corrosion-fatigue cracks formed in areas undergoing heavy plastic deformation. They also observed that in the bi-crystals, the grain boundaries were immune from attack. From the results of their experiments on fatigue followed by corrosion-fatigue, Evans and Whitwham (20) concluded that along small slip bands disarrayed material was produced locally and that this material was only susceptible to attack, if the environment reacted with it while the atoms were mobile.

Graphical Representation of Results

Stress/Endurance (S/N) curves obtained in corrosion-fatigue experiments show no sign of the 'fatigue limit' or safe range of stress encountered in fatigue tests on ferrous materials. Fig 3. gives a typical illustration of three different types of fatigue curve.

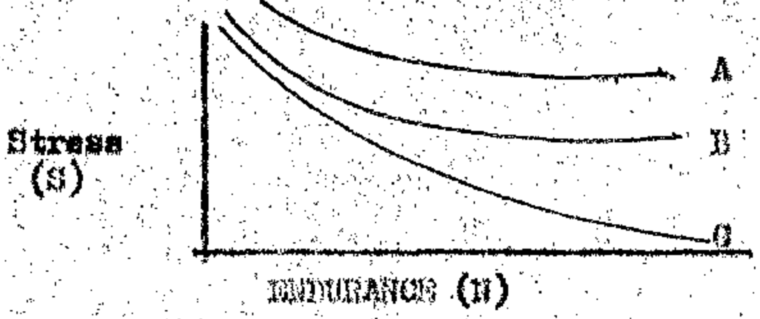

Fig 3.

[illegible]

[illegible]

[illegible]

Curve A shows the S/N curve for a ferrous material which possesses a marked fatigue limit. Curve B is for the same material, subjected to corrosive attack prior to normal fatigue testing. A lower value for the safe range of stress is shown in this instance. Curve C refers to the same material subjected to corrosion-fatigue and shows no fatigue limit. This curve is representative of all corrosive environments except air. Consequently a component in contact with a corrosive medium will eventually fail, even though subjected to a very small range of cyclic stress. Clearly then, the use of the term corrosion-fatigue limit should be avoided and replaced by 'endurance limit', which must be stated to some specific number of stress reversals.

Mechanism of Corrosion-Fatigue

The two main stages in the development of corrosion-fatigue cracks are crack initiation and crack propagation. Pit formation is the major factor associated with crack initiation and as such has been the subject of many investigations. McAdam & Geil (24) observed that corrosion pits formed during stressless corrosion differed from those formed during corrosion in the presence of alternating stress. In the former case, the corrosion pits were hemi-spherical in shape (Fig. 4) while in the/

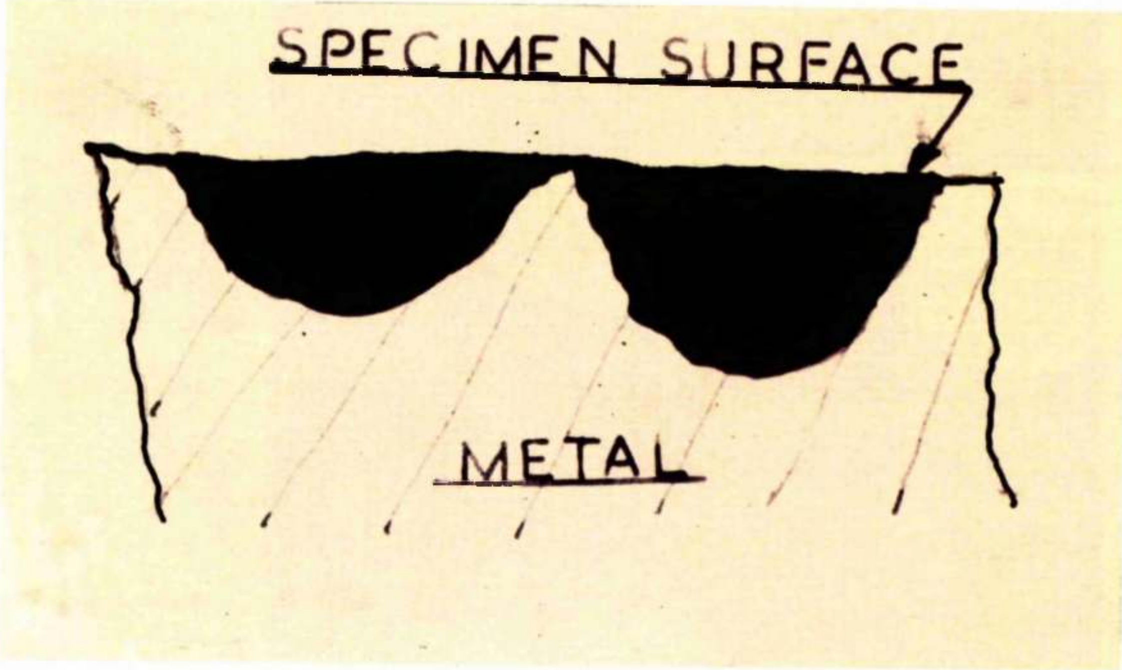

FIG 4

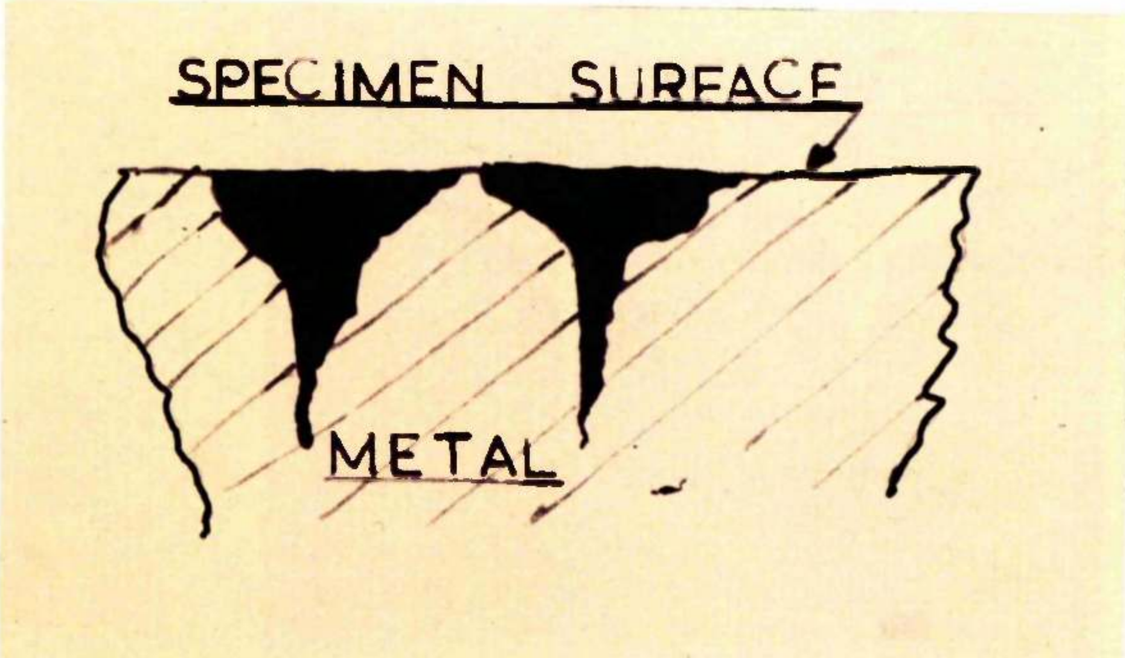

FIG 5

the latter case sharply pointed fissures were produced (Fig.5). These two types of pit have widely different stress concentration factors, that of a sharply pointed fissure being two to three times greater than that of the hemi-spherical type. This high stress concentration factor results in an intensification of stress around the tip of the fissure and promotes conditions favourable for local slip to take place during corrosion-fatigue.

Gough (21) suggested that the two primary factors which provide an adequate explanation of the mechanism of pitting are unequal oxygen distribution and the behaviour of protective films. Under corrosion-fatigue conditions, the velocity of corrosion increases and Gough attributed this to the effect of cyclic strain on the porosity and rupture of the protective films formed.

The mechanism of crack initiation is complicated in that only certain areas are attacked and form pits, some of which are deep and only some of the deep pits initiate cracks. McAdam (25) expressed the opinion that this was mainly due to the effects of cyclic stress, but the effects of protective films should be taken into account in the initial process of pit formation. On the other hand Aston (26) and Evans (27) suggested/

suggested that pit formation was associated with differential aeration and this also explained why some were deeper than others. Bengough (28) and his associates favoured a slightly different concept, concluding that corrosion was proportional to the available supply of oxygen provided the concentration of anions was sufficient and no protective films were formed.

Evans and Simnad (29) tested 0.19 per cent carbon steel wire specimens using a two stage procedure. The specimens were given a certain number of cycles of corrosion-fatigue, then treated with an inhibitor and the test completed at the same stress and frequency. The results they obtained are represented in Fig. 6.

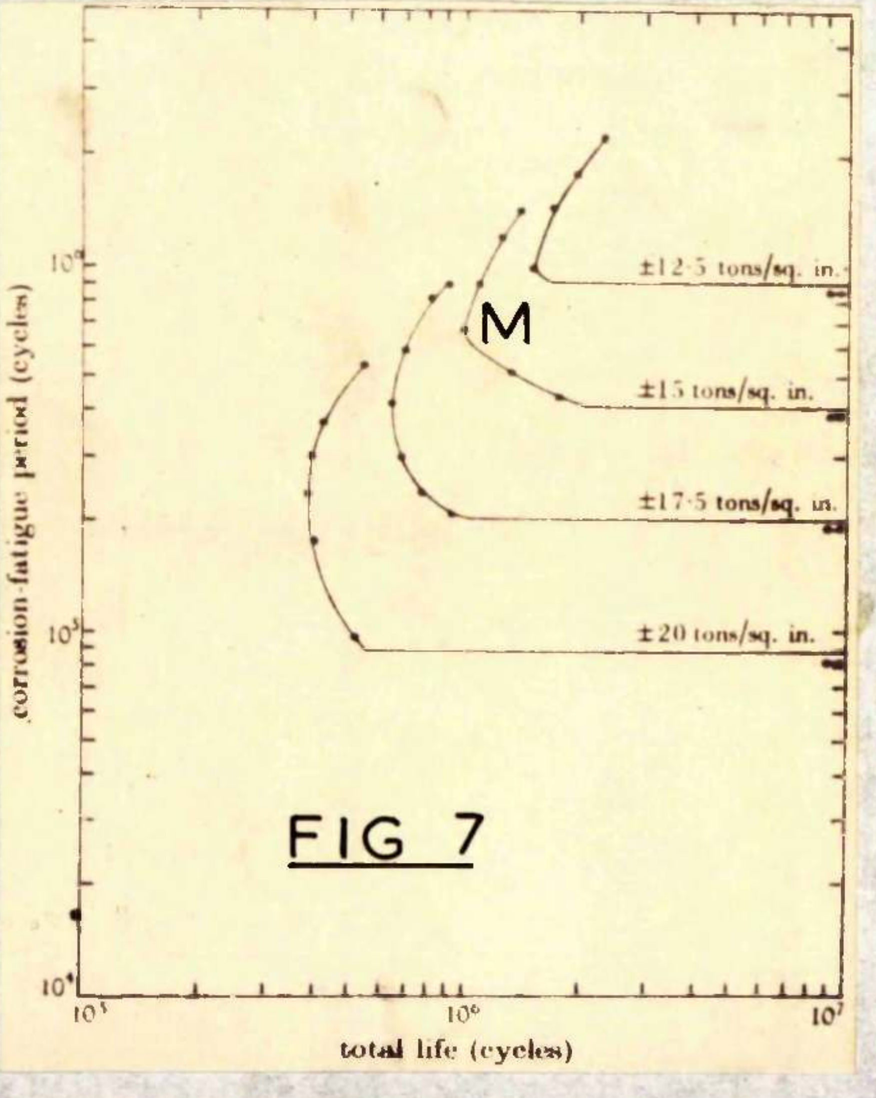

FIG 7

From this it will be seen that, for a given stress, if the specimen is subjected to less than a certain number of corrosion-fatigue cycles (for example $10^{4.9}$ at ± 20 tons per square inch) it can subsequently be subjected to an indefinite number of cycles in air without failure occurring As long as this number M (Fig. 6 - curve for 15 tons per square inch of corrosion-fatigue cycles is not exceeded the total life is drastically reduced with increases in the number of corrosion-fatigue cycles. As the number of corrosion-fatigue cycles is further increased beyond M the total life increases again.

It was suggested that corrosion-pits give rise to the development of a small number of cracks, when the number of cycles exceeded the above-mentioned limit M leading to a drastic reduction in life. For longer periods of corrosion-fatigue, more cracks were formed, resulting in a decrease in the stress concentration at the bottom of any one crack so that the total life became longer. As a result of these and other experiments on the effect of applied cathodic currents, Evans and Simnad proposed the following three effects of cyclic stress on the corrosion of a metal.

(a)/

(a) Diminution of Cathodic Polarisation (by improvement in the oxygen supply to the cathode).

(b) Diminution of Anodic Polarisation (by rupture of the protective films).

(c) Diminution of the resistance of the liquid path joining anodes and cathodes (by removal of corrosion products etc.)

Subsequent work by these two authors using mild steel and iron in acid solution ($\frac{N}{10}$ HCl) to avoid the complication of the oxide film, substantiated their conclusions.

It is generally agreed that crack propagation is not so important as crack initiation. This would seem to be the reason why much more work has been carried out on initiation than propagation.

Karpenko (30) has studied crack propagation during corrosion-fatigue and suggested that the surface of the metal became covered with a multitude of microcracks principally transcrystalline, containing products of corrosion. The number of microcracks produced was found to depend upon the activity of the medium and the coefficent of cyclic overloading. Karpenko concluded as had been shown earlier by Rebinder/

Robinder (31) that the occurrence of slip was facilitated by the adsorption of ions from the corrosive medium and since slip could occur more easily in corrosive conditions, microcracks formed more easily. Karpenko further concluded that electrochemical corrosion within these microcracks follows, and since the volume of the corrosion products which fill the cracks exceeds that of the starting material, this results in the growth of the cracks, both in depth and width. Thus this mechanism explains why transcrystalline cracks form and Karpenko concludes that it would be impossible to eliminate complete the drop in fatigue limit with the aid of electrical and other protective means.

Several factors affect the corrosion-fatigue strength of metals, the more important being the condition of the metal, the manner of testing and the corrosive environment.

Nature and Composition of the Metal.

Different metals and alloys have varying resistances to corrosion-fatigue attack. Generally the effects of alloying elements or of heat treatment are small unless they improve normal corrosion resistance (32). Thus, as shown in Fig. 7 D (33) in plain carbon steels, changes in composition and heat/

FIG 7A

FATIGUE LIMIT OF PLAIN CARBON STEELS

AS OBTAINED BY MCADAM (33)

Steel % C	Condition	Fatigue Limit (Tons./sq./in.)
0.003	Normalised	9.8
0.003	Heat Treated	10.7
0.11	Normalised	11.6
0.14	Heat Treated	16.0
0.24	Normalised	12.5
0.26	Heat Treated	17.0
0.36	Normalised	15.6
0.36	Heat Treated	23.3
0.49	Normalised	16.0
0.49	Heat Treated	24.1
1.1	Normalised	18.7

[illegible]

[illegible]

[illegible]

[illegible]	[illegible]	[illegible]
	[illegible]	[illegible]
[illegible]	[illegible]	[illegible]
[illegible]	[illegible]	[illegible]
[illegible]	[illegible]	[illegible]
[illegible]	[illegible]	[illegible]
[illegible]	[illegible]	[illegible]
[illegible]	[illegible]	[illegible]
[illegible]	[illegible]	[illegible]
[illegible]	[illegible]	[illegible]
[illegible]	[illegible]	[illegible]
[illegible]	[illegible]	[illegible]

FIG 7B

ENDURANCE LIMITS IN FRESH WATER OF PLAIN CARBON STEELS AS OBTAINED BY MCADAM (33)

Steel % C	Condition	Endurance Limit at 10^7 cycles (Tons./sq./in.)
0.003	Normalised	7.1
0.003	Heat Treated	9.0
0.11	Normalised	7.6
0.14	Heat Treated	10.7
0.24	Normalised	7.6
0.26	Heat Treated	10.7
0.36	Normalised	11.2
0.36	Heat Treated	9.8
0.49	Normalised	11.2
0.49	Heat Treated	10.3
1.1	Normalised	10.3

heat treatment make little difference to the sensitivity to corrosion-fatigue although the effect on normal fatigue is appreciable.

As might be expected, the stainless steels (greater than 12 per cent Cr) behave very differently and are much more resistant to attack. McAdam (34) carried out extensive research on the effects of alloying additions and found them to be relatively unimportant. Schulz and Buchholtz (35), however, found that the corrosion-fatigue resistance of structural steels was greatly improved by small additions of copper. McAdam also observed that heat treatment had little effect, but annealing gave a slight increase in the resistance to corrosion-fatigue attack. Although heat treatment of the whole specimen did not increase the corrosion-fatigue life, surface treatments, which increased the hardness of the surface layer were found to have a beneficial effect on the fatigue properties of metals. Gould and Evans (36) noted that the shot-peening of eutectoid carbon steels increased the corrosion-fatigue life in both dilute sulphuric acid and sea-water by over 100 per cent while Inglis and Lake (37) found surface nitriding produced a similar effect. Ryabchenkov and Abramova (38)/

(38) investigating methods for increasing the corrosion-fatigue strength of steels, found that shot-blasting, surface rolling and induction hardening gave remarkable increases in endurance. Increases in endurance as high as 250 per cent were obtained when an induction hardened 0.4 per cent carbon steel was tested in three per cent sodium chloride. It should be noted that all the methods mentioned above increase the hardness of the surface by the production of residual compressive stresses and this is the probable reason for the improvements in endurance.

Most of the work on protective coatings has been carried out on metallic coatings which can be applied in three different ways, namely:- spraying, electroplating or hot dipping. Gough and Sopwith (39) attributed the increased life given by galvanised and sherardised zinc coatings to cathodic protection. These results were confirmed by Gould and Evans (40) who found protection even at discontinuities in the zinc coating.

When metals which had previously been subjected to a surface hardening treatment were given a protective metallic coating, even greater increases in endurance were observed. Ryabchenkov/

Ryabchenkov and Abramova (38) found the imprvement over the normal endurance limit of a 0.4 per cent carbon steel (normalised) in three per cent NaCl could be as great as 500 per cent when surface hardening treatment was followed by electrolytic chormium plating, electrolytic zinc plating or cathodic protection by means of a zinc disc round the specimen. In certain cases the endurance limit exceeded the normal endurance limit in air.

Little work has been done on the effects of varying the surface roughness of specimens subjected to corrosion-fatigue tests. A decrease in fatigue life with roughened specimens was observed by Karpenko (41).

Testing Procedure

The two main methods of applying cyclic stressing are push-pull (compression-tension) loading, and rotating bending loading, as in the Wöhler fatigue machine. Gough and Sopwith (42) and Gould (43) found considerable differences in the endurance of similar material when subjected to both types of test. This is not unexpected since in push-pull loading all the specimen is in tension or compression at the same time, whereas in rotating bending, regions of the specimen are at all points/

points on the sinusoidal curve of the loading. This means that in the latter case there is a greater chance of electrochemical corrosion taking place, because of the difference in potential between areas in compression and those in tension. The rate of stressing is also important and McAdam (44) has shown that a low frequency of cyclic stressing is more damaging than higher frequencies.

The effect of specimen dimensions on the endurance limit was demonstrated by McAdam (45) and Karpenko (46). Both have shown that an increase in the diameter of the specimen will result in a decrease in the endurance limit.

The method by which the corrosive fluid is brought into contact with the specimen is important but this will be considered more fully in the subsequent discussion on experimental equipment.

Corrosive Environment

The nature of the corrosive environment has an important effect on the susceptibility of metals to corrosion-fatigue. Thus additions of chlorides to the environment increase the susceptibility of carbon steels to corrosion-fatigue as was demonstrated by Speller, McCorkle and Mumma (47) who found a considerable reduction in the endurance limit of a normalised 0.35 per cent carbon steel with the addition of 25 parts per

million/

million (p.p.m.) NaCl plus 25 P.p.m. Na_2SO_4 to a distilled water environment. Further additions caused a less drastic reduction in the endurance limit. They state that the addition of acid had a similar effect.

The susceptibility to corrosion-fatigue attack can be greatly reduced by the addition of suitable inhibitors to the corrosive environment. The effects of these inhibitors have been fully discussed in the text books by Evans (27) and Speller (48). In his book, Evans has divided inhibitors into the following three main classes.

1. Adsorption Inhibitors- These are predominantly organic compounds which appear to form surface films, generally reducing the attack. For example, Agar, thiourea, certain amines, soluble oils and organic colloids.
2. Anodic Inhibitors - These are mainly sodium or potassium salts containing anions which form sparingly soluble salts with the metal under test. The best known inhibitors in this class are, caustic soda ($Na\,OH$) potassium dihydrogen phosphate KH_2PO_4) potassium dichromate ($K_2Cr_2O_7$) and sodium chromate (Na_2CrO_4). These salts tend to stifle the anodic reaction which would normally give rise to the formation of ferrous hydroxide.

3./

3. Cathodic Inhibitors - These tend to hinder the reactions which would take place at Cathodic areas during corrosion. There are two main cathodic reactions, one leading to the liberation of hydrogen and the other to the adsorption of oxygen from solution, with subsequent formation of hydroxyl ions. There are, therefore, two types of cathodic inhibitors, namely:-

(a) Those which prevent liberation of hydrogen:- These are mainly salts of arsenic and antimony, which can restrain the evolution of hydrogen at cathodic areas because of the high hydrogen overvoltage on the arsenic and antimony deposited at those areas.

(b) Those which prevent the adsorption of oxygen from solution:- These are mainly salts of metals (for example zinc and nickel salts) which form sparingly soluble hydroxides at the cathodic areas, thus preventing the movement of hydroxyl ions from the cathodic area to the anodic area, thereby reducing the attack.

Evans stated that 'Anodic inhibitors are usually efficient but dangerous, whereas cathodic inhibitors tend to be inefficient but/

but safe'. The reason for this statement will be appreciated after a consideration of their respective actions. If insufficient anodic inhibitor is added to the solution, so that corrosion takes place only at the most susceptible regions, the area subjected to attack is greatly reduced but the amount of corrosion remains the same. This means that the intensity of corrosion will be accelerated at these unprotected points, leading to an early failure in the presence of cyclic stressing. On the other hand, cathodic inhibitors will not cause the anodic areas to shrink and therefore as the amount of corrosion is diminished, it follows that the intensity will be diminished.

There are other classifications of inhibitors but the above is more generally accepted. Reference lists of inhibitors are frequently published, but the data supplied therein usually refer to stressless corrosion conditions. Those inhibitors which are in common use today comprise chromates, phosphates, nitrites, mixtures of these three and proprietary makes of 'soluble' oils and amines.

Chromates, including dichromates, are the most used, both in industry and in research. Speller, McCorkle and

Mumma/

Mumma (47) observed that even in 3 per cent NaCl, considerable protection was conferred by an 0.5 per cent addition of sodium chromate. Gould and Evans (36) confirmed this, but also observed sodium chromate to be superior to the dichromate.

Watcher (49), Cohen (50) and Wyllie and Cheeseman (51) showed that sodium nitrite in chloride solutions had similar inhibiting effects, one per cent conferring very good protection, but with an increase in the temperature, an increase in this concentration was necessary. However, the most important factor in the use of sodium nitrite is the control of the pH of the solution. Watcher and Wyllie and Cheeseman emphasised the importance of keeping the pH in the range 9-10 and both used phosphates as their buffering agents. Phosphates can be used by themselves to inhibit corrosion in boiler drums, but it is essential that the supply of phosphate be maintained. Mixtures of phosphate and chromate, and phosphate and nitrite have proved superior to either of the three when used alone.

The proprietary makes of inhibitor like 'Rust-Lick' and 'Corrokos' are nearly all of the amine type (for example cyclohexylamine, benzylamine, morphine). They have proved of value in boiler practice and recirculating cooling systems such as central heating.

On/

On the other hand considerable experimental evidence has been produced to show that a strongly adherent hydrated iron-chromium oxide film ($Cr(OH)_3$ γ Fe_2O_3 H_2O) is formed, as found by Mayne, Mentor and Pryor (52) from electron diffraction studies. Using other inhibitors the surface film was invariably found to be γ Fe_2O_3. H_2O. Experimental evidence for the above oxide layers has also been obtained by Cohen and Palmer (53).

CHAPTER THREE

EXPERIMENTAL EQUIPMENT. II.

The most common methods of applying corrosive environments in corrosion-fatigue testing use either a drip or wick feed on to the specimen. These methods suffer from the following three disadvantages:-

(a) Accelerated corrosion at the air/liquid interface due to differential aeration and concentration effects.

(b) Possibility of lack of homogenity in the corrosion environment.

(c) Difficulty of temperature control, especially when operating at elevated temperatures.

Although these methods have been widely used, it was thought that a procedure in which the specimen was completely immersed in the corrosive fluid would give more accurate and reliable results, because the occurrence of the three above factors would be minimised. It was therefore necessary to choose a fatigue machine which would facilitate testing under complete immersion conditions. The rotating load type of machine designed and developed by the British Non-Ferrous Metals/

Metals Research Association, in which the specimen does not revolve, thereby simplifying fluid sealing, appeared to be the most suitable for this purpose. Six machines were made from the B.N.F.M.R.A. design. Another factor influencing the choice was the speed of testing - 3000 cycles per minute. This enabled an endurance of 50 million to be reached in 12 days.

Fatigue Machine - Fig 8 shows plan, elevation and end elevation views of the fatigue machines used. The specimen S is held vertically in the machine between the brack A and the clamping block B. The upper end of the specimen is attached to a rotating head C by means of a capstan nut L and a ball race J. The rotating head C is driven through a flexible coupling F attached to the motor shaft M. The drive is supplied by a synchronous motor operating at 3000 r.p.m. The head is normally perfectly balanced but the adjustable weights W in the head generate a centrifugal force which supplies the bending moment. The adjustment of these weights allows a range of stresses from 3 tons per square inch to 22 tons per square inch to be used. An aluminium clamp D attached to the specimen contains a small hole H (0.008 in diameter) through which light from 12 volt/

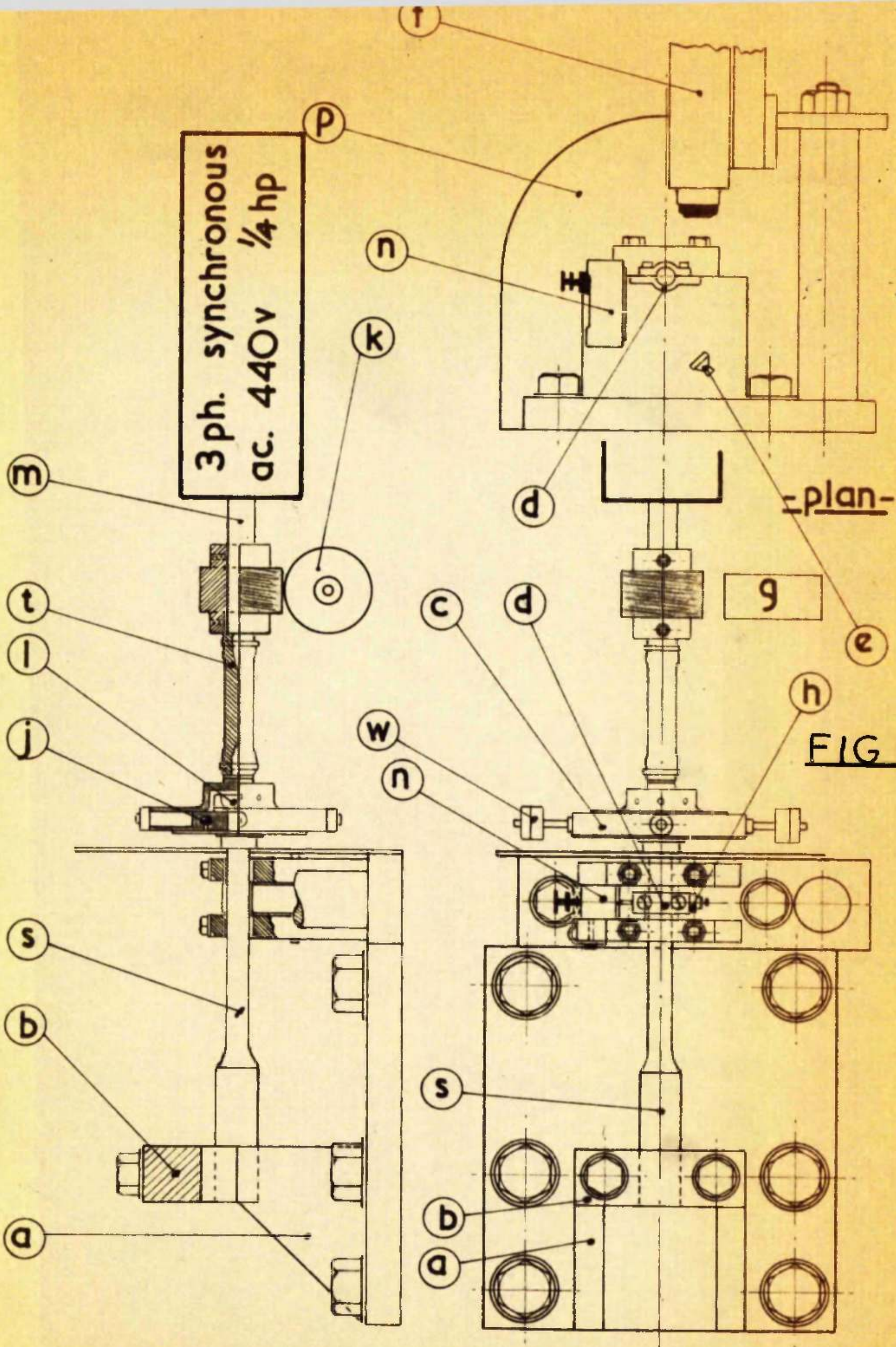

- end elevation -

-elevation-

-plan-

FIG 8

volt bulb is reflected by a steel mirror E into the microscope F. When the machine is in operation the reflection appears as a band of light, the length of which is measured by adjustable shutters in the microscope. This length is directly proportional to the load applied, the precise relationship being obtained from a static calibration, which is discussed later. Cairney (54) found some difficulty in the accurate determination of the applied stress. By increasing the magnification of the microscope this difficulty was overcome. The fatigue life of the specimen is recorded on a six digit counter G driven through a 100: 1 reduction K. The micro-switch N through a relay, cuts off the current to the motor when the specimen fractures. A perspex cage P provides protection for the user from all moving parts.

Fig. 9 illustrates diagrammatically the arrangement of all the apparatus used during corrosion-fatigue tests, and Fig. 10 is a photograph of the apparatus in operation.

Corrosion Circuit - The corrosion fluid is drawn from the glass reservoir by a pump, which pumps it through a heater, into a thermostat tube, thence round the specimen and back into the reservoir. The reservoir holds 2.5 litres, and has a small reflux condenser to cut down the evaporation losses.

This/

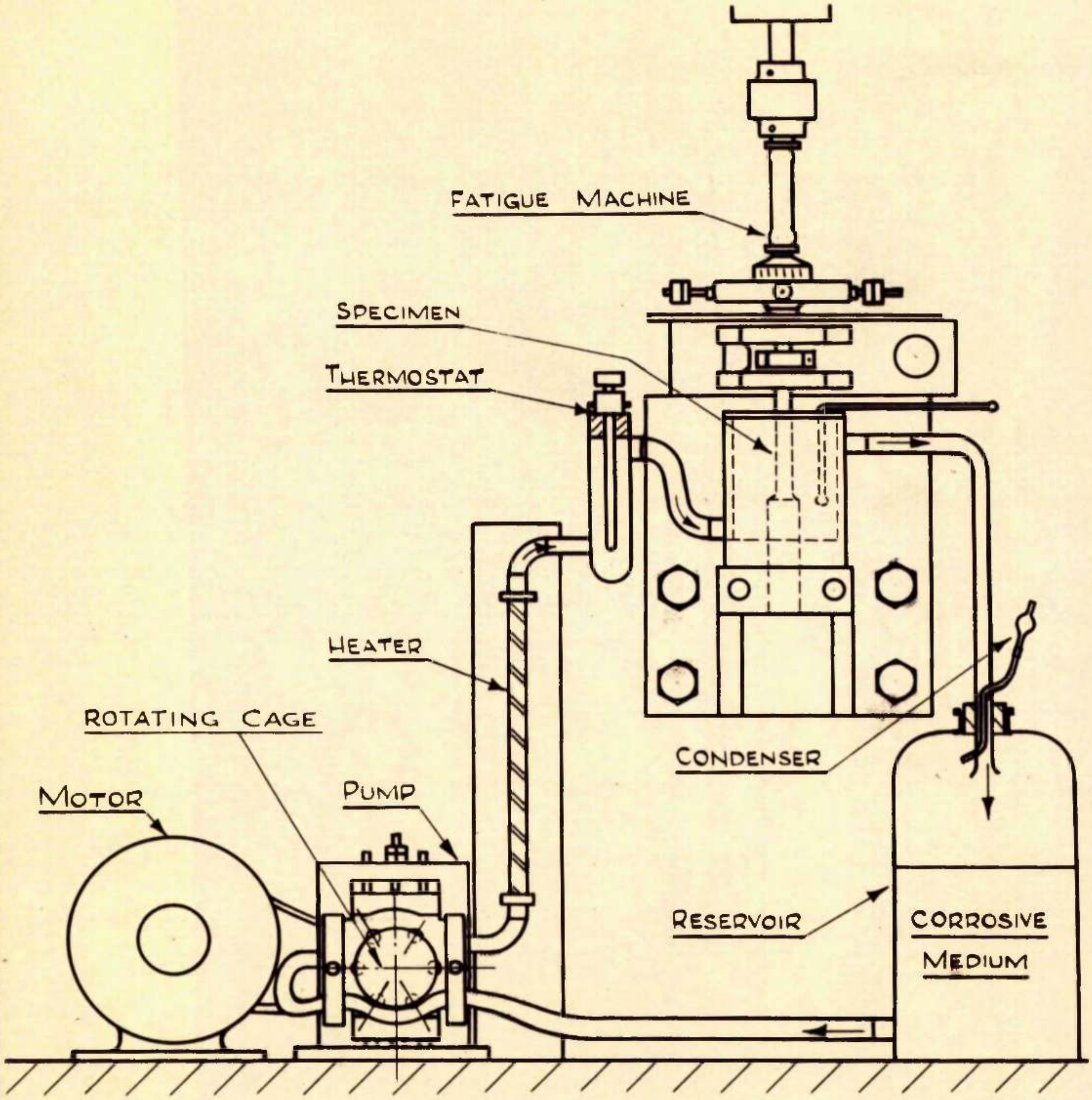

ARRANGEMENT OF CORROSION CIRCUIT AND FATIGUE MACHINE

FIG 9

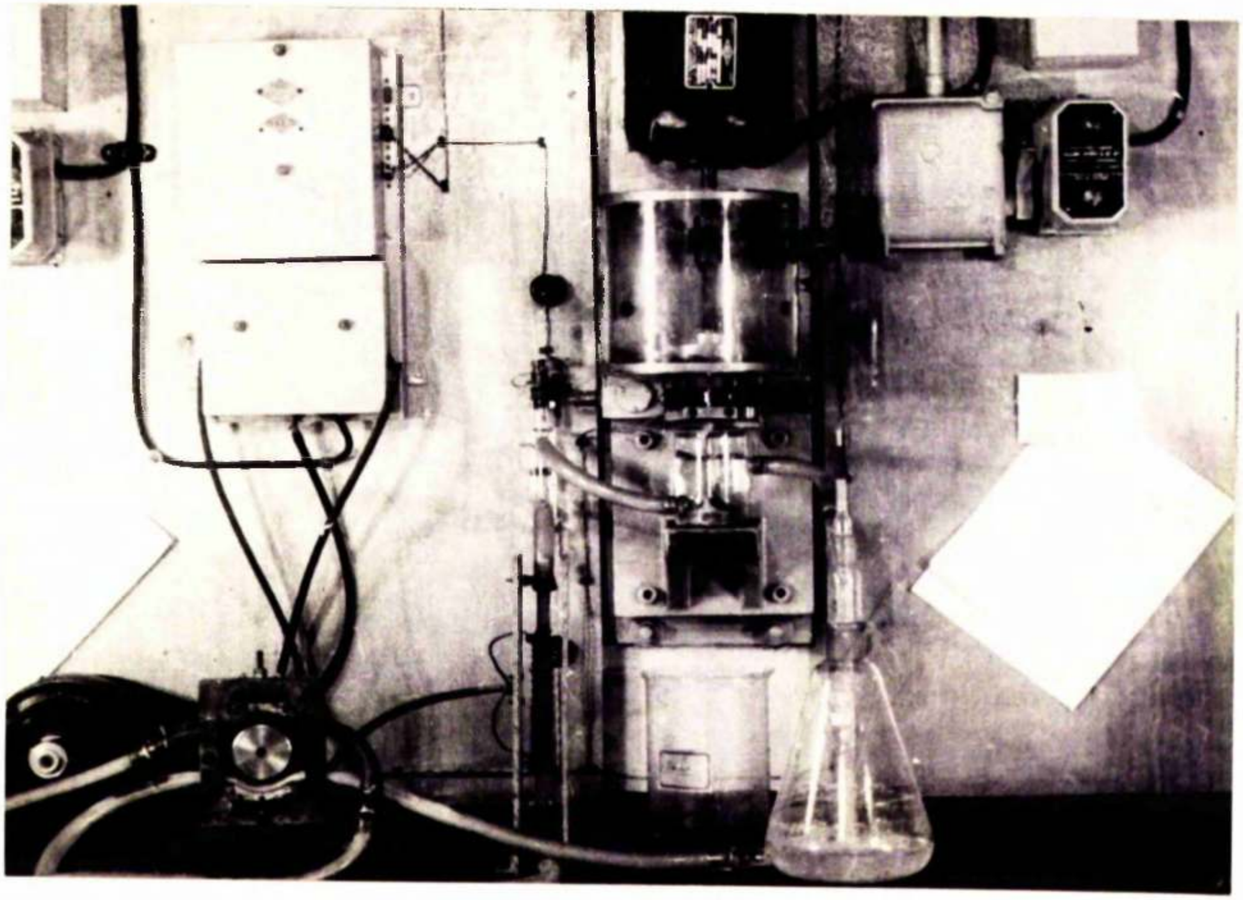

FIG 10

This ensures little change in the solution concentration. Cairney (54) used a centrifugal pump, made from bakelite, for circulating the corrosive medium. It was hoped that this would overcome the corrosion problem. However, Cairney had difficulties due to the corrosive medium seeping up the shaft of the pump and into the bearings. This created an electrochemical cell causing the specimen to corrode more quickly. In the present work, this was overcome by the pump illustrated in Fig. 11. This enabled the aqueous medium to be circulated without any break in the tubing, and eliminated the possibility of extraneous metallic materials which might give rise to electrochemical corrosion cells entering the system. A cross-section of the pump is shown in Fig. 12. The fluid is propelled through flexible PVC tubing in a succession of waves due to a displacement caused by a series of roller bearings (8) mounted on a rotating cage (7). The rollers must be free to rotate, so that no abrasion of the tubing takes place. They must also be arranged at such a distance apart that at least one always presses on the tubing, thus preventing any backward flow. The rate of flow can be altered by moving the adjustable block (2) up or down. The tubing/

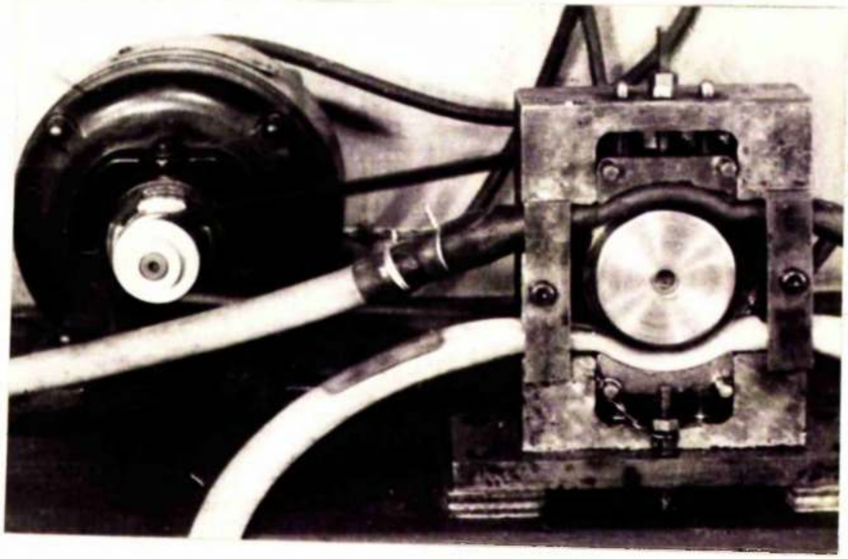

FIG 11

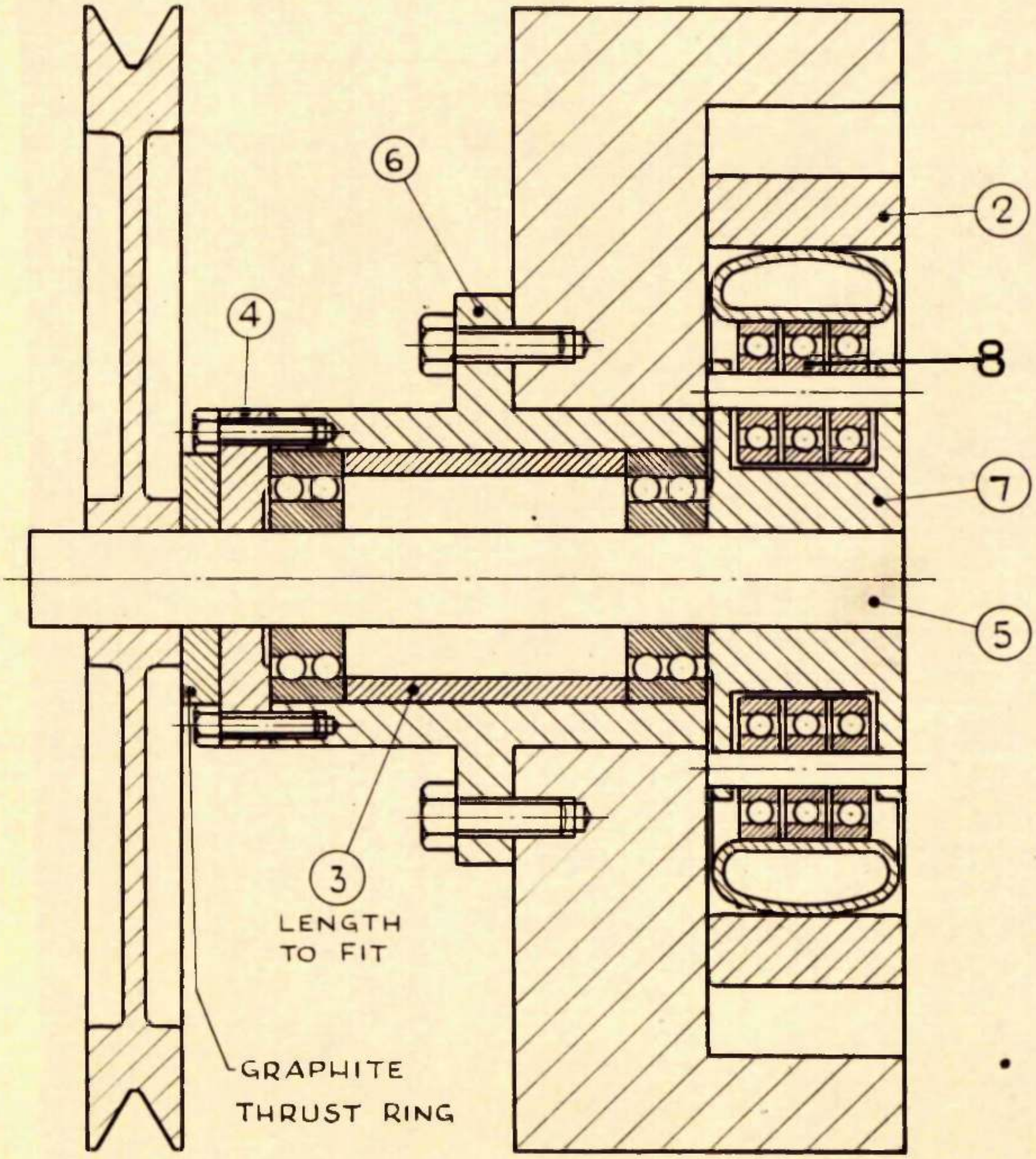

FIG 12

tubing is held in position by two flat plates, facilitating removal of the tubing by unscrewing a single 'Allen' screw. The pump is driven through a 3:1 reduction gear by a 1500 r.p.m. ¼ H.P., A.C. motor, and serves two fatigue machines as shown in Fig. 10.

On leaving the pump the fluid passes through a vertical silica tube round which is wound a 750 watt spiral nichrome element. This element is controlled from a 'Tem-Con' relay operated by the thermostat which can control the temperature to ± 0.5°C.

The details of the heater and thermostat relay circuit are shown in Fig. 13. The thermostat contains a bimetallic expansion element in the stem which operates finely adjusted contacts in the head. The sensitivity of the system is dependent upon the length of the expansion element and for the present work a 4 inch stem length, enclosed in a mercury glass sheath has proved most satisfactory. The closing of the contacts in the head raises the grid potential of the amplifier, from which current flows to energise a solenoid-operated relay.

Cairney (54) experienced great difficulty with the heating circuit failing overnight, causing the fluid to be circulated/

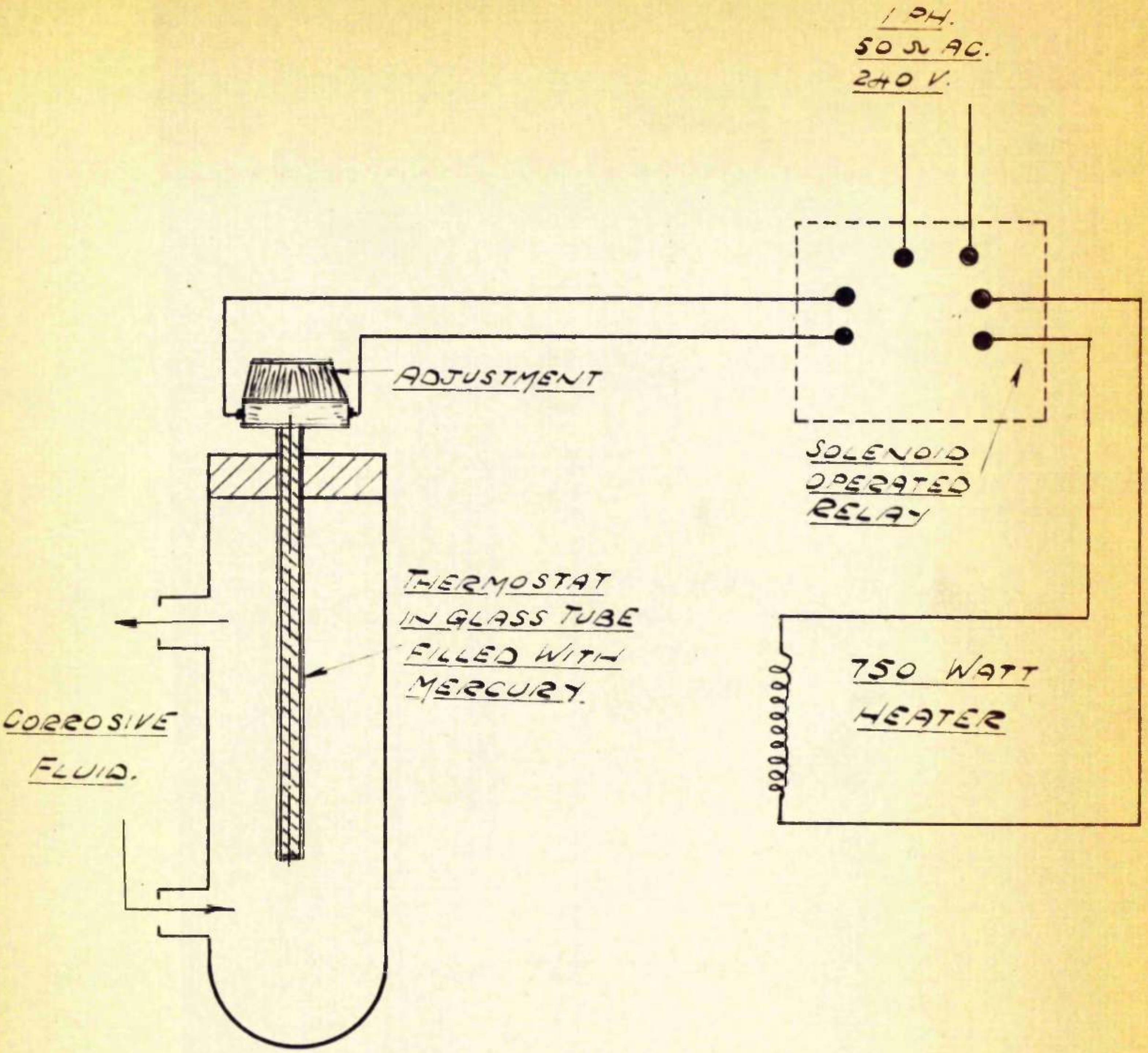

—THERMOSTAT RELAY CIRCUIT.—

FIG 13.

circulated cold, and thereby increasing the rate of corrosive attack. At other times, a connection might have failed, and the fluid in the corrosive circuit would be drained. This caused the heater to continue burning so creating the danger of fire. To overcome these difficulties, a heat fuse was incorporated in the heater, enabling the heater to be cut out if a leak developed in the circuit. The heater was enclosed in 'Sindanyo' to cut down heat losses and this also helps to minimise fire risks. One of the chief locations of the leaks was at the inlet to the specimen tanks.

The specimen tanks which Cairney used were made in heat resistant glass having an tangential inlet and a radial outlet. The bottom of the tank was made from ebonite, being sealed to the vessel by an 'O' ring and having another 'O' ring seal where the specimen was inserted. This was found unsatisfactory, so a new type of tank made from rigid PVC was used with similar attachments, except that the bottom was sealed to the rigid PVC by 'Bostik' adhesive. The top was also made from ebonite and had a centre hole for the specimen. This hole had a lip round it to take a thin rubber seal. Another small hole in the top was made for holding a thermometer. The main advantages of using a rigid PVC vessels were that breakages were minimised and it was easier to attach the PVC tubing to the vessel.

The/

The motor driving the fatigue machine had a very fast acceleration to its working speed, so resistances were incorporated in the circuit as shown in Fig. 14. These resistances were only used for starting to enable any overload caused by the sudden acceleration to be kept to a minimum. This overloading occurred because the flexible drive lagged behind the motor for the first few seconds and when the working speed was reached the rotating head exceeded this speed momentarily, so causing an overload.

There is also incorporated in the circuit shown in Fig. 14 a cut-out which was usually successful in stopping the machine when a crack developed (that is before final fracture occurred), thereby allowing subsequent examination of the partly developed crack to be carried out.

The specimens used in the present study and illustrated in Fig. 15 had a longer length (six inches in place of five inches) and a small diameter (0.4 inches compared with 0.5 inches) than the usual specimen used in the B.N.F.M.R.A. fatigue machines. This enabled higher stresses to be obtained at the critical section without much change in the position of the out of balance weights.

The/

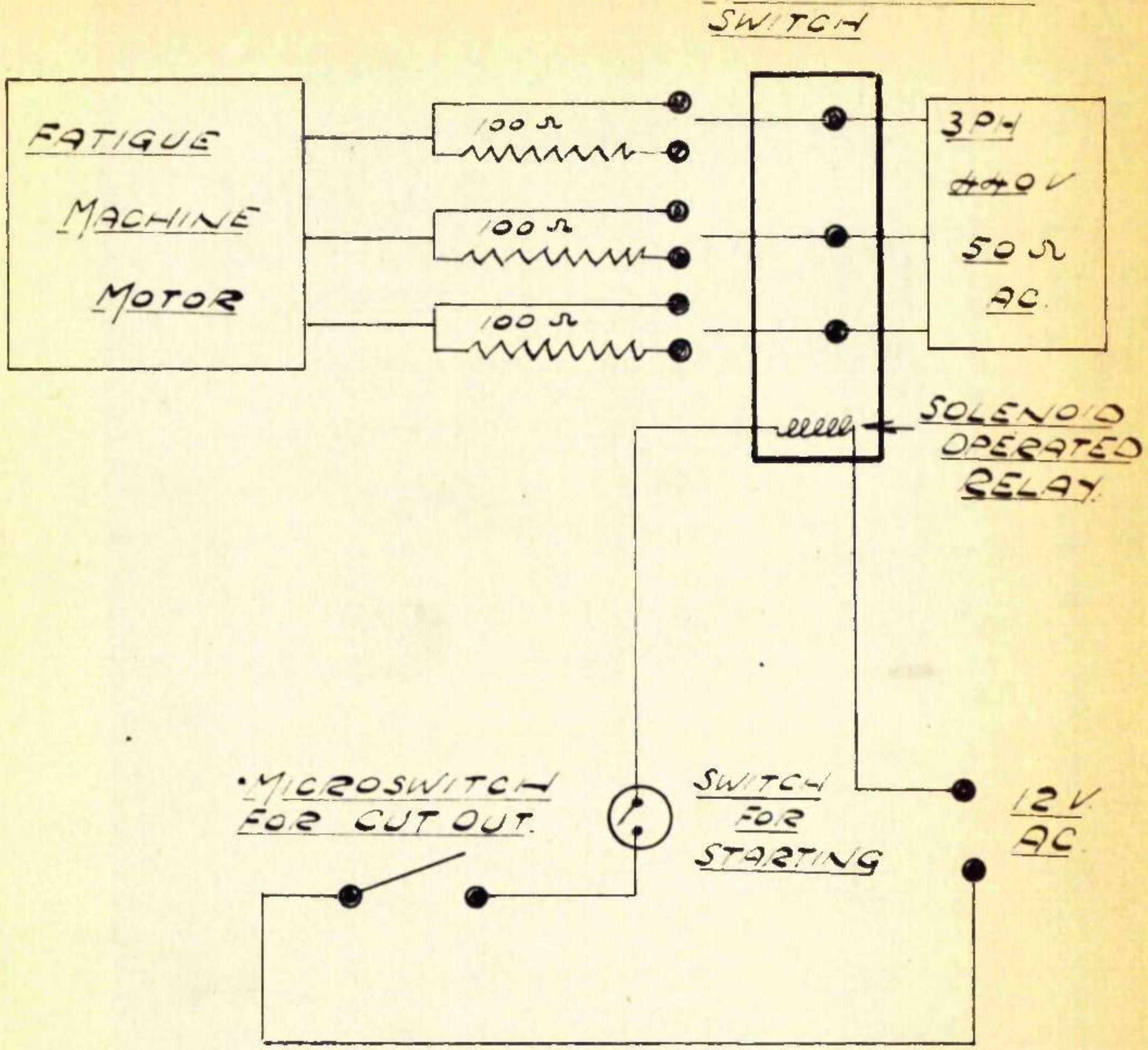

— STARTING AND CUT OUT CIRCUIT. —

FIG 14.

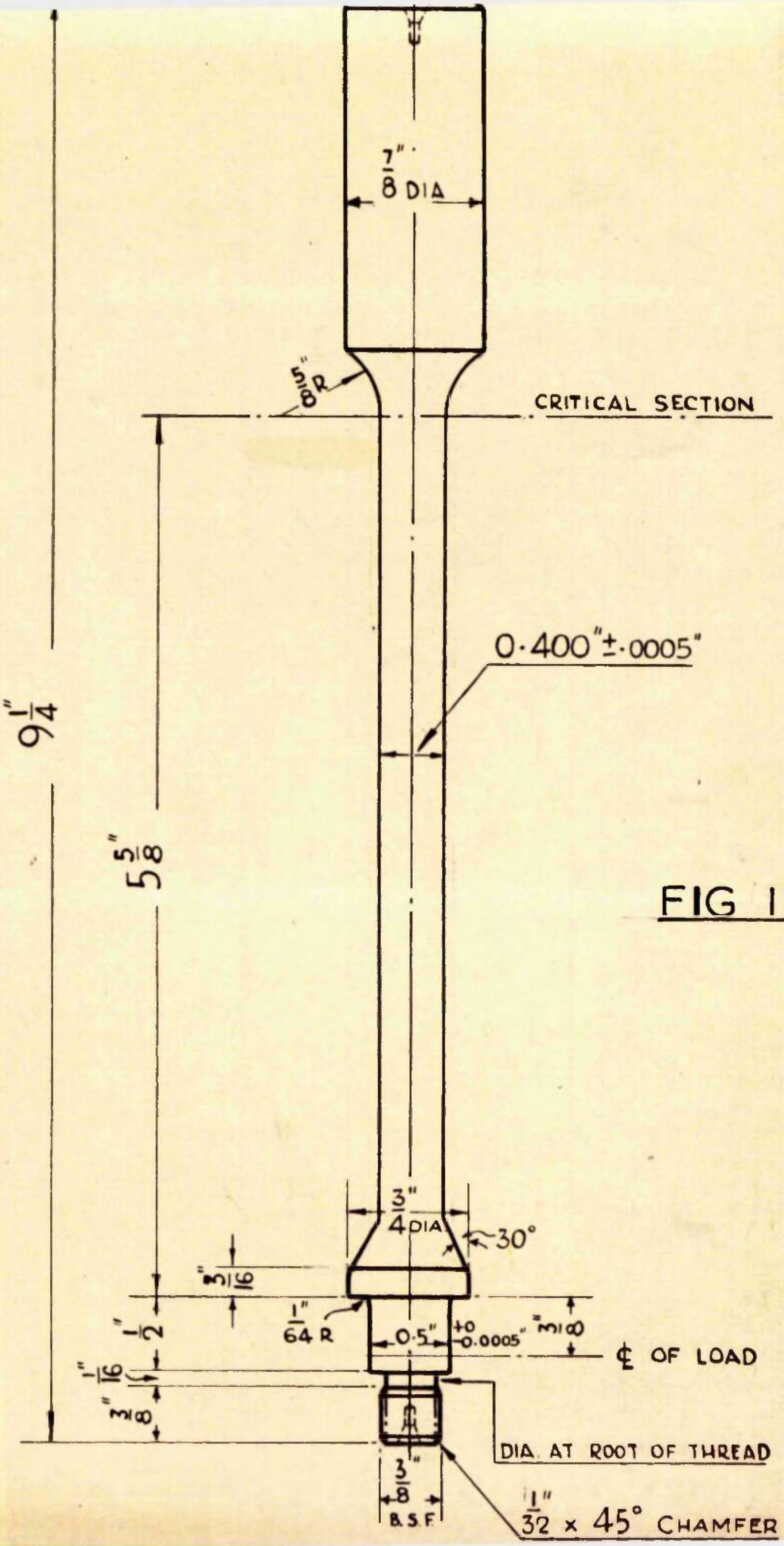
9 1/4"
7/8" DIA
5/8" R
CRITICAL SECTION
5 5/8"
0·400"±·0005"
3/4" DIA
30°
3/16"
1/64" R
1/2"
0.5" +0 -0.0005"
3/8"
℄ OF LOAD
1/16"
3/8"
DIA. AT ROOT OF THREAD
3/8" B.S.F.
1/32" × 45° CHAMFER

FIG 15

The preparation of the specimen is most important when reproducibility of results is required, and surface finishes should be as identical as possible. If the dimensions (particularly the length) were not constant, much time would have to be spent on measuring them and on the subsequent calculation of the stresses.

The specimens were roughed out on a copying lathe from one inch diameter steel bar having the following composition and properties:-

0.21% Carbon
0.32% Silicon
0.54% Sulphur
0.02% Phosphorus
0.55% Manganese
Ultimate tensile strength 28.8 tons per square inch
Elongation 40%
Reduction in Area 60%
Yield stress 17.95 tons per square inch

Five hundred feet of this steel, which had been rolled from a single ingot was obtained to ensure maximum uniformity of composition and properties.

To/

To ensure a uniform finish of the specimen great care was necessary. The specimens were finished to a wet scrape (about 20 micro-inches) in a centre lathe. When the final polishing of the specimen was carried out by hand the finish from one specimen to another varied between 2 and 3 micro-inches, but was very non-uniform. In the present work, a machine was specially designed for this purpose, and this is shown in Fig. 16. The specimen in the machine rotates at four revolutions per minute and the arms carrying the emery paper reciprocate at ninety times per minute. The specimen was polished through the following grades of emery paper:- 1G, 1, 1/0, 2/0, and 3/0. The mirror finish obtained was very regular and consistent in uniformity. The grade of finish was of the order or 2½ micro-inches, with very little variation. Using this machine any emery surface finish between 2μ and 40μ was reproducible and variations in surface finish were easily obtained. The surface finishes were checked by using the Taylor-Hobson 'Talysurf' shown in Fig. 17. This gave a centre line average (C.L.A.) value for the trace of the surface finish, one of which is shown in Fig. 18.

After polishing, the specimen diameter was measured to an accuracy/

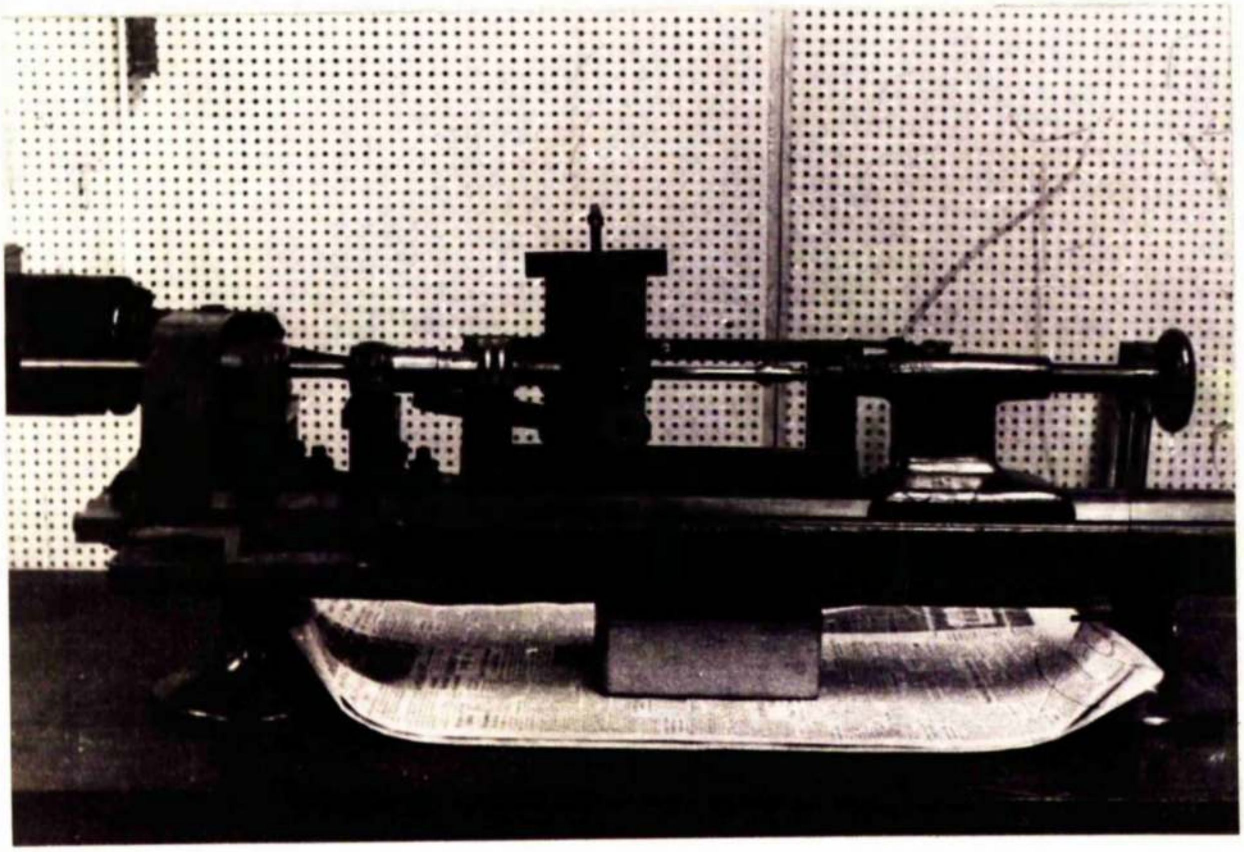

FIG 16

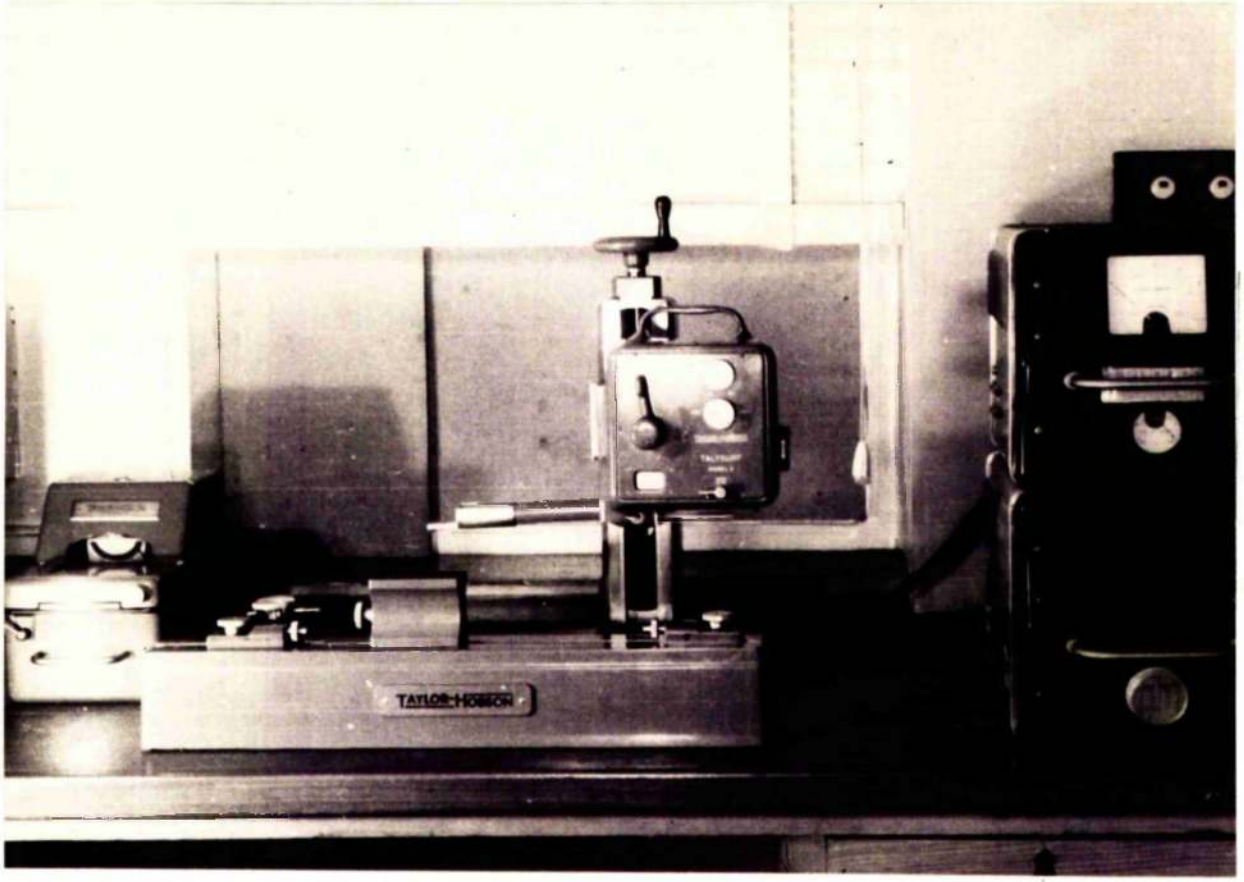

FIG 17

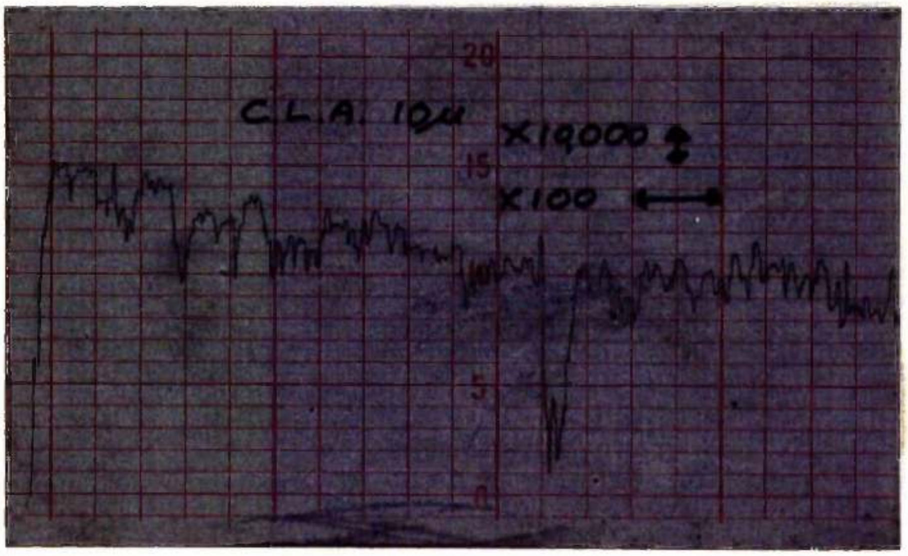

FIG 18

accuracy of 0.001 inches using a bull-nosed micrometer. Care must be taken to ensure that the micrometer did not damage the surface finish. The specimen was then thoroughly degreased with trichlorethylene and its surface finally examined for defects through a hand glass.

The prepared specimen was inserted through the base of the specimen tank and the cover placed in position. The membranous rubber seal was affixed and the thermometer inserted into the hole provided for it.

The tank containing the specimen was now transferred to the fatigue machine bracket and the specimen clamped in position. The rotating head and the flexible coupling were brought into position and fixed both to the specimen and the driving shaft of the motor.

The small aluminium clamp, containing the pinhole was fixed in position and aligned so that the light shone through the hole on to the centre of the microscope objective. Before the spot diameter was measured, the shutters were brought together and the counter set at zero. The spot diameter was then measured.

The specimen was then calibrated statically, and Fig. 19 illustrates a specimen undergoing calibration. A thin steel wire/

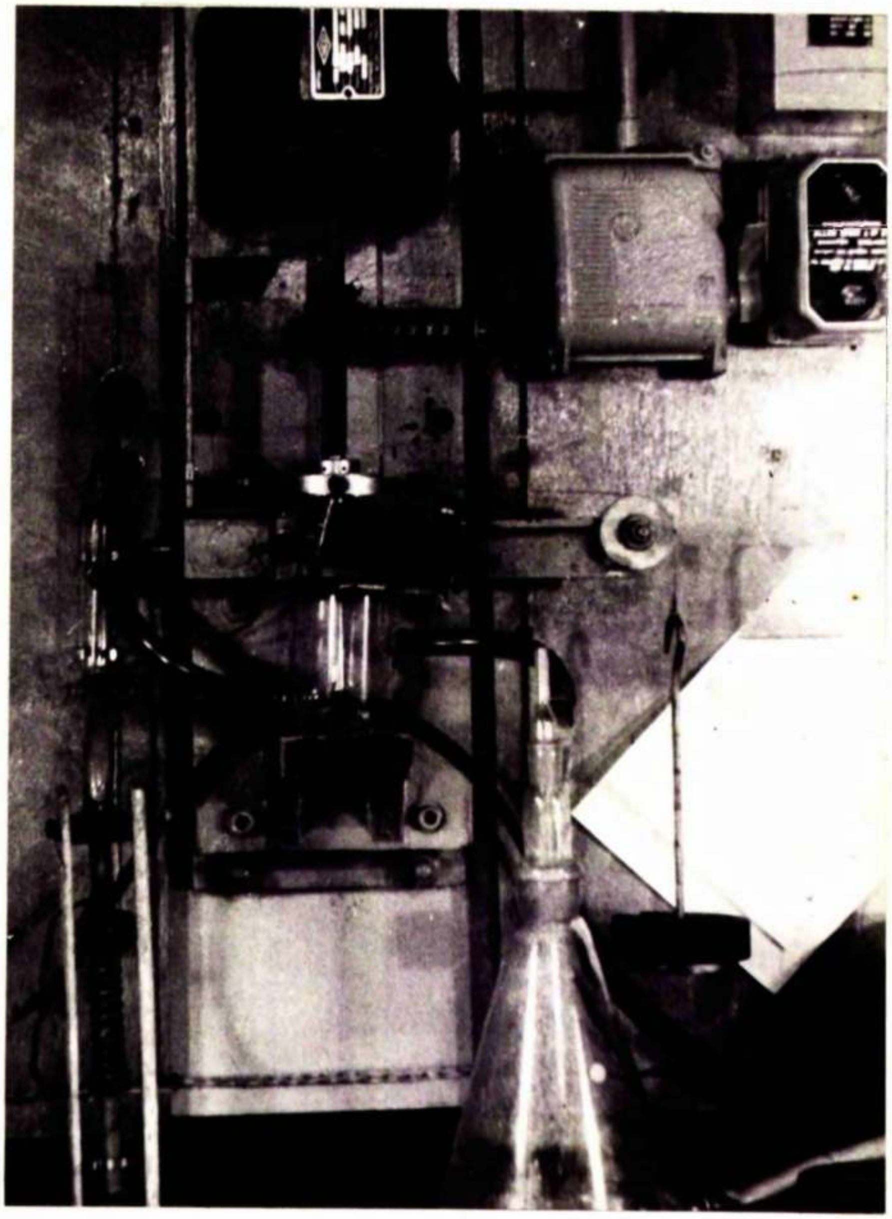

FIG 19

wire was attached to one of the adjustable weights of the rotating head, brought over a pulley on the end of an adjustable arm and a one lb. hanger suspended from it.

Weights were added in three lb. increments; the deflection obtained being measured by means of the movement of the light spot viewed through the microscope.

The stress was calculated in the following manner.

$M = WL$ where M = Bending Moment.

W = Load Applied

and L = distance from point of application of the load to the critical section.

The stress $S = \frac{My}{I}$ where y = the distance from the neutral axis to the extreme fibre.

$\therefore y = \frac{d}{2}$ (d is the diamter of the specimen)

I = Moment of Inertia

$= \frac{\pi d^4}{64}$ for a round bar.

$S = \frac{My}{I}$ lbs per square inch.

$= \frac{WLy}{I}$ lbs per square inch

For the present series of tests the length was six inches

$\therefore L = 6$

$$\therefore S = \frac{W \times 6 \times d/2}{\frac{\pi}{64} \times d^4} \text{ lbs. per square inch}$$

$$= \frac{192\, W}{\pi d^3} \text{ lbs per square inch}$$

$$= \frac{192\, W}{2240 \pi d^3} \text{ Tons per square inch}$$

$$\text{Hence Stress} = 0.02727 \times \frac{W}{d^3} \text{ Tons per square inch}$$

Hence as the diameter of the specimen and the loads applied were known, the various stresses could be calculated. These were plotted against the measured spot deflections as shown in Fig. 20. A straight line relationship exists which can be extrapolated as far as the elastic limit. The appropriate deflection was then obtained for any desired stress e.g. in Fig. 20 if 10 tons per square inch is the desired stress, the appropriate deflection is 180.

During the static calibration, one side of the specimen was in compression and the other in tension, therefore, in the present fatigue testing procedure, the above deflection must be doubled. Furthermore since the shutters of the microscope only read to the edges of the spot, the spot diameter must be added to give the final desired 'band length'.

For example, if a test was to be run at 10 tons per square inch.

Desired Deflection = 180

Spot Diameter = 56

∴ Desired total band length = (2 x 180) + 56 = 416

After this calculation of the desired band length, the out/

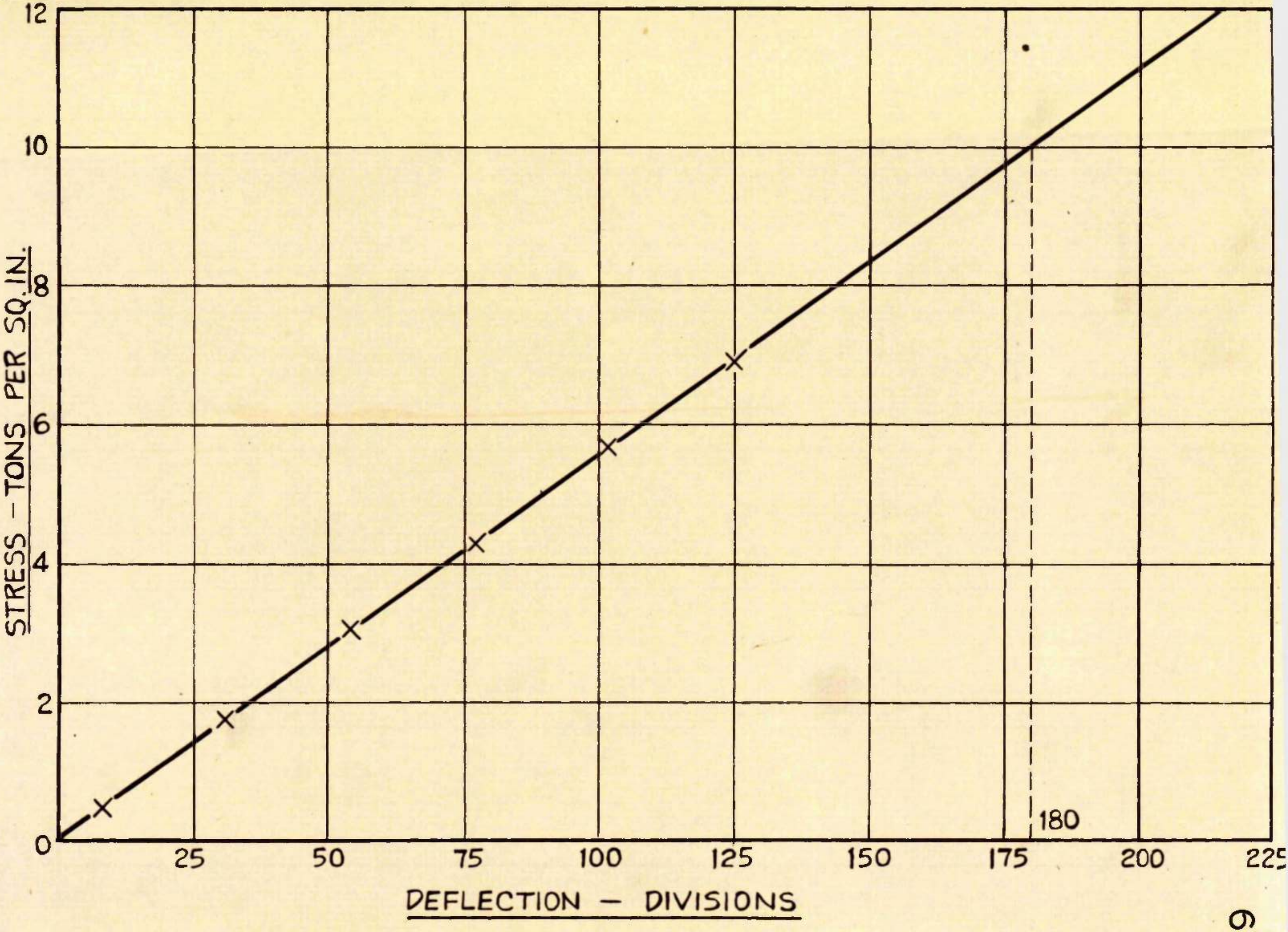
STRESS - TONS PER SQ.IN.
12
10
8
6
4
2
0
25
50
75
100
125
150
175
180
200
225
DEFLECTION - DIVISIONS

FIG 20

out of balance weights were adjusted until this bend length was obtained.

It was necessary to calibrate each specimen individually due to small variations (.395 - .403 in) in the specimen diameter and in the positioning of the aluminium clamp on the specimen. During the calibration the specimen was subjected to fatigue although not in the corrosive environment. This amount of fatigue was small (~ 35,000 reversals of stress) and could normally be ignored.

When the calibration was completed the appropriate corrosive solution was made up using synthetic sea-water, distilled water and various inhibitor solutions. When making up a solution it was customary to measure all the additions by pipettes into a two litre measuring flask, then fill this flask up to the mark with distilled water.

For example, if a 10 per cent sea water plus 250 p.p.m. sodium chromate solution was required, 200 c.c. of sea water were pipetted into the two litre graduated flask, followed by 10 c.c. of a 5 per cent solution of sodium chromate. The flask was then filled up to the mark with distilled water. Similarly, if 1000 p.p.m. of Oil C was required, some distilled water (or the required measured quantity of sea-water) was first put into the flask to ensure proper emulsification/

emulsification then 2 c.c. of Oil C were added, and the solution made up to the mark with distilled water.

Careful preparation of the solution is necessary, since slight changes in composition affect the reproducibility of results. Synthetic sea water was made up according to a D.S.I.R. formula, viz:-

27.26 gms/litre anhydrous sodium chloride (Analar)
0.11 gms/litre anhydrous sodium bicarbonate (Analar)
0.69 gms/litre anhydrous potassium chloride (Analar)
0.09 gms/litre anhydrous potassium bromide (Analar)
1.29 gms/litre anhydrous calcium sulphate (Analar)
3.51 gms/litre anhydrous magnesium chloride (Analar)
1.84 gms/litre anhydrous magnesium sulphate (Analar)

This was stored in an aspirator as a 100 per cent solution and 10 litres were made up as and when required. The inorganic inhibitors were stored as 5 per cent solutions, but the oils were used as received from the manufacturers.

After preparation, the appropriate solution was heated almost to boiling point in a round bottomed flask, and transferred to the reservoir from where it could flow into the PVC tubing (precautions were taken to ensure that no air was trapped in the latter). When the tubing was sufficiently softened/

softened by the hot solution, the pump could be started and the tubing inserted, forcing the solution round the test specimen. When the solution had reached the correct working temperature, the motor of the fatigue machine was switched on, the starter resistances switched out, and the revolution counter set at zero. The microswitch was adjusted so that a 50 per cent increase in the band length beyond the setting would trip the motor relay. The pump was also adjusted to enable the solution to be circulated fast enough to ensure maximum aeration of the solution, caused by the turbulent flow into the reservoir.

During the course of the test, the working temperature was checked at least twice daily, to ensure that the thermostat was set correctly and that the relays were working satisfactorily. The solution was changed every forty eight hours to minimise any changes in concentration due to evaporation or interaction with the specimen.

The test was completed when the specimen failed or survived fifty million stress reversals. Any result where the test had to be stopped for more than thirty minutes for maintenance work on the apparatus was discontinued due to the effects of static corrosion etc.

To ensure that the performances of the inhibitors were compared with their electrochemical data an attempt was made to follow the process of protective film breakdown during a test. Fig. 21 shows the method which was used. A cell was formed by the specimen, corrosive fluid and a standard calomel electrode, and the resultant cell potential was measured by an electronic millivoltmeter which required no current. The potential difference set up in the cell was a direct measure of the susceptibility of the metal to corrode in the electrolyte of the cell. The results obtained in this series of tests enabled inhibitors to be compared on an electrochemical basis.

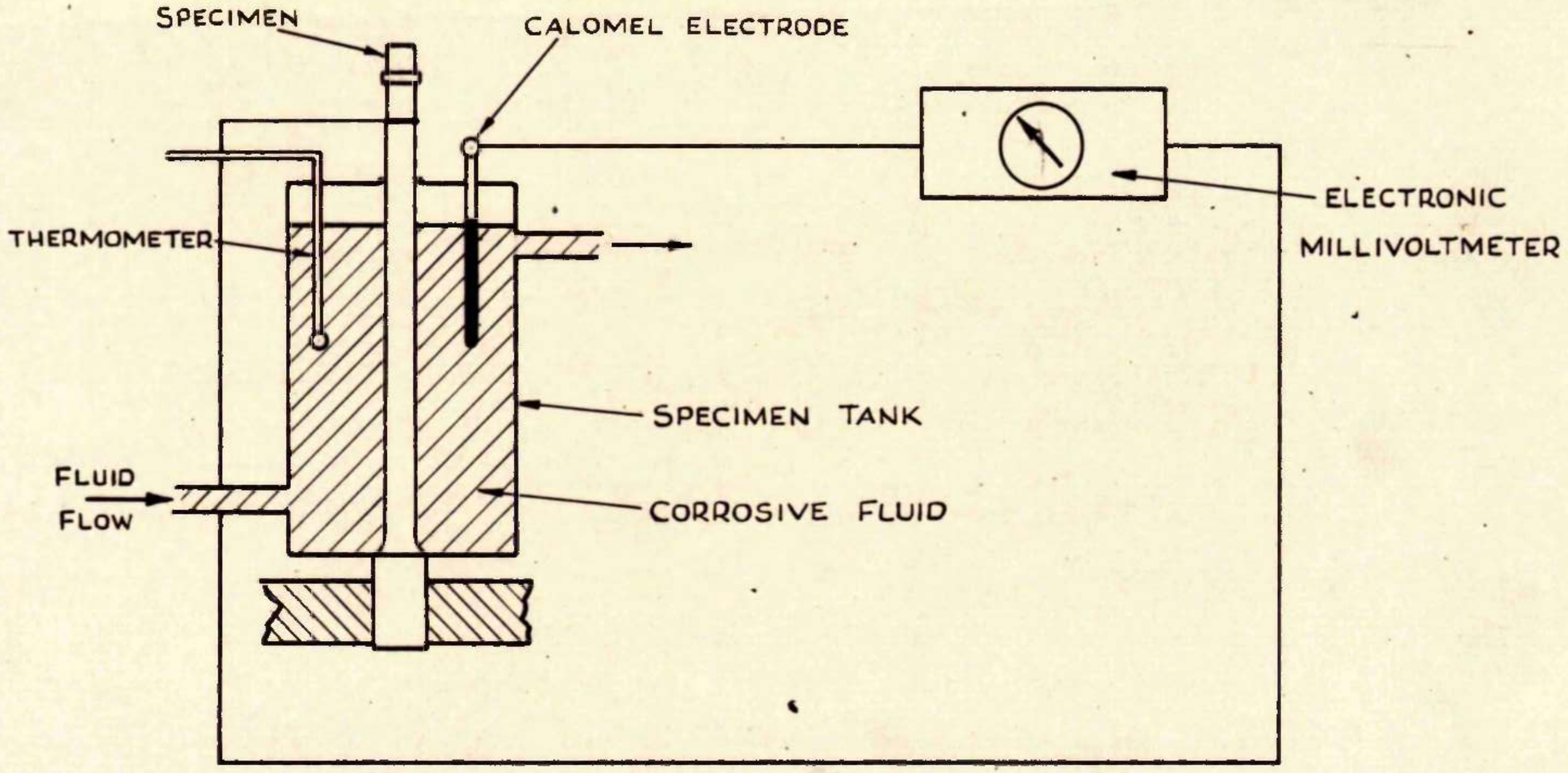

FIG. 21. CIRCUIT POTENTIAL MEASUREMENT.

CHAPTER FOUR

PRESENTATION OF RESULTS

It is most convenient to present the results of the investigation in graphical form, because this greatly facilitates the discussion of the results. Fig 22. shows the progressive changes in endurance as the environment was changed from air to distilled water. These curves show the main effects of varying the chloride concentration at 35°C. The next figure Fig. 23 is a cross plot of Fig. 22 and shows the effect of sea water concentration on the endurance limit.

When corrosion-fatigue tests are carried out in the presence of an inhibitor the concentration of the latter represents an additional variable. The initial tests were carried out at 35°C and at constant stress (12 tons per square inch) in order to evaluate the comparative performances of various inhibitors. These tests were carried out in 2.5 per cent 5 per cent and 10 per cent sea water solutions. The results obtained are shown in Figs. 24 and 25. Fig. 24 shows the results of the anodic inhibitors added to 2.5 per cent sea water solutions and Fig. 25 shows the results of the inhibitors in 5 per cent and 10 per cent sea/

sea water. Typical results showing the potential of a specimen during corrosion-fatigue testing in various solutions are shown in Fig 26.

The results shown in Fig. 24 and 25 indicate what inhibitors are the most efficient. Tests were carried out using these inhibitors to enable S/N diagrams to be constructed for the effects of varying percentages of these inhibitors in 2.5 per cent, 5 per cent and 10 per cent sea water solutions. The results obtained are shown in Figs. 27 to 32.

Figs. 27, 28 and 29 respectively show the S/N curves for sodium chromate in 2.5 per cent, 5 per cent and 10 per cent sea water at 88°C. The corresponding results for sodium nitrite in 2.5 per cent, 5 per cent and 10 per cent sea water at 88°C are shown in Figs. 30 to 32. The results shown in Figs. 27 to 32 have been used in the preparation of Fig. 33 where the concentration of inhibitor is plotted against the endurance limit obtained in 2.5 per cent, 5 per cent and 10 per cent sea water solutions for 25 million reversals of stress.

The comparison of the efficiency of adsorption inhibitors is shown in Fig 34. The results obtained were for

a/

a constant stress of ± 12 tons per square inch and for a temperature of 88°C. Fig. 35 shows the effects of varying the percentage of sea water during tests using the most efficient of the series of the adsorption inhibitors. These tests were also carried out at a constant stress of 12 tons per square inch and a temperature of 88°C.

Figs. 36 to 38 give the S/N curves for oil F in 2.5 per cent, 5 per cent and 10 per cent sea water respectively. The results from Fig. 36 were used to construct curves shown for Oil F in Fig. 33, which represents the effect on the endurance limit at 25 million cycles of adding the inhibitor to 2.5 per cent, 5 per cent and 10 per cent sea water at 88°C.

As the temperature of the environment was increased from 25°C to 88°C the endurance limit showed a progressive change as shown by Fig. 39 and from a cross plot of Fig.39, Fig. 40 is obtained. This shows the effect of temperature on the endurance limit.

The results for the tests on specimens having different surface finishes are shown in Figs. 41 to Figs 43. Fig. 41 represents the effect of variations in the surface finish of specimens tested in corrosive environments with various sea water concentrations. The effects of adding an anodic inhibitor/

inhibitor (sodium chromate) to the most corrosive solutions used in the tests are shown in Fig. 42. Fig. 43 shows the results obtained when an adsorption inhibitor (oil F) was used.

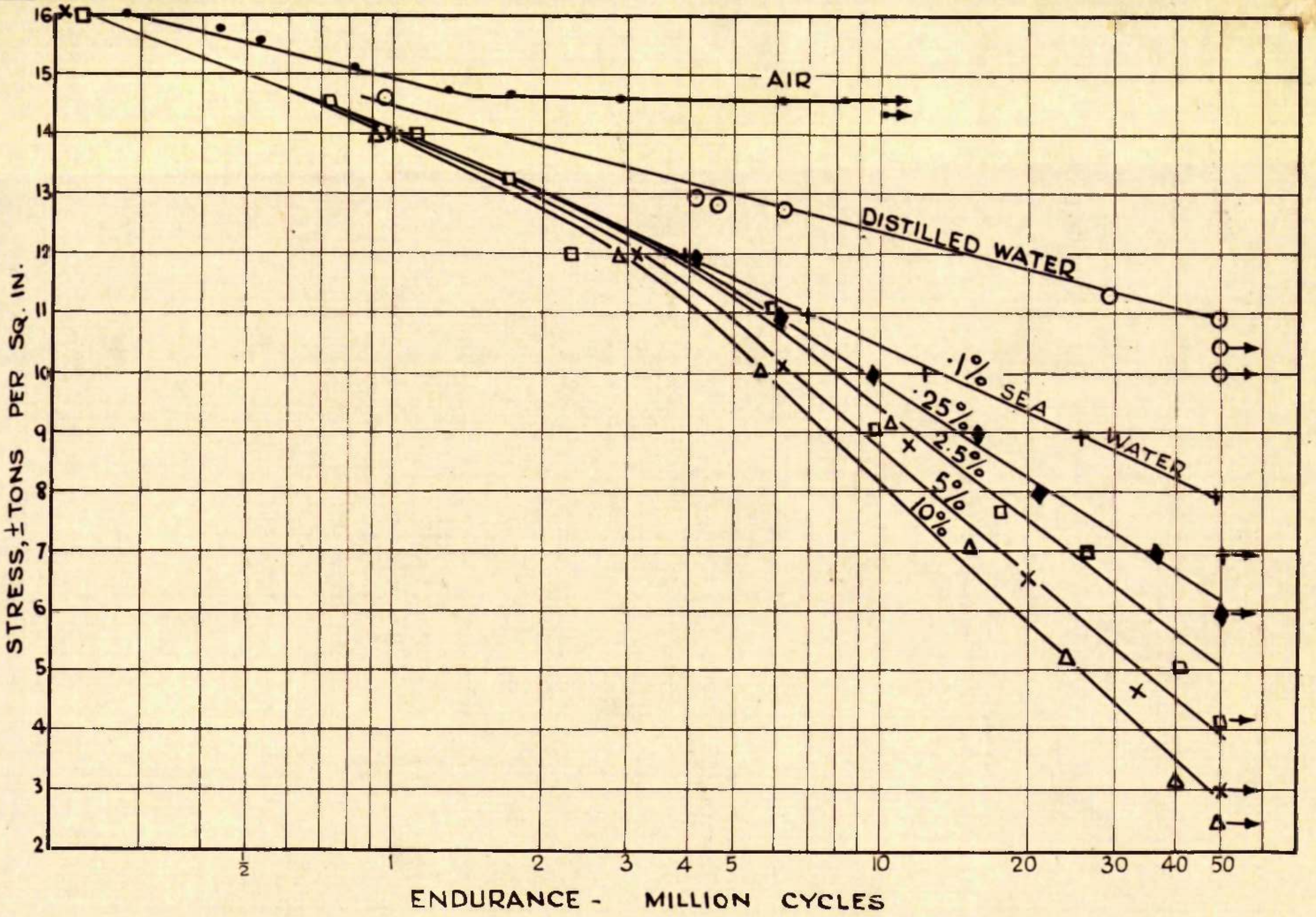

FIG 22 S - LOG N CURVES FOR MILD STEEL IN AIR, DISTILLED WATER AND VARIOUS SEA WATER ENVIRONMENTS AT 88°C

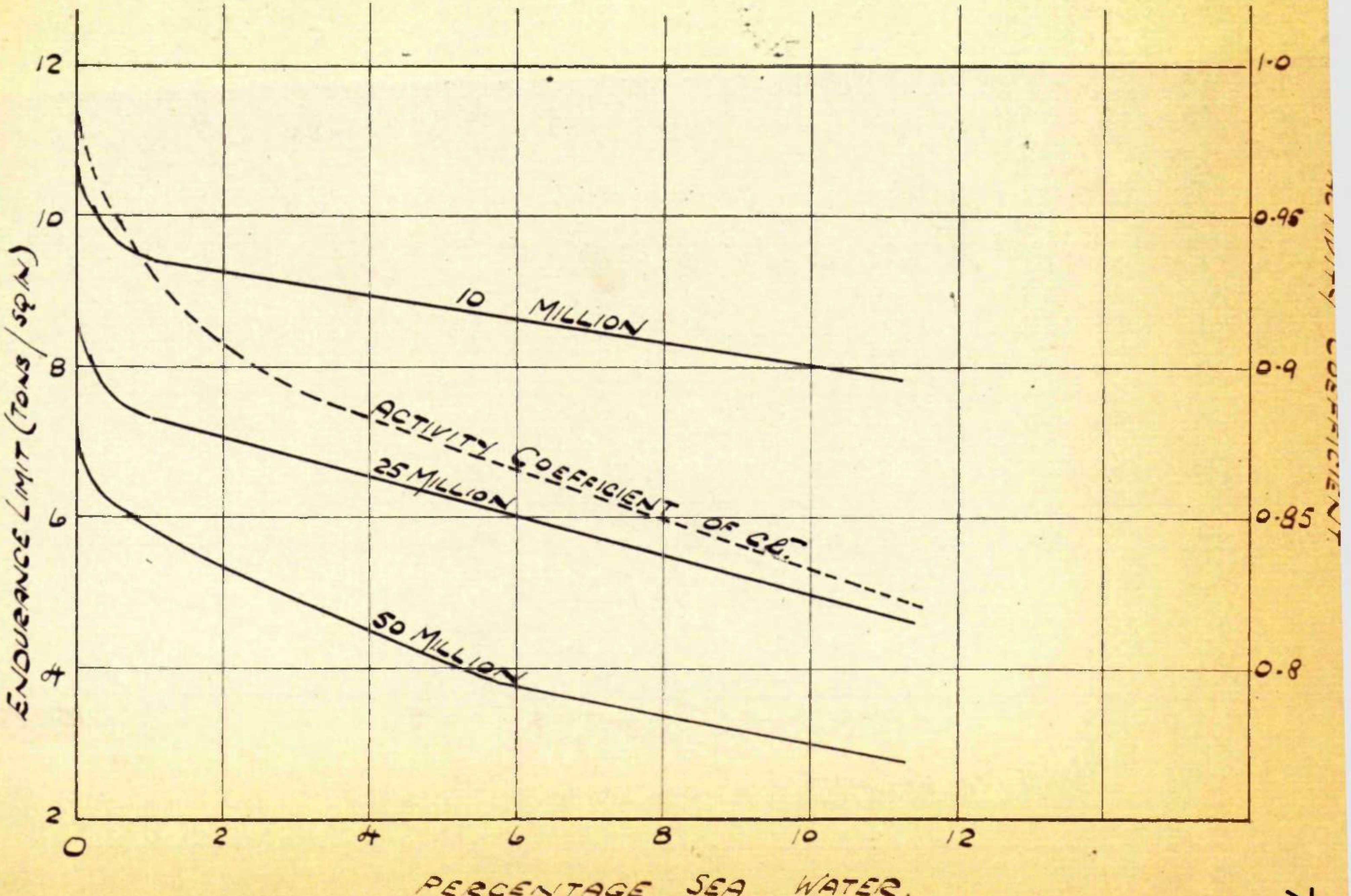
ENDURANCE LIMIT (TONS / SQ IN)
12
10
8
6
4
2
0
2
4
6
8
10
12
PERCENTAGE SEA WATER.
ACTIVITY COEFFICIENT
1·0
0·95
0·9
0·85
0·8
10 MILLION
ACTIVITY COEFFICIENT OF CL⁻
25 MILLION
50 MILLION

FIG 23

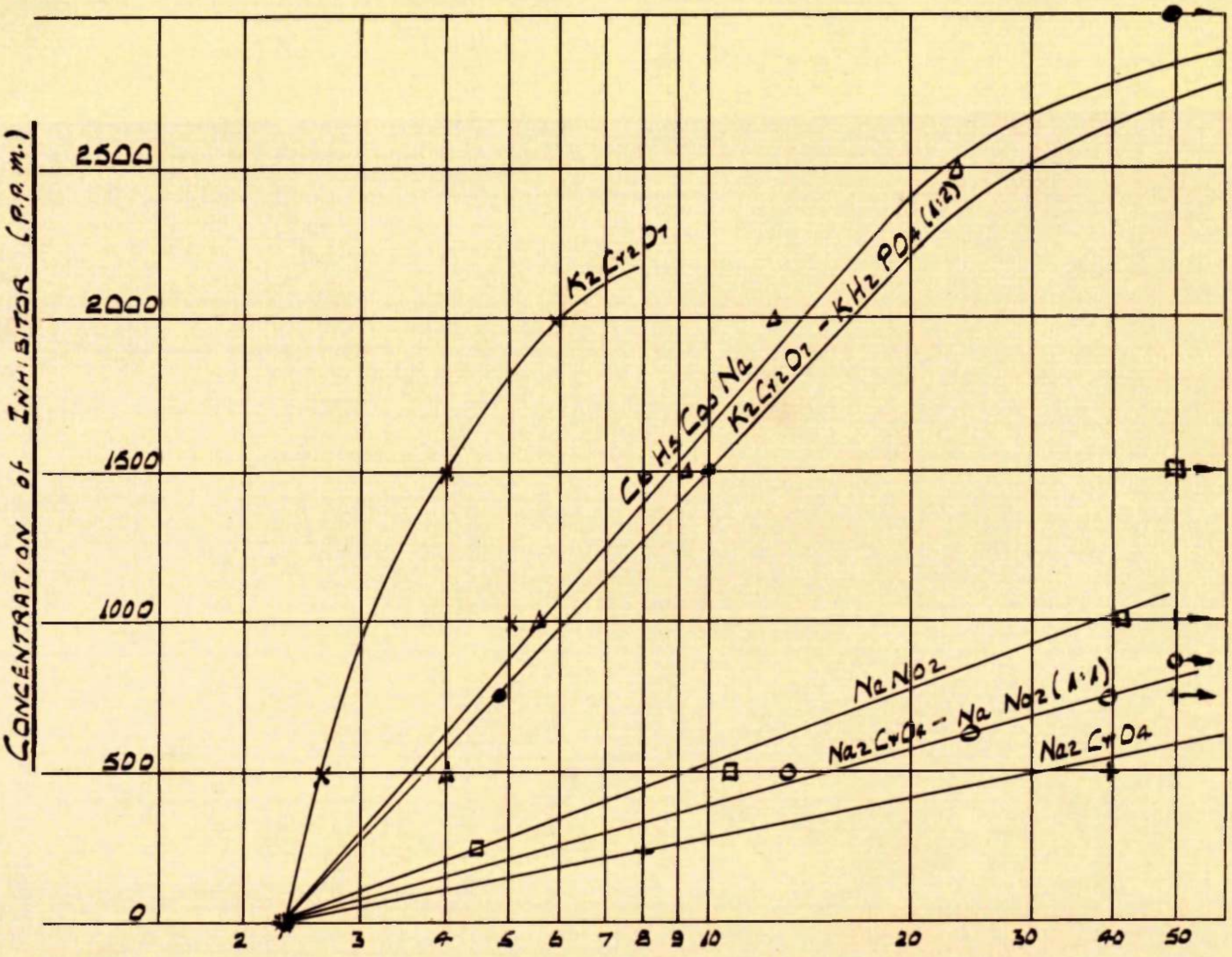
CONCENTRATION of INHIBITOR (P.P.M.)
2500
2000
1500
1000
500
0
2
3
4
5
6
7
8
9
10
20
30
40
50
$K_2Cr_2O_7$
C_6H_5COONa
$K_2Cr_2O_7 - KH_2PO_4$ (1:2)
$NaNO_2$
$Na_2CrO_4 - NaNO_2$ (1:1)
Na_2CrO_4
ENDURANCE – MILLION CYCLES

FIG 24

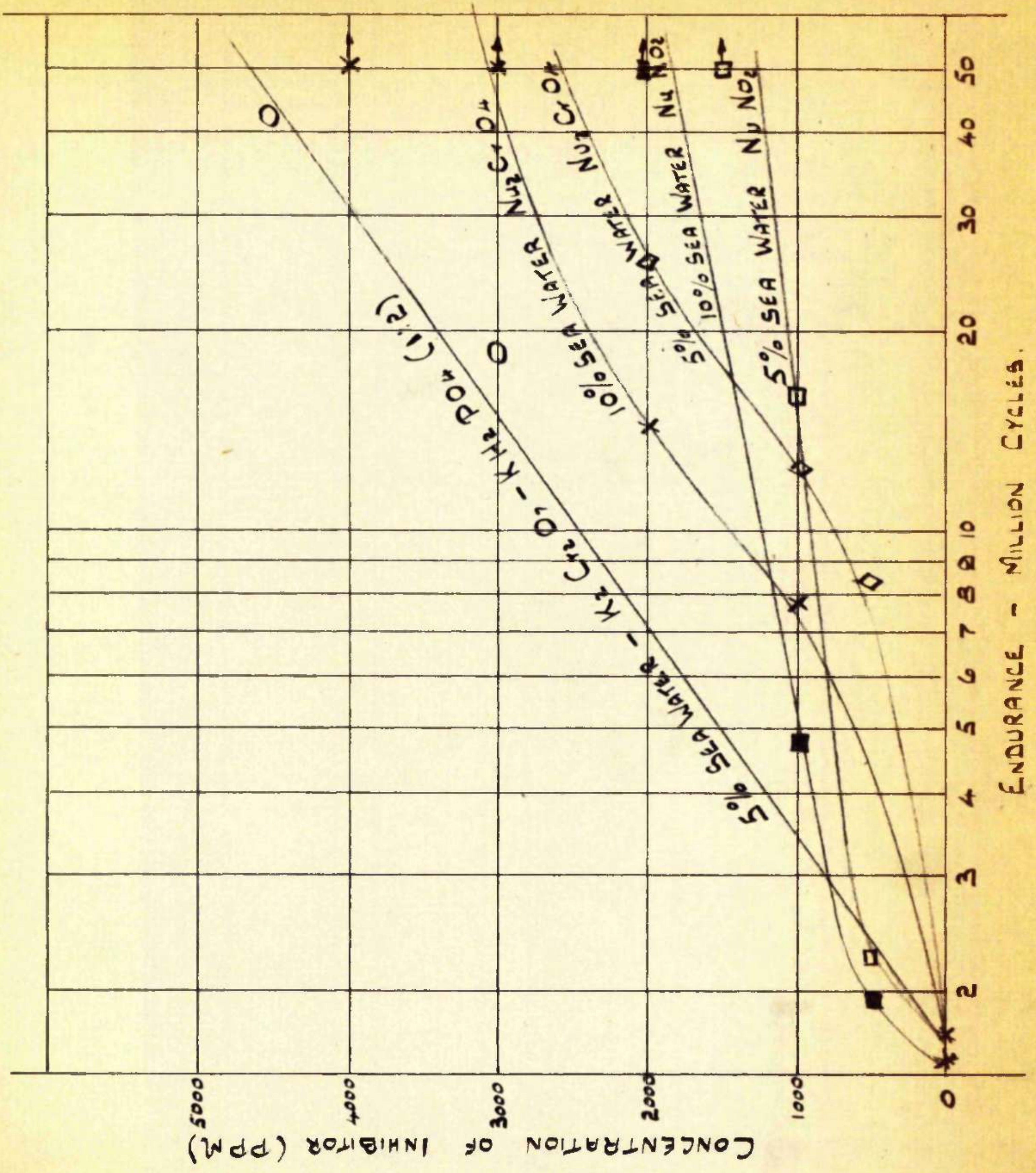
5% SEA WATER - $K_2Cr_2O_7$ - KH_2PO_4 (1:2)
10% SEA WATER Na_2CrO_4
5% SEA WATER Na_2CrO_4
10% SEA WATER $NaNO_2$
5% SEA WATER $NaNO_2$
0
1000
2000
3000
4000
5000
CONCENTRATION OF INHIBITOR (PPM)
2
3
4
5
6
7
8
9
10
20
30
40
50
ENDURANCE - MILLION CYCLES

FIG. 25

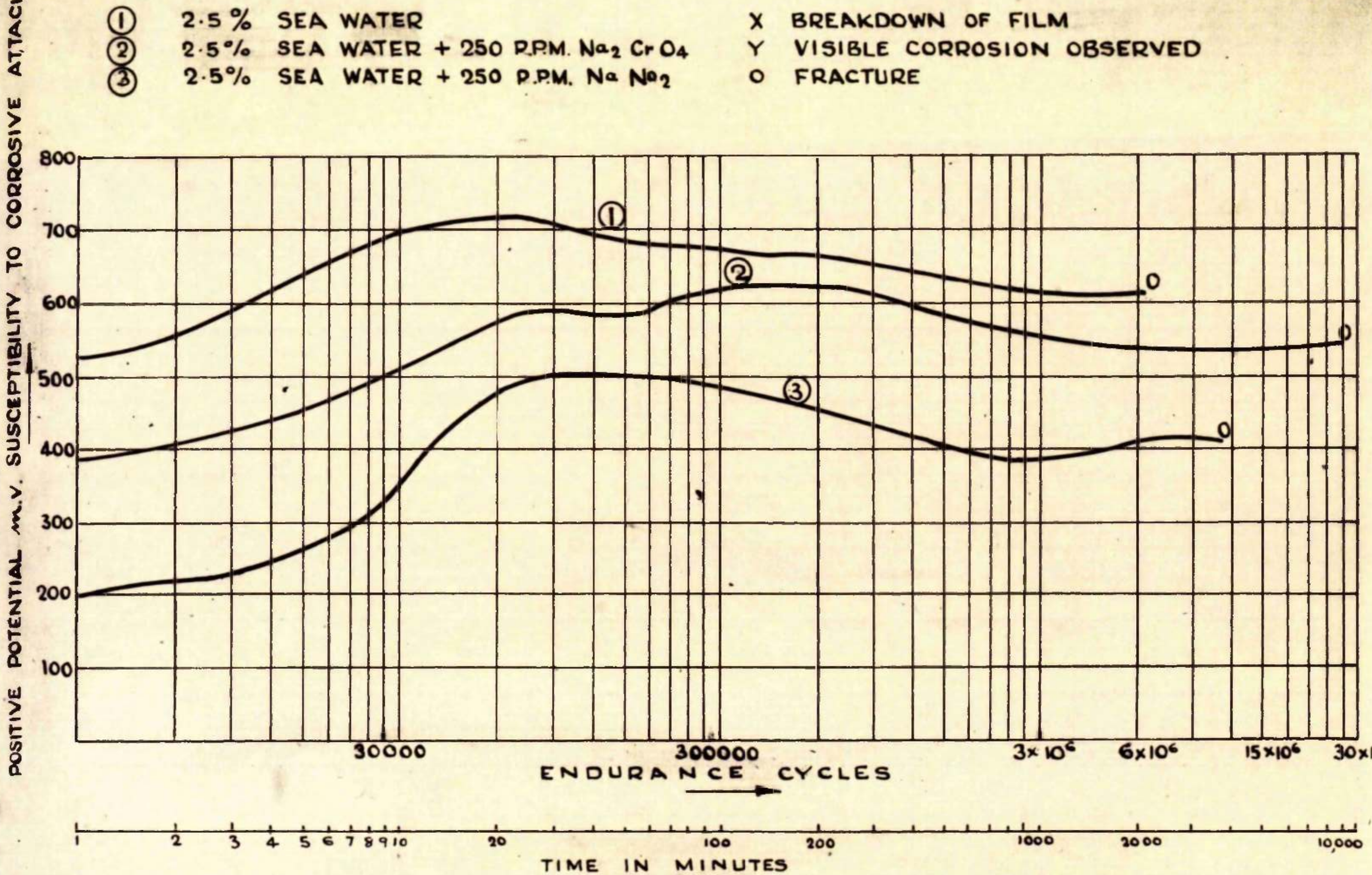

FIG. 26 ELECTRO-POTENTIAL OF SPECIMEN IN VARIOUS CORROSIVE SOLUTIONS

STRESS RANGE ± 10 TONS/IN². TEMPERATURE 88°C

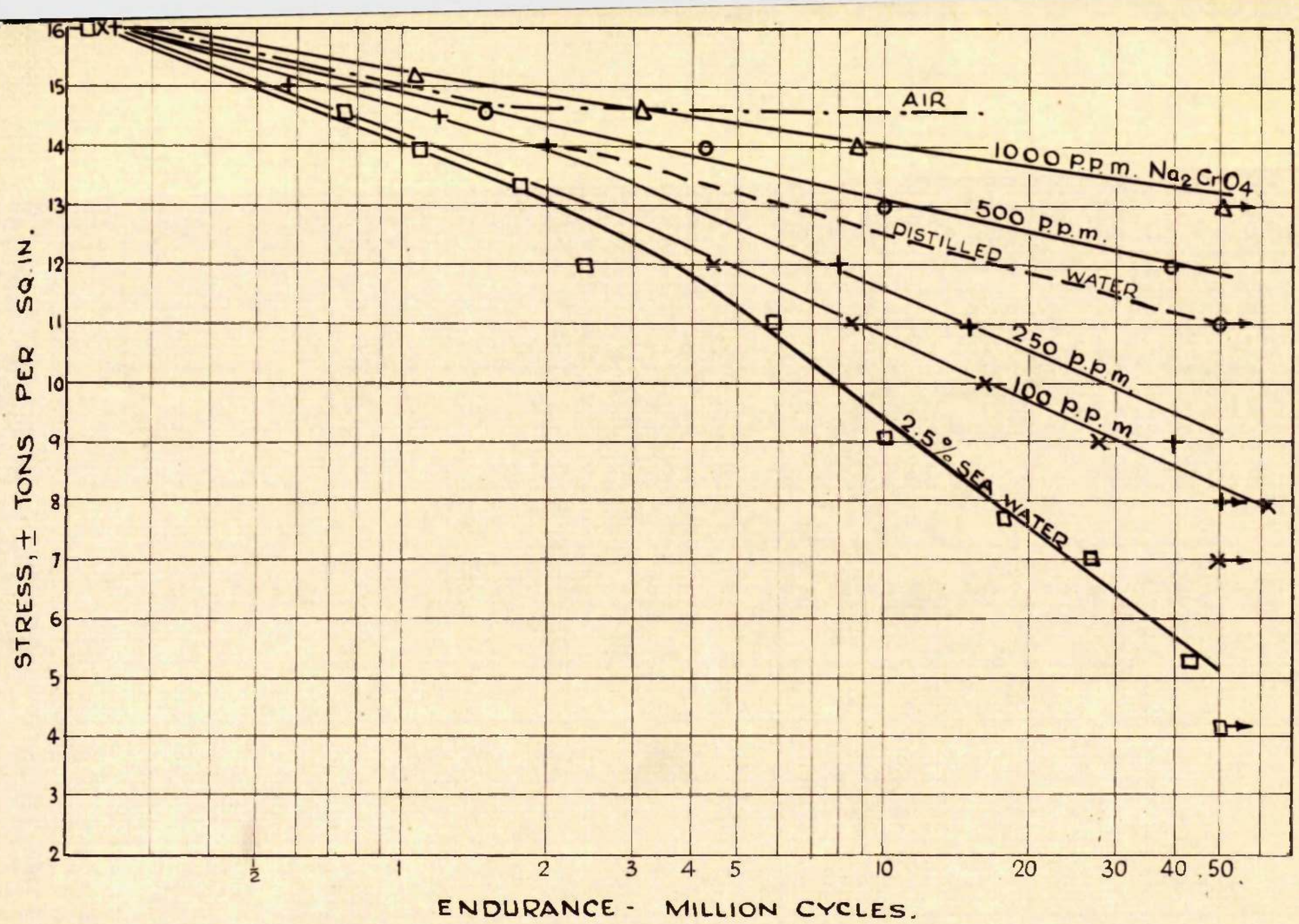

FIG 27 S - LOG N CURVES FOR SODIUM CHROMATE INHIBITORS IN 2.5% SEA WATER AT 88°C

4

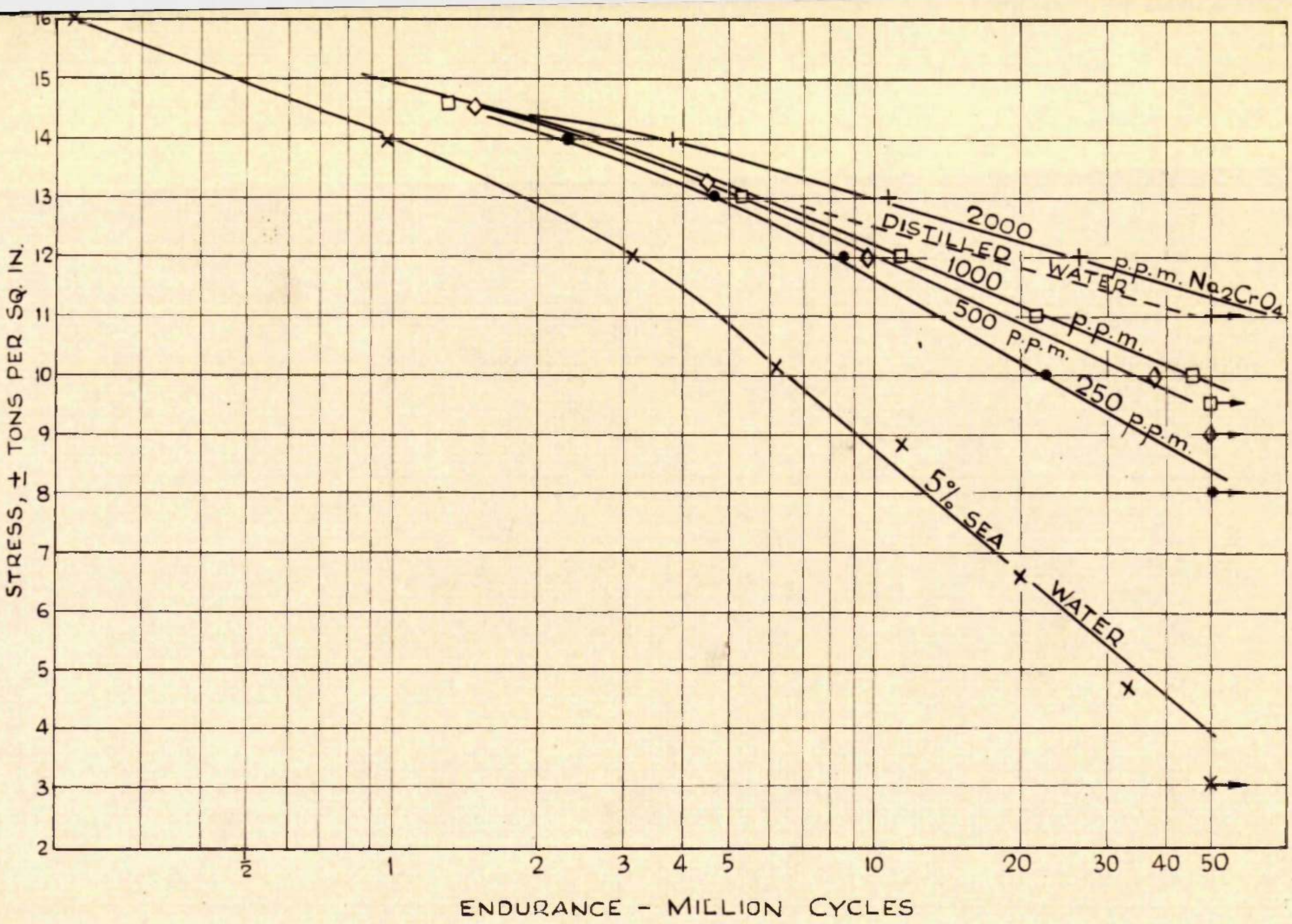

FIG 28 S - LOG N CURVES FOR SODIUM CHROMATE INHIBITOR IN 5% SEA WATER AT 88°C

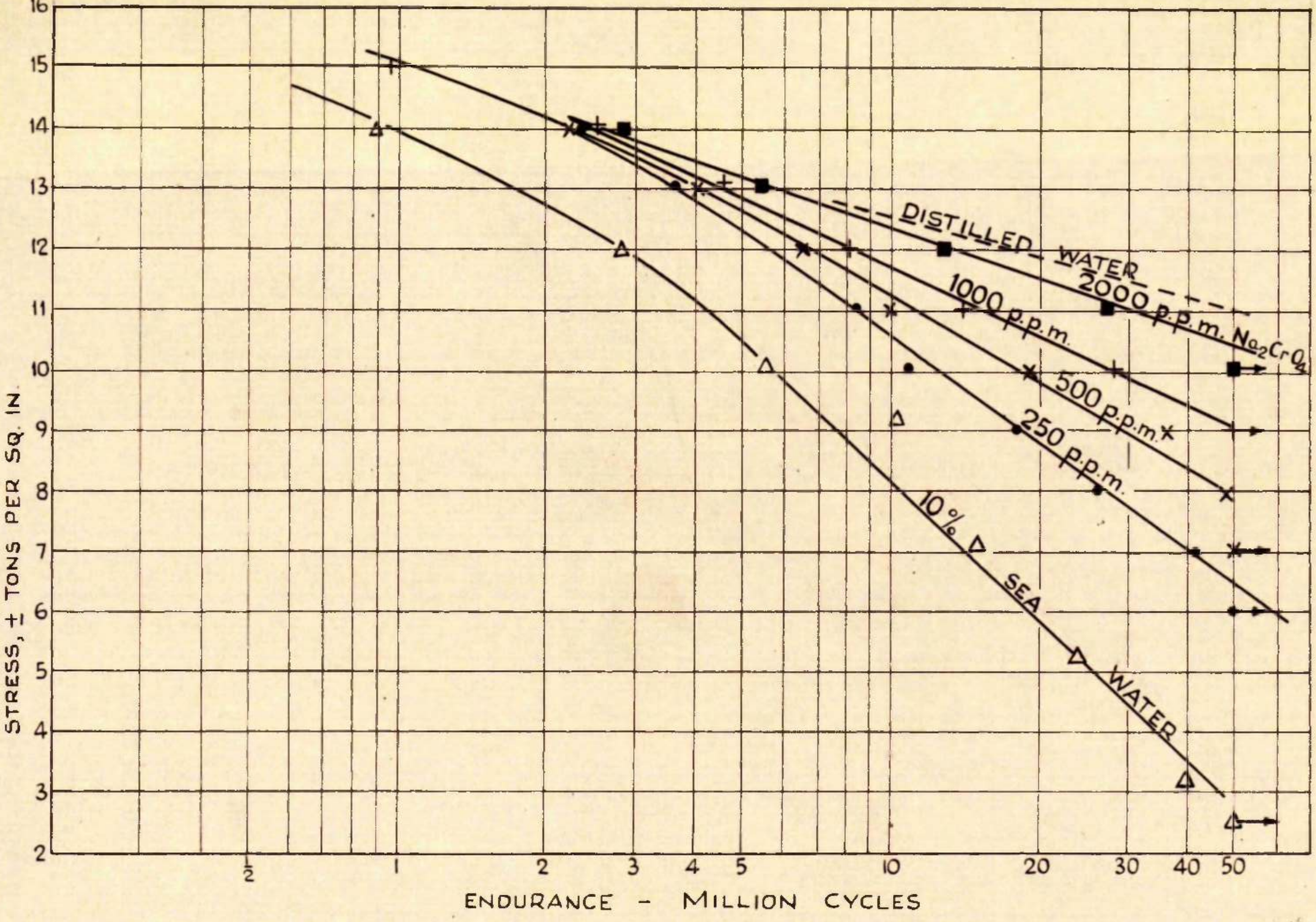

FIG 29 S - LOG N CURVES FOR SODIUM CHROMATE INHIBITOR IN 10% SEA WATER AT 88°C

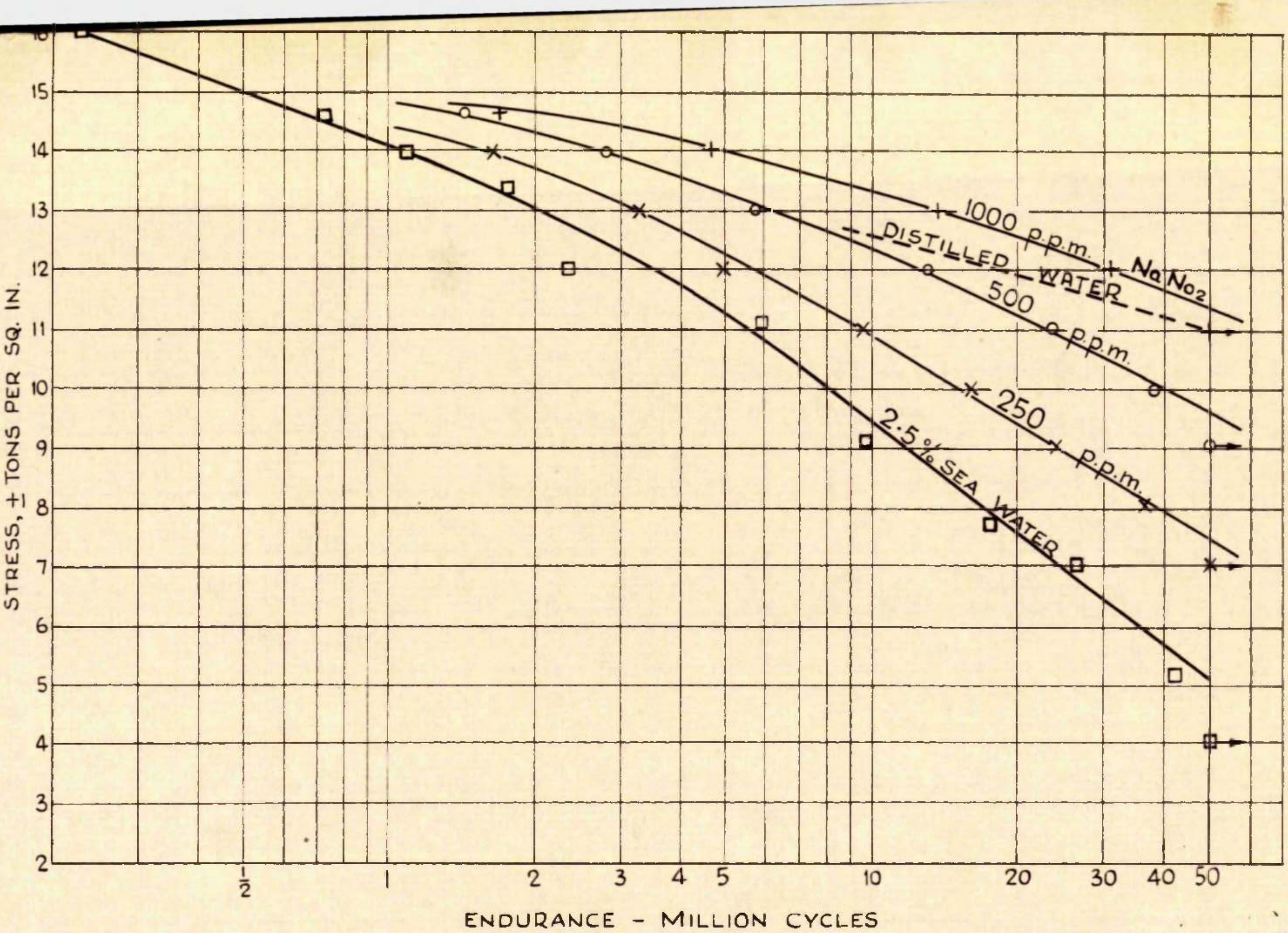

FIG 30 S - LOG N CURVES FOR SODIUM NITRITE INHIBITOR IN 2.5% SEA WATER AT 88°C

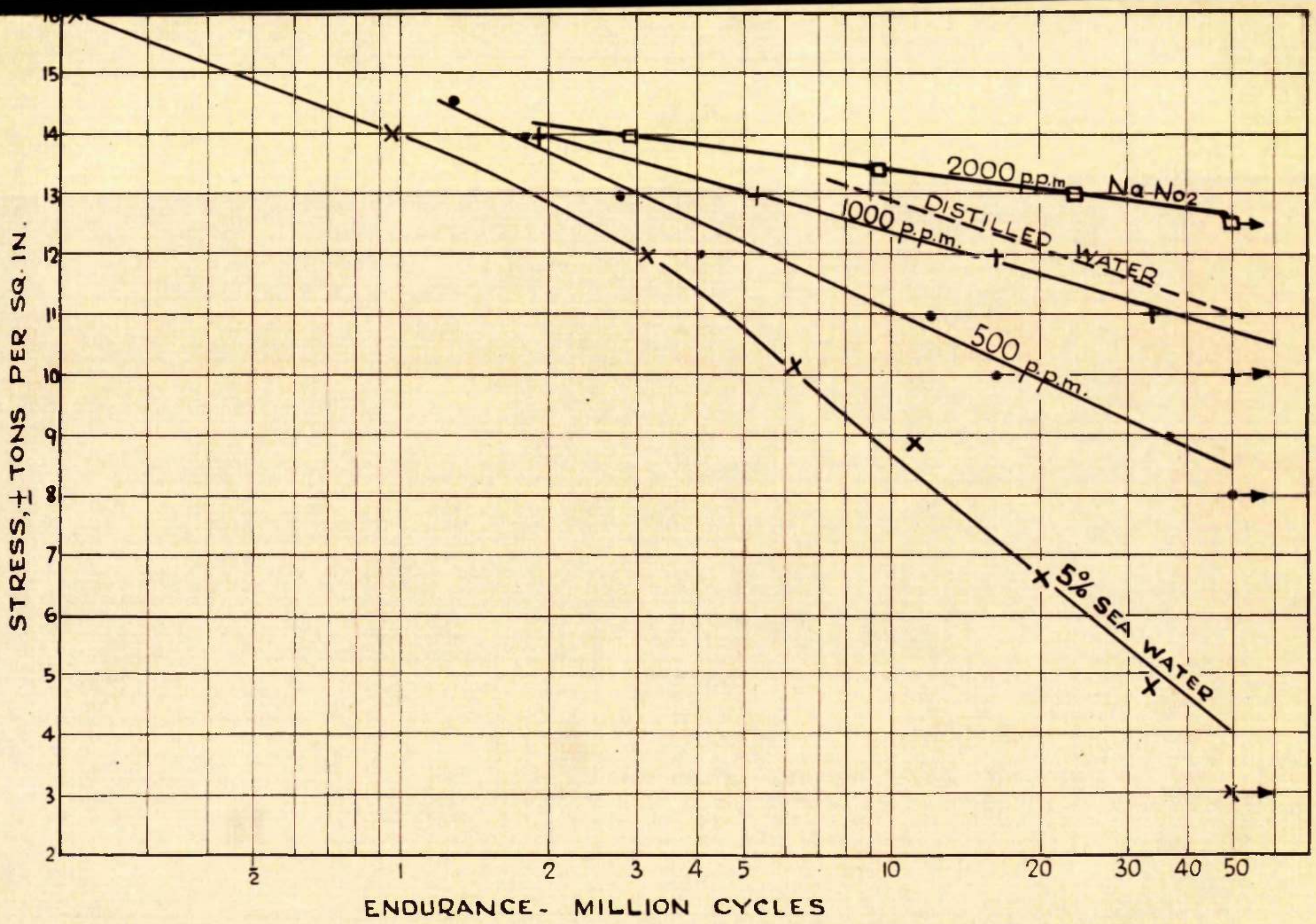

FIG 31 S - LOG N CURVES FOR SODIUM NITRITE INHIBITOR IN 5% SEA WATER AT 88°C

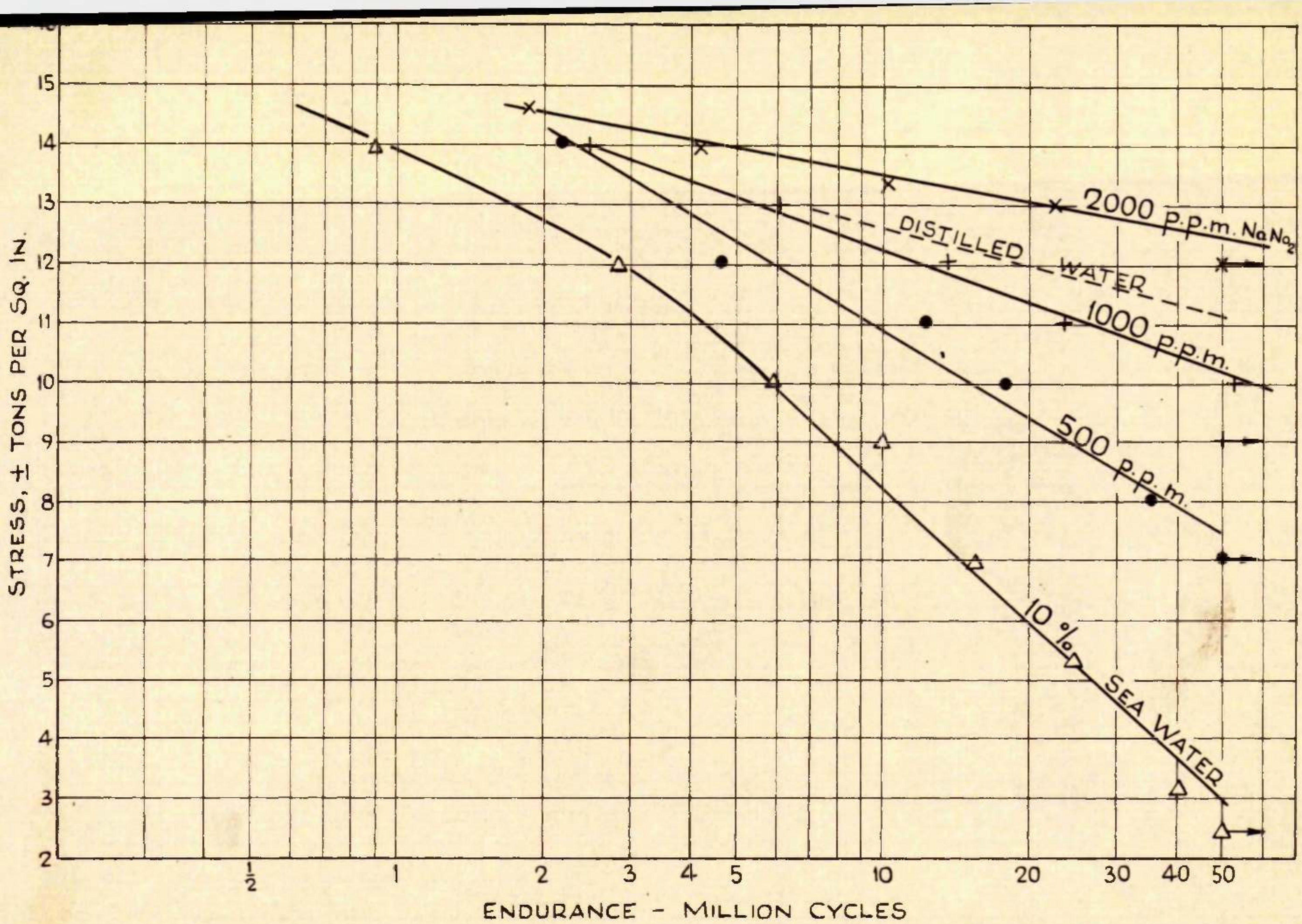

FIG 32 S - LOG N CURVES FOR SODIUM NITRITE INHIBITOR IN 10% SEA WATER AT 88°C

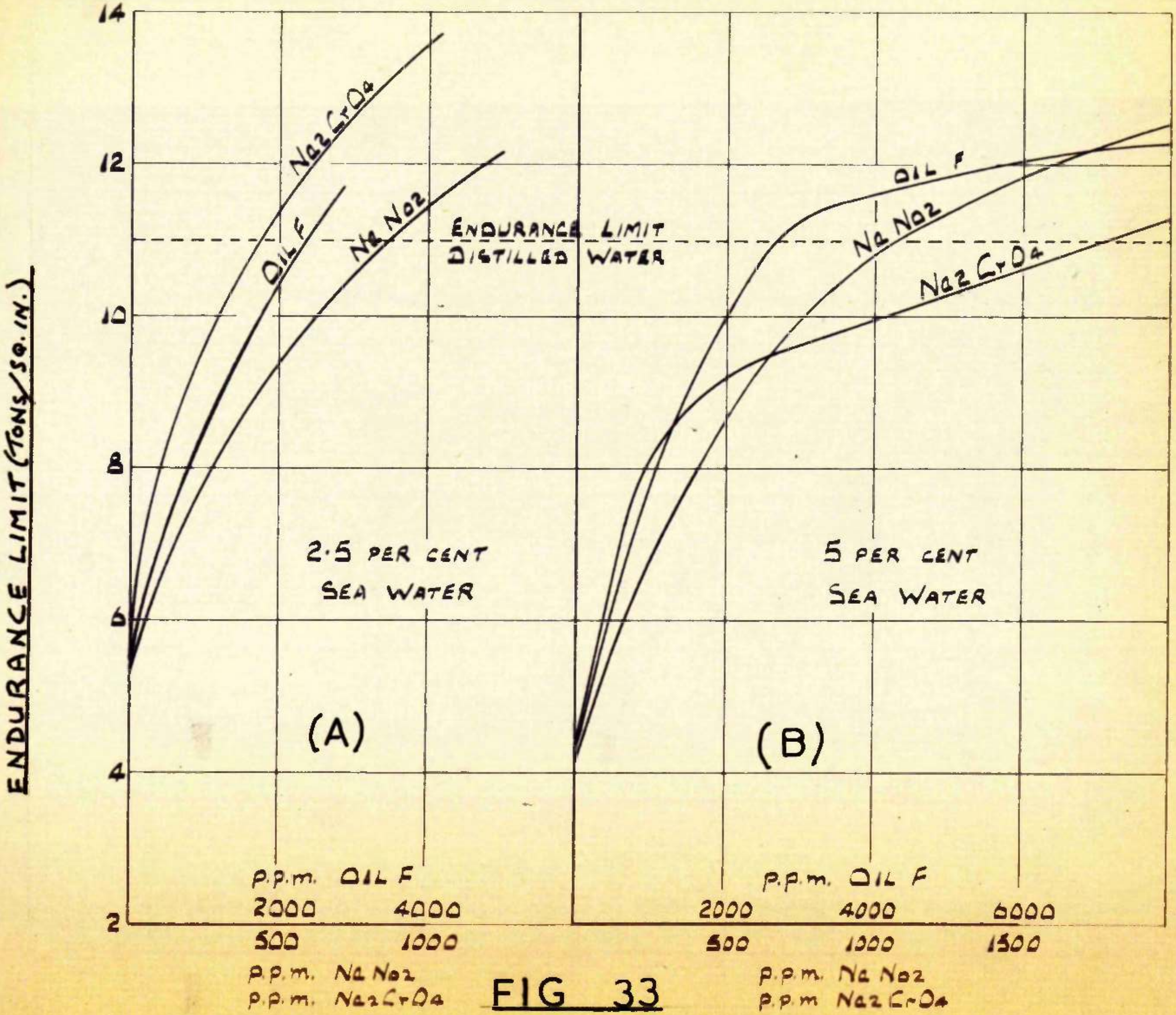
ENDURANCE LIMIT (TONS/SQ. IN.)
14
12
10
8
6
4
2
Na2 Cr O4
OIL F
Na NO2
ENDURANCE LIMIT
DISTILLED WATER
OIL F
Na NO2
Na2 Cr O4
2·5 PER CENT
SEA WATER
5 PER CENT
SEA WATER
(A)
(B)
P.P.M. OIL F
2000
4000
500
1000
P.P.M. Na No2
P.P.M. Na2 Cr O4
P.P.M. OIL F
2000
4000
6000
500
1000
1500
P.P.M. Na No2
P.P.M. Na2 Cr O4

FIG 33

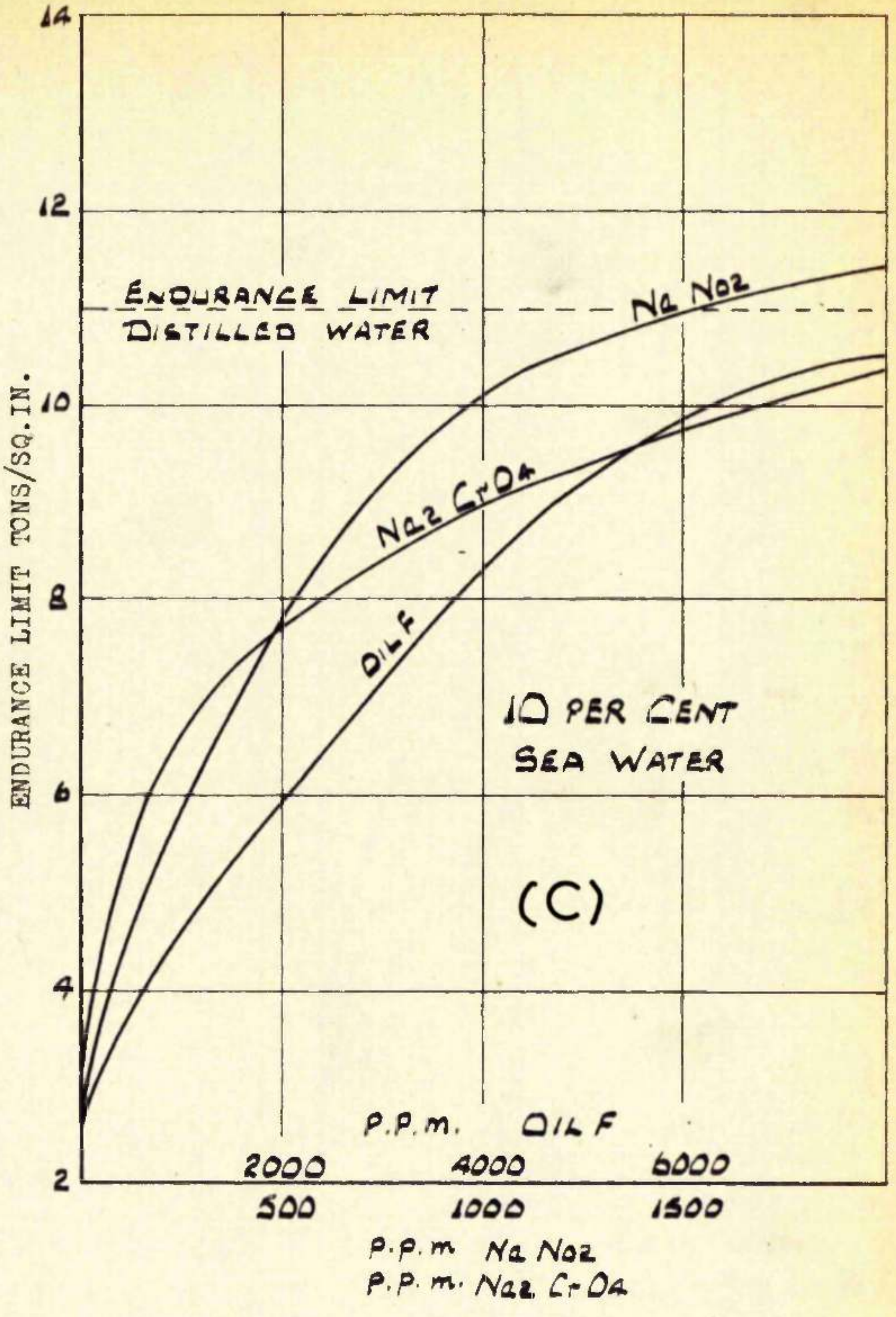
14
12
10
8
6
4
2
ENDURANCE LIMIT TONS/SQ.IN.
ENDURANCE LIMIT
DISTILLED WATER
Na NO2
Na2 Cr O4
OIL F
10 PER CENT
SEA WATER
(C)
P.P.m. OIL F
2000
4000
6000
500
1000
1500
P.P.m Na NO2
P.P.m. Na2 Cr O4

FIG 33

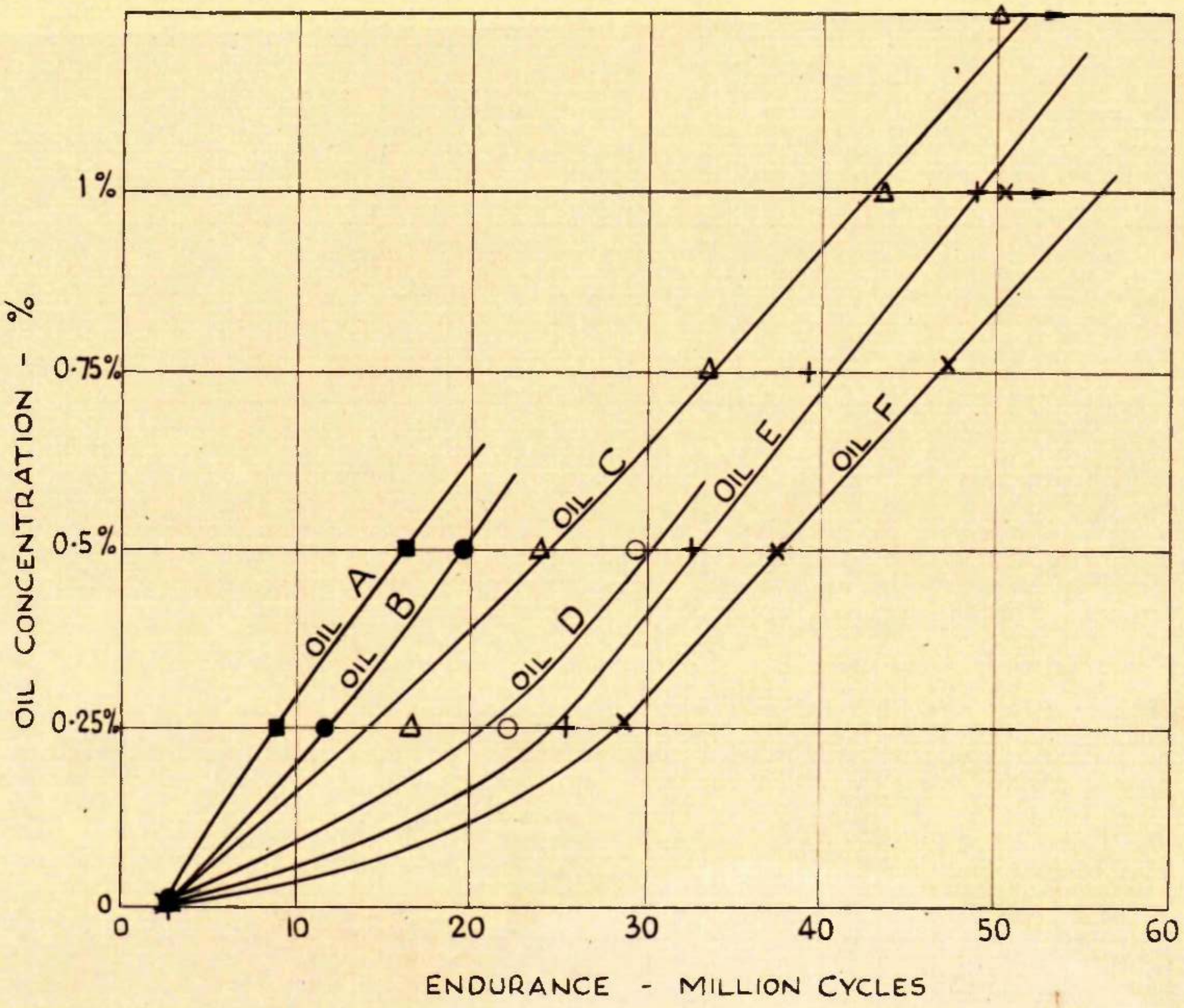
OIL CONCENTRATION - %
1%
0·75%
0·5%
0·25%
0
0
10
20
30
40
50
60
ENDURANCE - MILLION CYCLES
OIL A
OIL B
OIL C
OIL D
OIL E
OIL F

FIG. 34

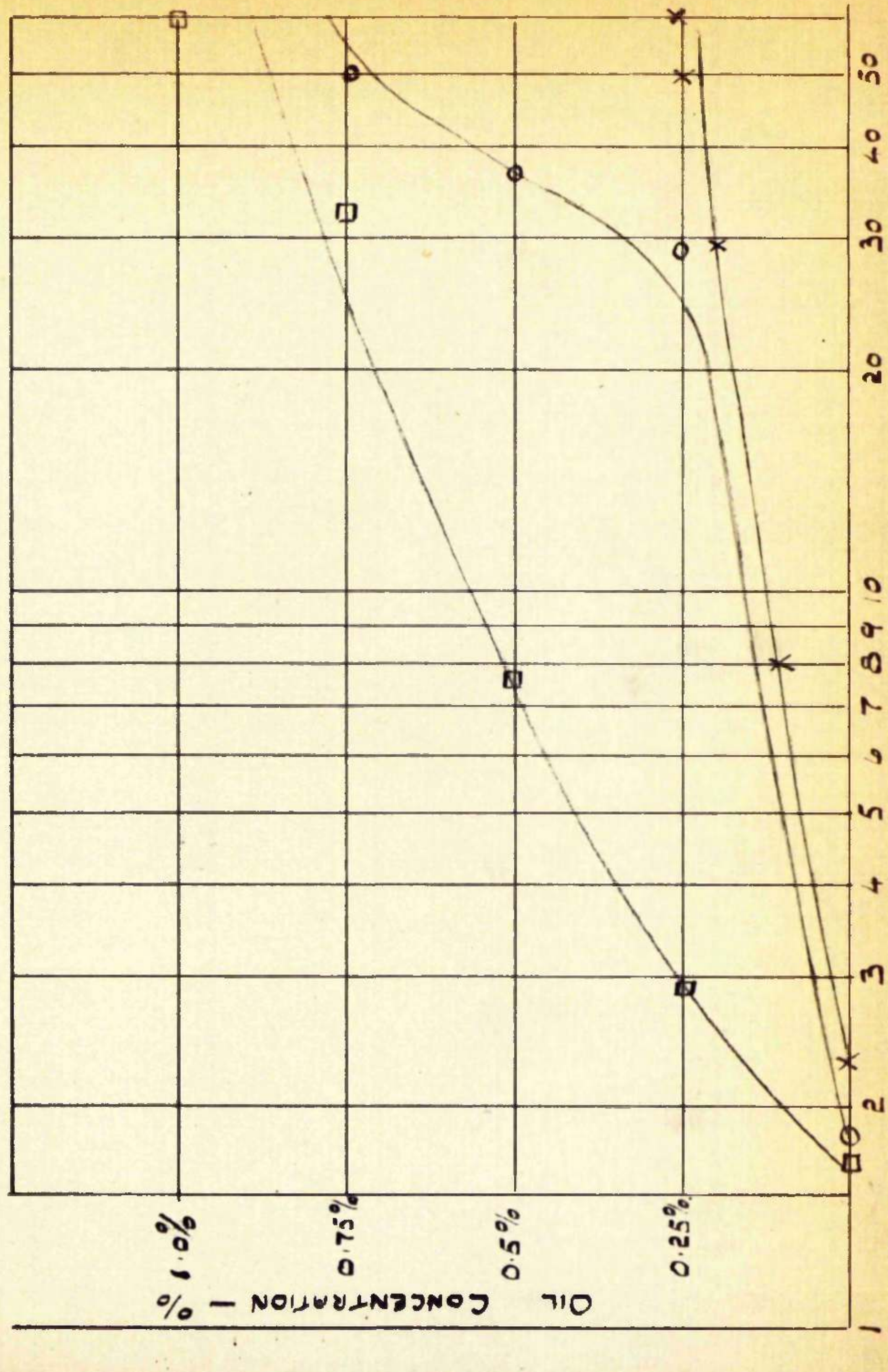
OIL CONCENTRATION - %
1.0%
0.75%
0.5%
0.25%
1
2
3
4
5
6
7
8
9
10
20
30
40
50
ENDURANCE - MILLION CYCLES

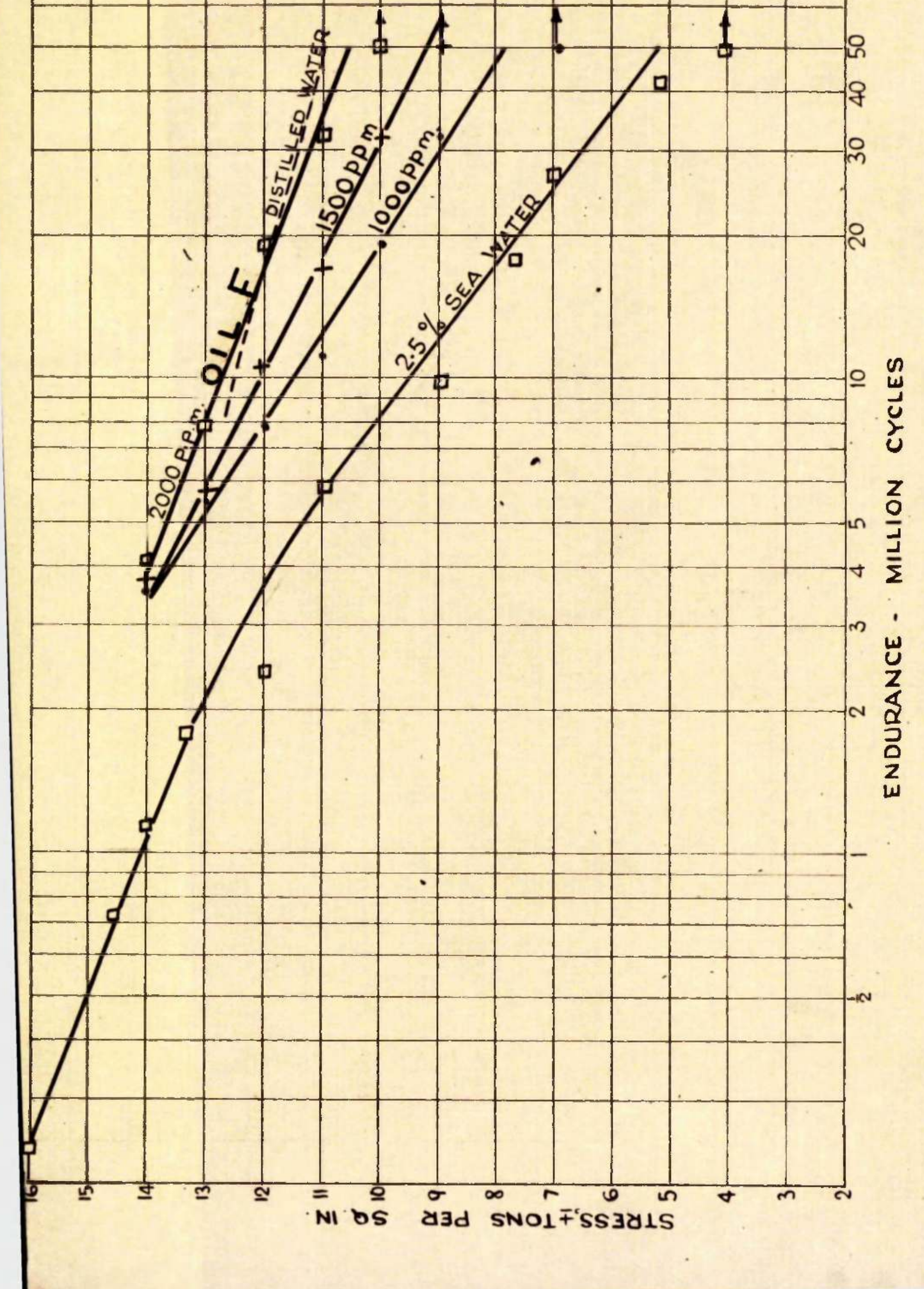

FIG. 36 S-LOG N CURVES FOR 2·5 PER CENT SEA WATER WITH VARYING OIL F ADDITIONS. TEMP. 88°C

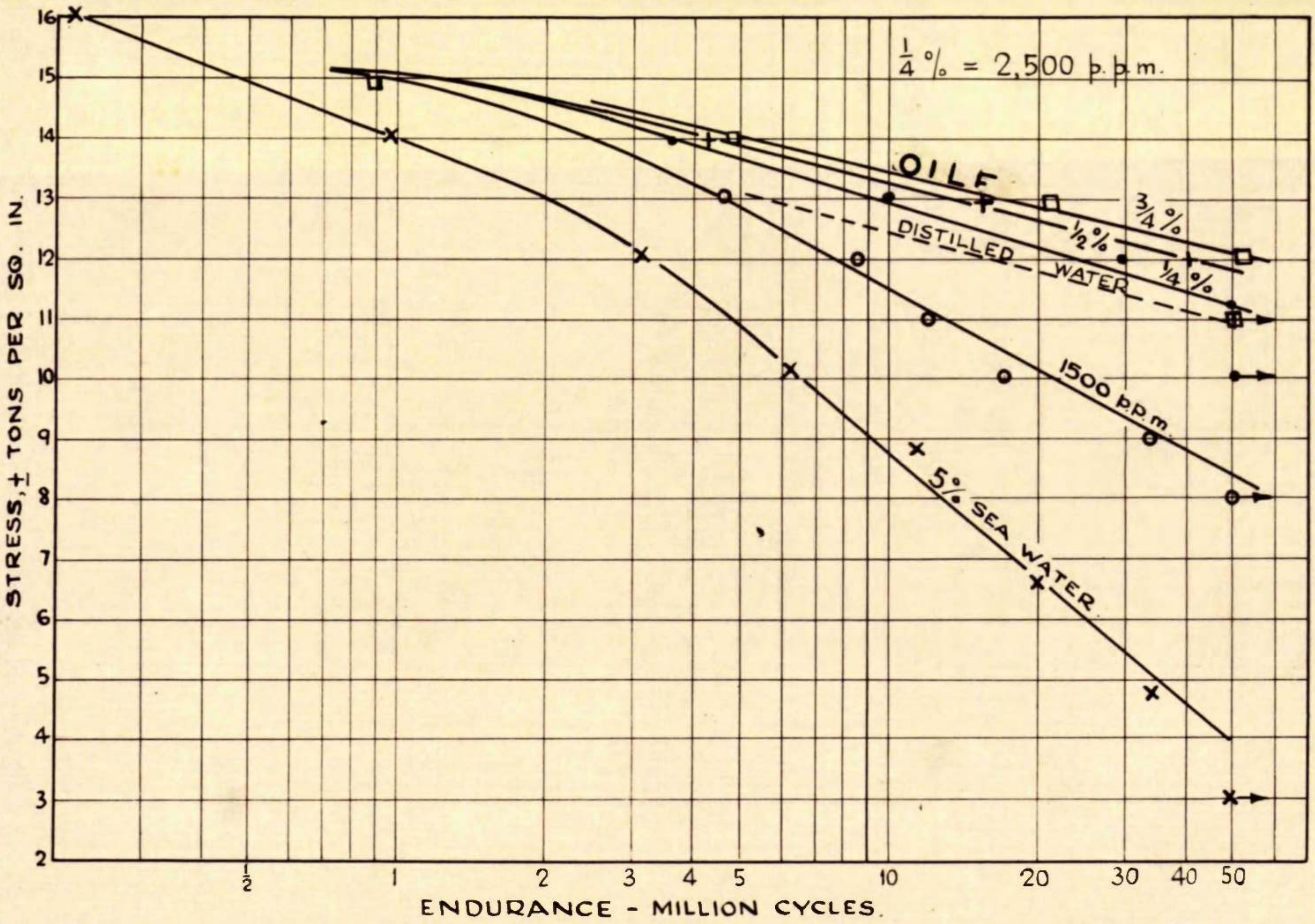

FIG. 37 S-LOG N CURVES FOR 5 PER CENT SEA WATER WITH VARYING OIL F ADDITIONS. TEMP 88°C

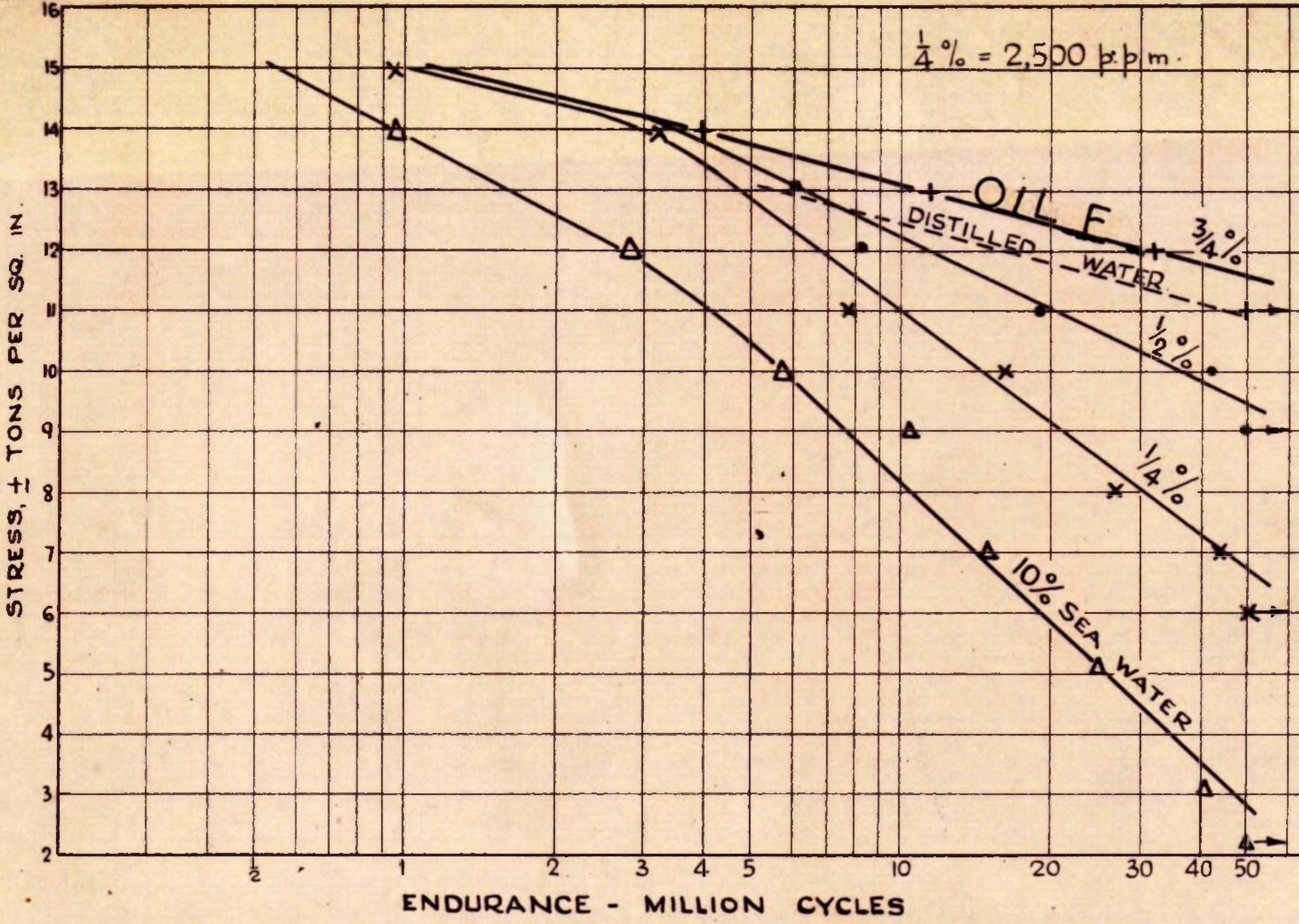

FIG. 38 S-LOG. N CURVES FOR 10 PER CENT SEA WATER WITH VARYING **OIL F** ADDITIONS. TEMP. 88°C

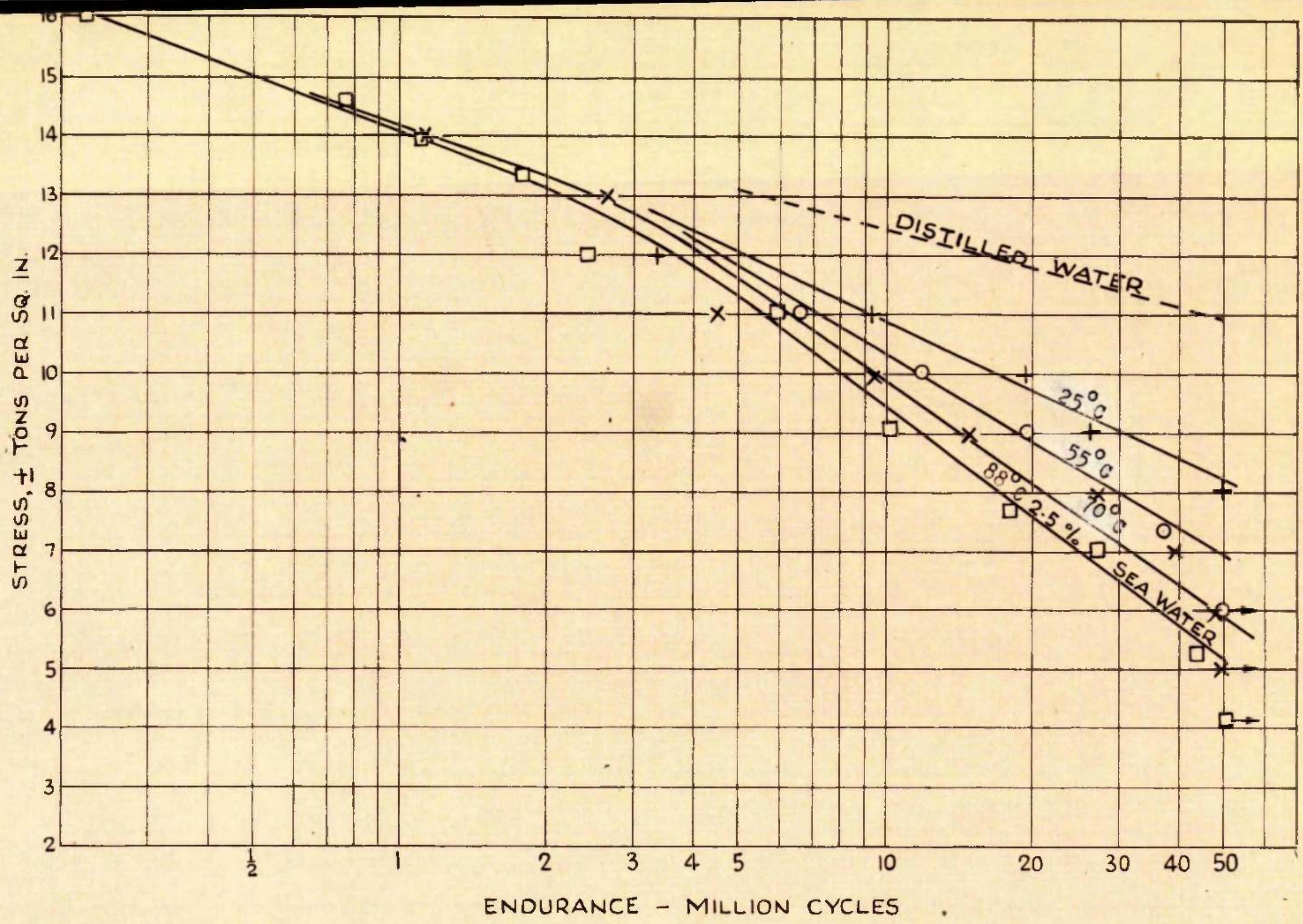

FIG. 39 EFFECT OF TEMPERATURE ON ENDURANCE IN 2·5 PER CENT SEA WATER NO INHIBITOR

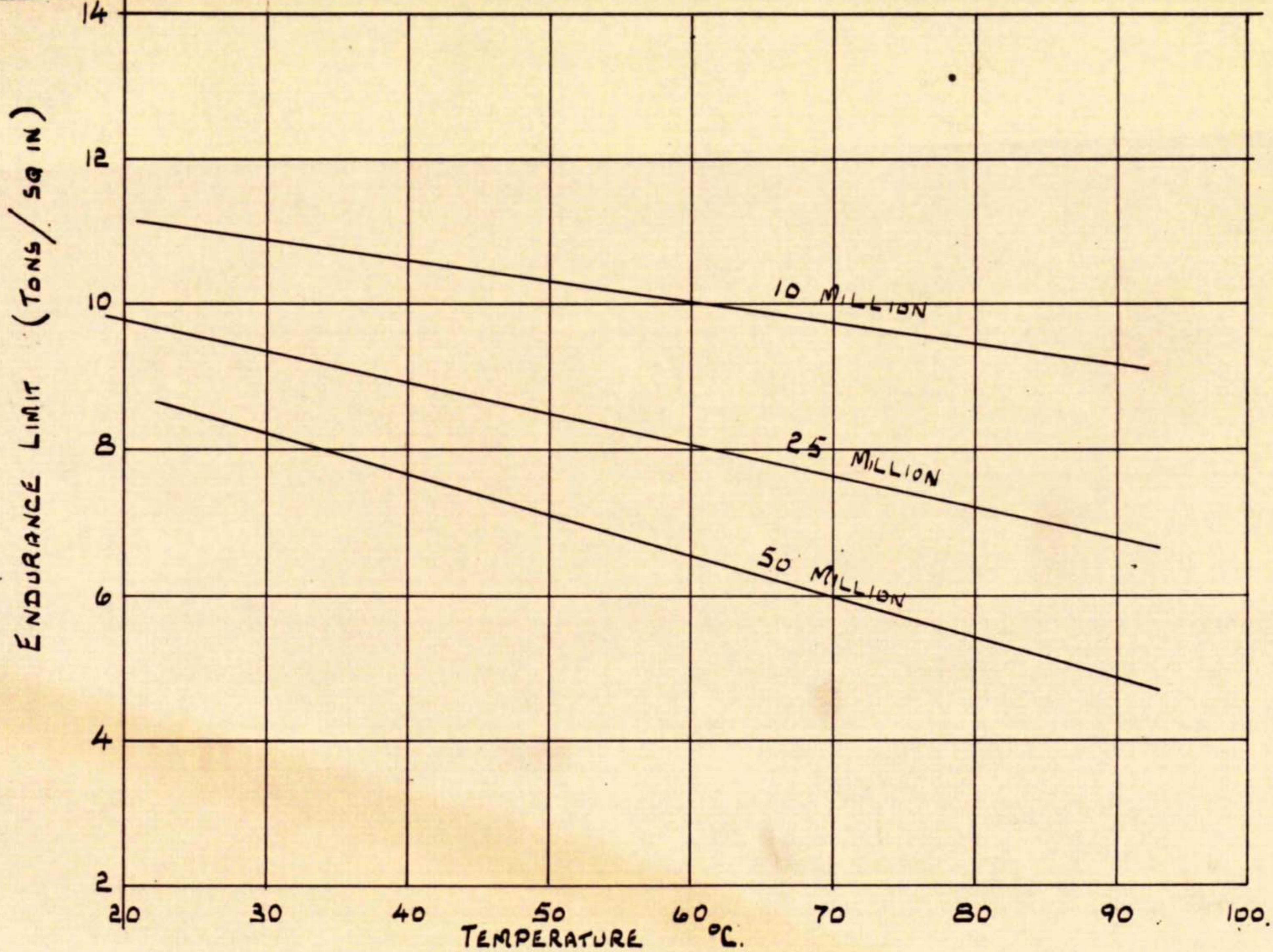
14
12
10
8
6
4
2
ENDURANCE LIMIT (TONS/ SQ IN)
20
30
40
50
60
70
80
90
100.
TEMPERATURE °C.
10 MILLION
25 MILLION
50 MILLION

FIG 40

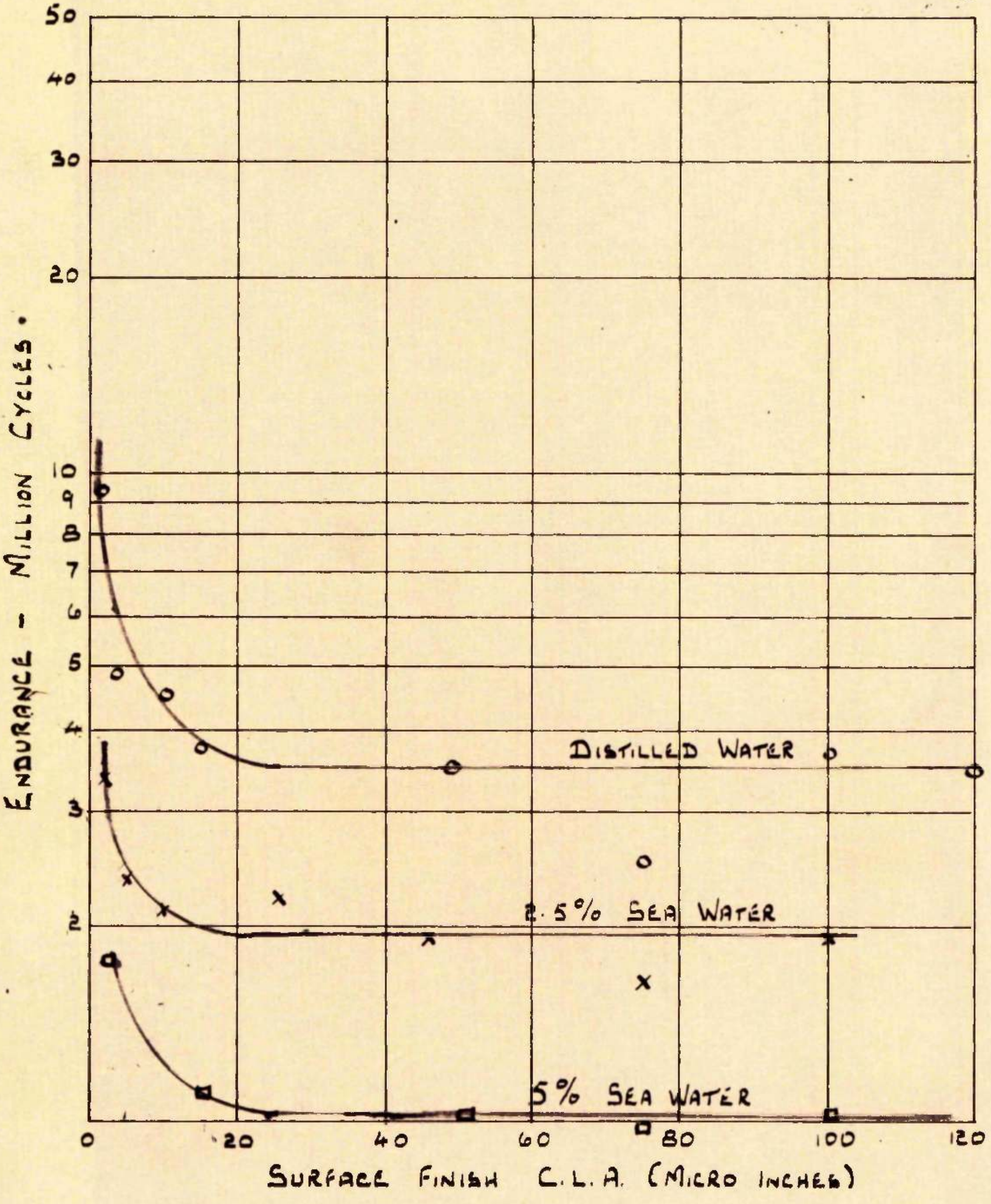
50
40
30
20
10
9
8
7
6
5
4
3
2
0
20
40
60
80
100
120
ENDURANCE - MILLION CYCLES.
SURFACE FINISH C.L.A. (MICRO INCHES)
DISTILLED WATER
2.5% SEA WATER
5% SEA WATER

FIG 41

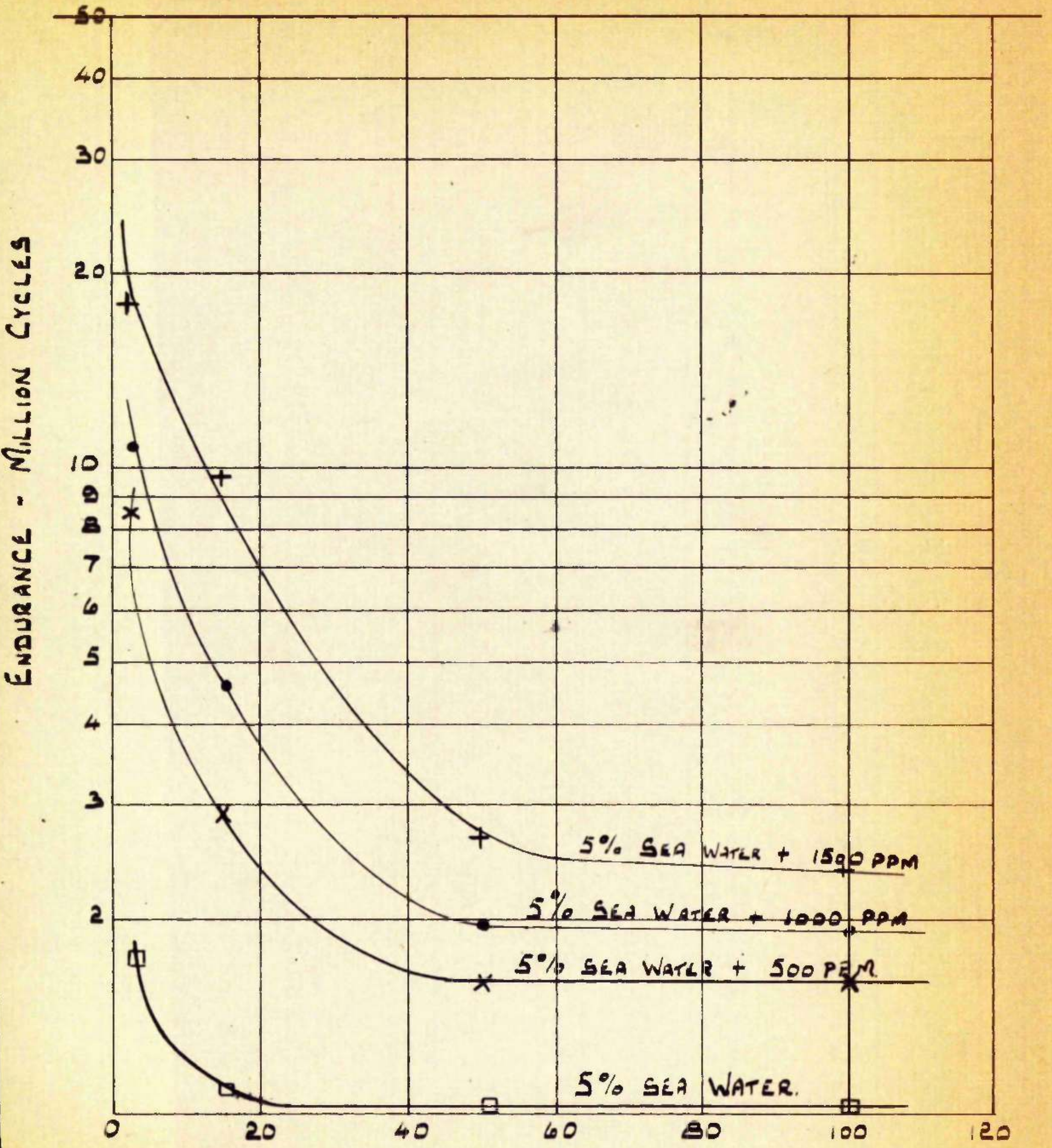
50
40
30
20
10
9
8
7
6
5
4
3
2
ENDURANCE - MILLION CYCLES
0
20
40
60
80
100
120
5% SEA WATER + 1500 PPM
5% SEA WATER + 1000 PPM
5% SEA WATER + 500 PPM.
5% SEA WATER.
SURFACE FINISH C.L.A. (MICRO INCHES)

FIG 42

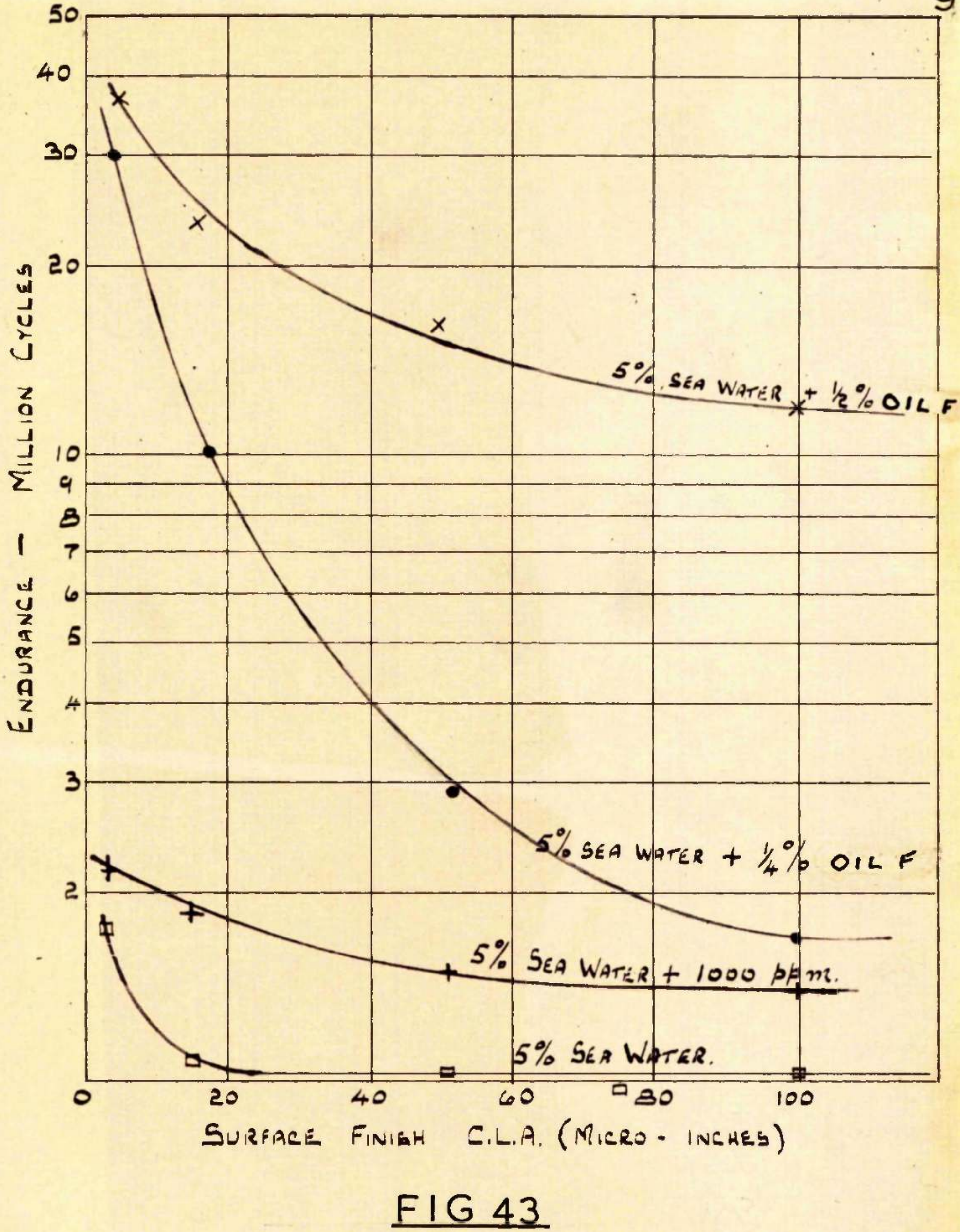
50
40
30
20
10
9
8
7
6
5
4
3
2
0
20
40
60
80
100
ENDURANCE - MILLION CYCLES
SURFACE FINISH C.L.A. (MICRO - INCHES)
5% SEA WATER + ½% OIL F
5% SEA WATER + ¼% OIL F
5% SEA WATER + 1000 p.p.m.
5% SEA WATER.

FIG 43

CHAPTER FIVE

DISCUSSION OF EXPERIMENTAL RESULTS

The results presented in the last chapter may conveniently be considered under the following four headings:-

1. Effect of chloride concentration
2. Effect of Inhibitors
3. Effect of Temperature
4. Effect of Surface Finish.

1. Effect of Chloride Concentration

Fig. 22 shows the main effects of varying the chloride concentration of the corrosive environment at 88°C. It will be noted that even in distilled water the safe limit obtained in air, no longer exists, and is replaced by an endurance limit, which lies substantially below the former. Thus, after 50 million reversals of stress, the endurance limit in distilled water is only 11 tons per square inch compared with a fatigue limit of 14.6 tons per square inch obtained in air. The effect of the presence of varying amounts of seawater is to cause further significant decreases in the endurance limit; even small additions of sea water have a very pronounced effect./

effect. Thus an addition of only 0.1 per cent of synthetic sea water (equivalent to 0.005 per cent chlorides) lowers the endurance limit (at 50 million cycles) to 7.9 tons per square inch. This rapid fall in the endurance limit, with increasing chloride concentrations up to 10 per cent sea water is shown in Fig. 23. It will be seen that the decrease in the endurance limit is rapid up to about 0.25 per cent sea water, further additions causing a much more gradual but continuing decrease. The endurance limit after 50 million cycles of stress at 88°C in 10 per cent sea water is 2.9 tons per square inch and it would appear that lower endurance limits would be obtained at higher chloride concentrations.

This lowering of the endurance limit when chlorides are present was also observed by Speller, McCorkle and Mumma (47) who carried out tests on a 0.35 per cent carbon steel. Fig. 44 shows that a comparison between results obtained in the present work, with those obtained by Speller, McCorkle and Mumma. Although their fatigue limit (in air) for the 0.35 per cent carbon steel was 15.1 tons per square inch compared with 14.6 tons per square inch for the present series, the endurance limits (at 10 million cycles) for similar chloride concentrations, were 11.7 and 10.6 respectively. This difference can be partly accounted for by the difference in temperature between/

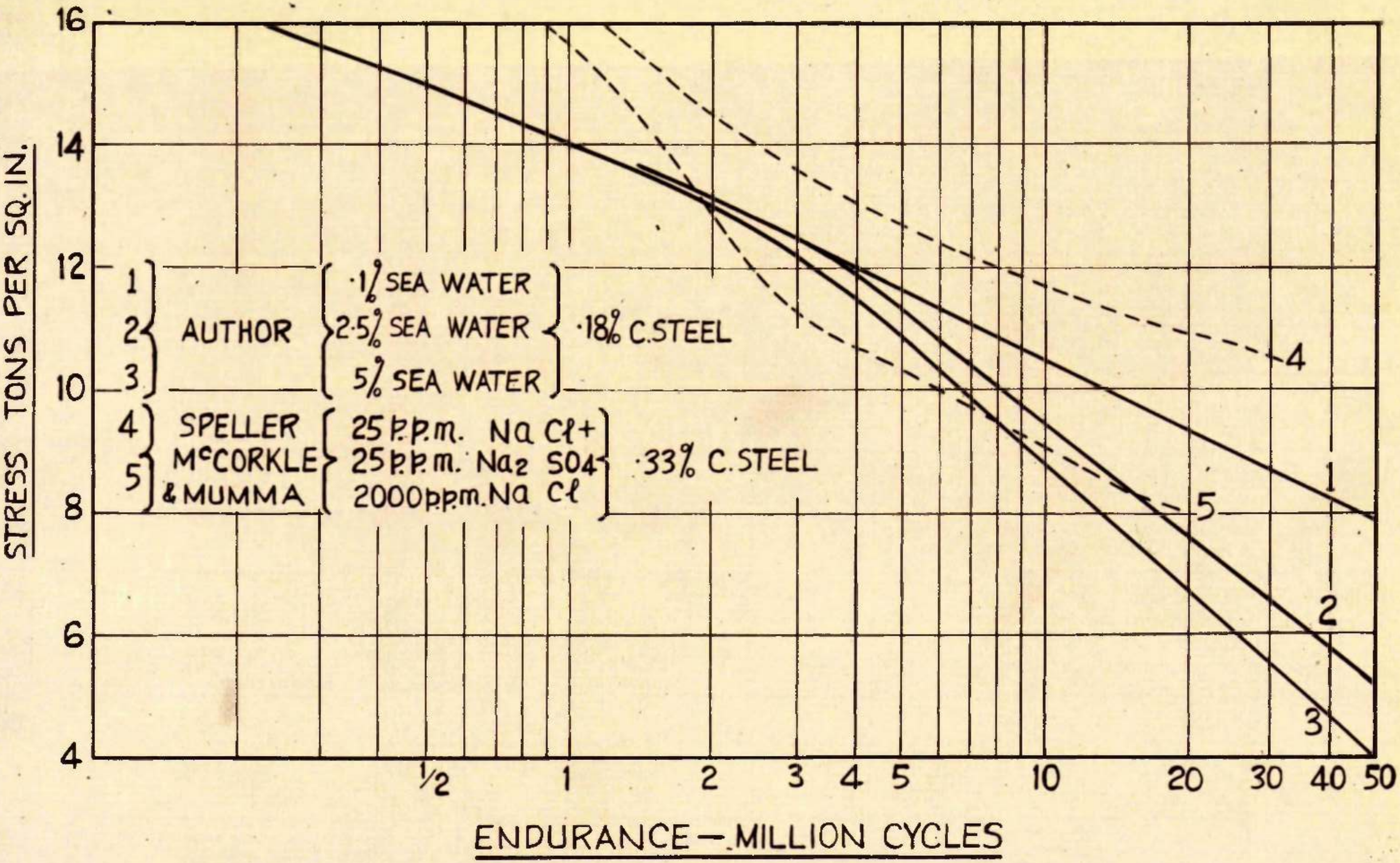
STRESS TONS PER SQ. IN.
16
14
12
10
8
6
4
ENDURANCE — MILLION CYCLES
½
1
2
3
4
5
10
20
30
40
50
1
2
3
4
5
AUTHOR
·1% SEA WATER
2·5% SEA WATER
5% SEA WATER
·18% C.STEEL
SPELLER McCORKLE & MUMMA
25 p.p.m. Na Cl +
25 p.p.m. Na_2SO_4
2000 p.p.m. Na Cl
·33% C. STEEL

FIG 44

between the two sets of results. Speller, McCorkle and Mumma (47) worked at room temperature which would increase the endurance. The only work done at temperatures similarly to those used in the present work was by Lehmann (55) who carried out corrosion-fatigue tests on a normalised 0.33 per cent carbon steel at 96°C. He found that the fatigue limit of 18.3 tons per square inch was reduced to an endurance limit (at 10 million cycles) of 16.9 tons per square inch with a distilled water environment, but a solution of three parts water and one part sodium chloride gave an endurance limit of 18.4 tons per square inch. This peculiar effect could be due to the fact that the high chloride concentration means that the oxygen concentration of the solution would be very low, and furthermore the solution was used in an enclosed vessel out of contact with the atmosphere. This effect of a fall in oxygen concentration had been noted by Uhlig (56).

Binnie (57) showed that when carrying out corrosion-fatigue tests by dripping a sodium chloride solution through a hydrogen atmosphere, a considerable improvement in the endurance limit was observed, when compared with the tests carried out in the air. Binnie concluded that the improvement was due to the absence of dissolved oxygen. The lowering of the/

the endurance limit by distilled water could therefore be attributed to the oxygen dissolved in the water. This oxygen was absorbed by the water as it dropped through the air space in the reservoir. This would then cause the occurrence of the corrosion reaction specified below.

At anodic areas $\mathrm{Fe} \rightarrow \mathrm{Fe}^{++} + 2e^{-}$ ....(1)

$\mathrm{Fe}^{++} \rightarrow \mathrm{Fe}^{+++} + e^{-}$ ....(2)

At cathodic areas $\mathrm{H}^{+} + e^{-} \rightarrow \frac{1}{2}\mathrm{H}_2$ ....(3)

(in acid solutions)

$\frac{1}{2}\mathrm{O}_2 + \mathrm{H}_2\mathrm{O} + 2e^{-} \rightarrow 2\,(\mathrm{OH}^{-})$ ....(4)

(In Alkaline solutions)

Reaction (3) is very slow in neutral or alkaline solutions and accounts for only a small proportion of the observed corrosion, most of the corrosion being due to the oxygen consuming reaction (4). Both oxygen and the aqueous media are necessary for these reactions to take place, the former providing the means of oxidation and the latter a medium for the conduction of electrons outwith the metal, between the anodes and cathodes. Fig. 45 is a schematic representation of the corrosion of mild steel in distilled water. The metal is normally covered with an oxide film, but the ability of this film to protect the metal from corrosion will depend on the nature of the medium on contact with the metal and the film.

In/

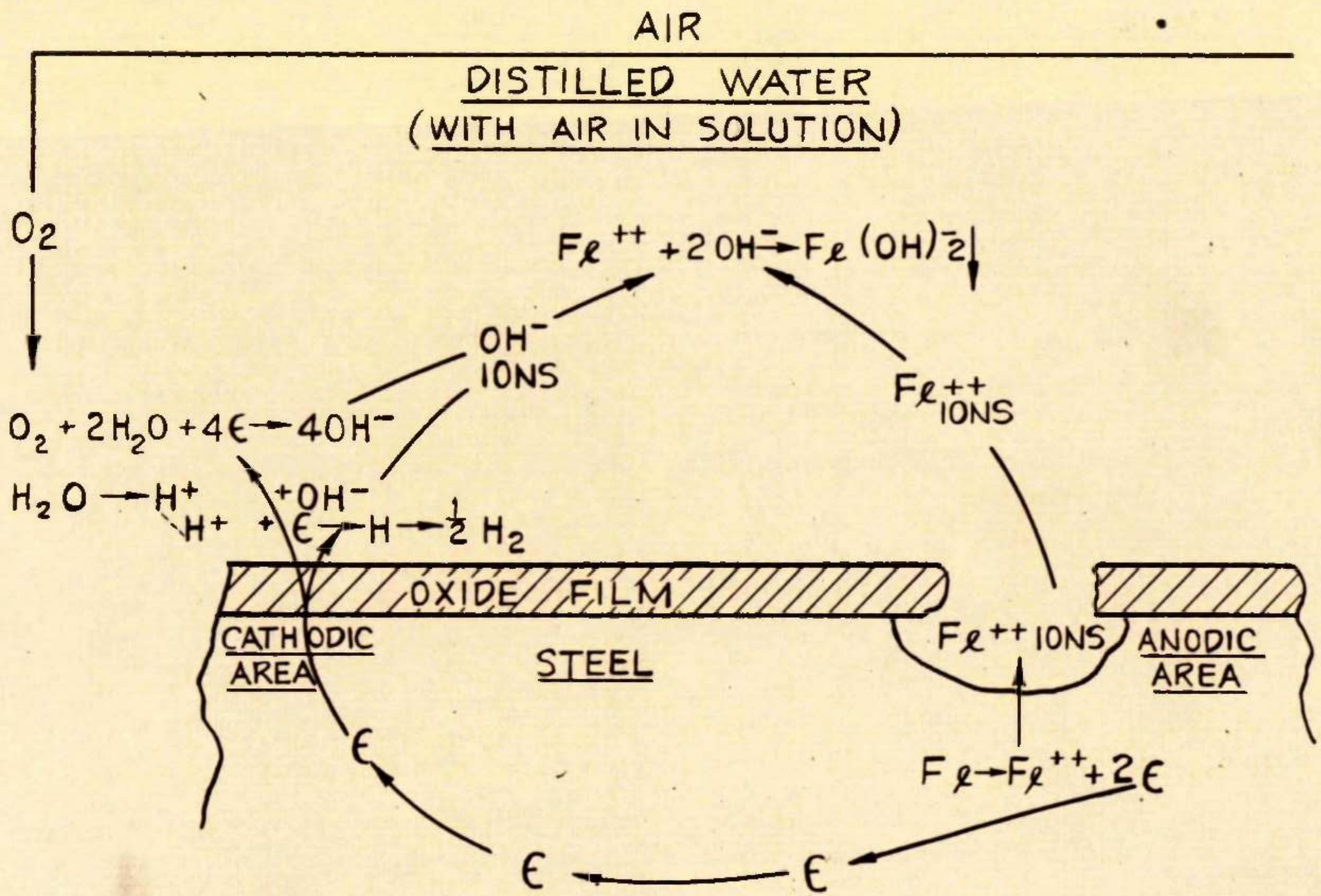
AIR
DISTILLED WATER
(WITH AIR IN SOLUTION)
O2
Fe++ + 2OH− → Fe(OH)2
OH− IONS
Fe++ IONS
O2 + 2H2O + 4ε → 4OH−
H2O → H+ + OH−
H+ + ε → H → ½ H2
OXIDE FILM
CATHODIC AREA
STEEL
Fe++ IONS
ANODIC AREA
Fe → Fe++ + 2ε
ε
ε
ε

FIG 45

In the case of steel, this film generally affords little protection, and although it may be impervious to molecular oxygen, it is usually incapable of preventing access of ions to the metal. These ions react to form salts, which may or may not stifle further corrosion depending on the prevailing conditions.

In Fig. 45 hydrogen ions come mainly from the dissociation of water, which also provides one of the sources of hydroxyl ions. These hydrogen ions take up electrons at the cathodic areas, forming atomic hydrogen, which polarises the cathode. The cathode is depolarised either by oxygen combining with the atomic hydrogen to give water for example

$$4H + O_2 \longrightarrow 2H_2O \ldots\ldots\ldots\ldots\ldots (5)$$

or by the formation of molecular hydrogen. Hydroxyl ions which combine with the ferrous ions, come from two sources, the dissociation of water or from the following reaction:-

$$2H_2O + 4e^- + O_2 \longrightarrow 4(OH)^- \ldots\ldots (6)$$

These hydroxyl ions also oxidise the ferrous hydroxide to ferric hydroxide at the anodic areas as follows:-

$$Fe(OH)_2 + (OH)^- \longrightarrow Fe(OH)_3 + e^- \ldots\ldots (7)$$

Fig. 46 is a schematic representation of the corrosive attack/

OXYGEN FREE ATMOSPHERE
DISTILLED WATER

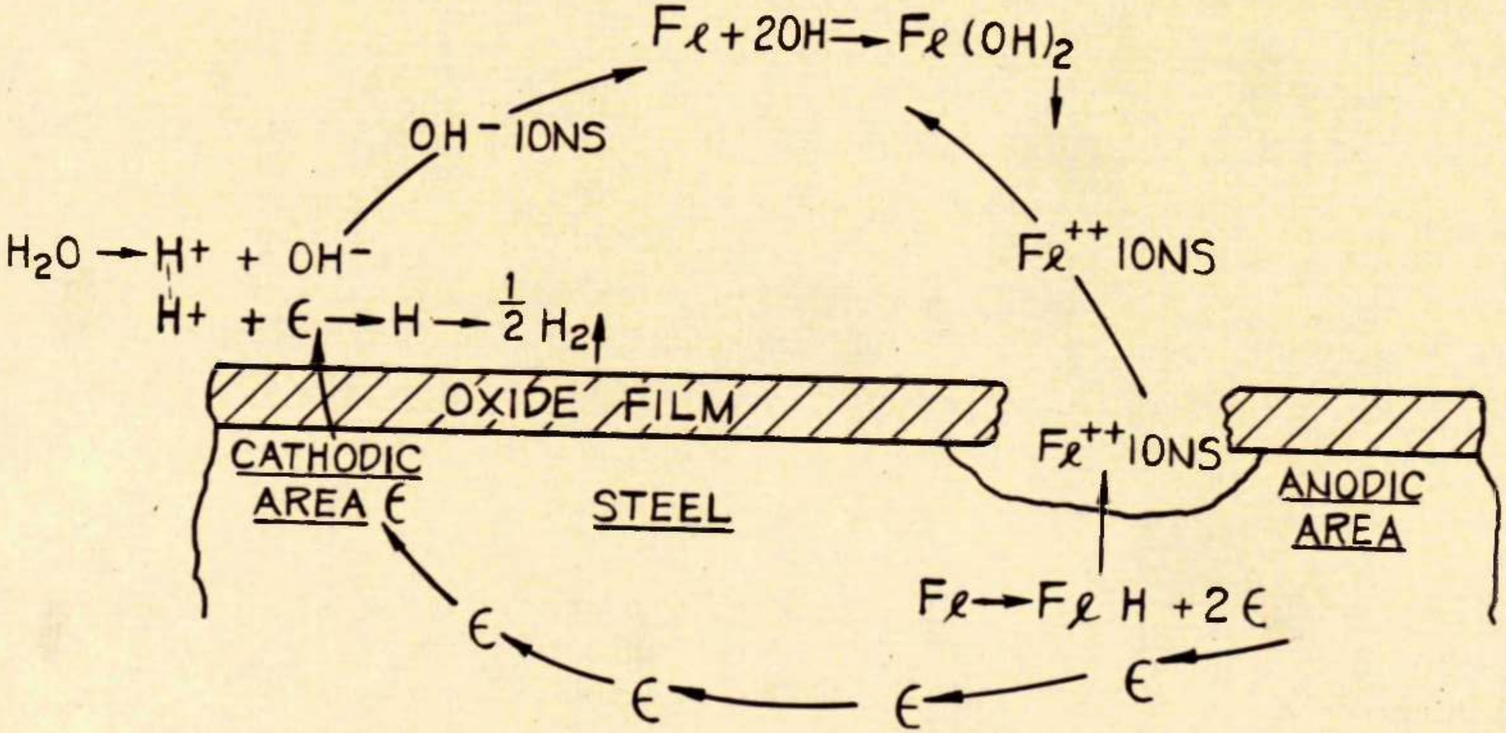

FIG 46

attack when no oxygen is present. This shows that when oxygen is absent, some corrosion does take place, but it is greatly reduced in quantity, since the main reaction for the production of hydroxyl ions is the one involving the adsorption of oxygen((6) above), and there is also more polarisation at the cathode because the dissolved oxygen removes the atomic hydrogen. This film of atomic hydrogen can virtually prevent the passage of current when no dissolved oxygen is present.

Chloride additions caused a further lowering of the endurance limit and by examining Fig. 47, the additional corrosion caused by these additions is clearly demonstrated. As might be expected, additions of soluble salts like NaCl, to aqueous media affect the corrosion and Uhlig (56) attributed the observed increase in corrosion rate to the following two factors:-

(1) The addition of salt increases the conductivity of the solution and enables passage of electric current between anodic and cathodic areas further apart.

(2) The type of corrosion product produced is less adherent and therefore its protective action is lessened.

As/

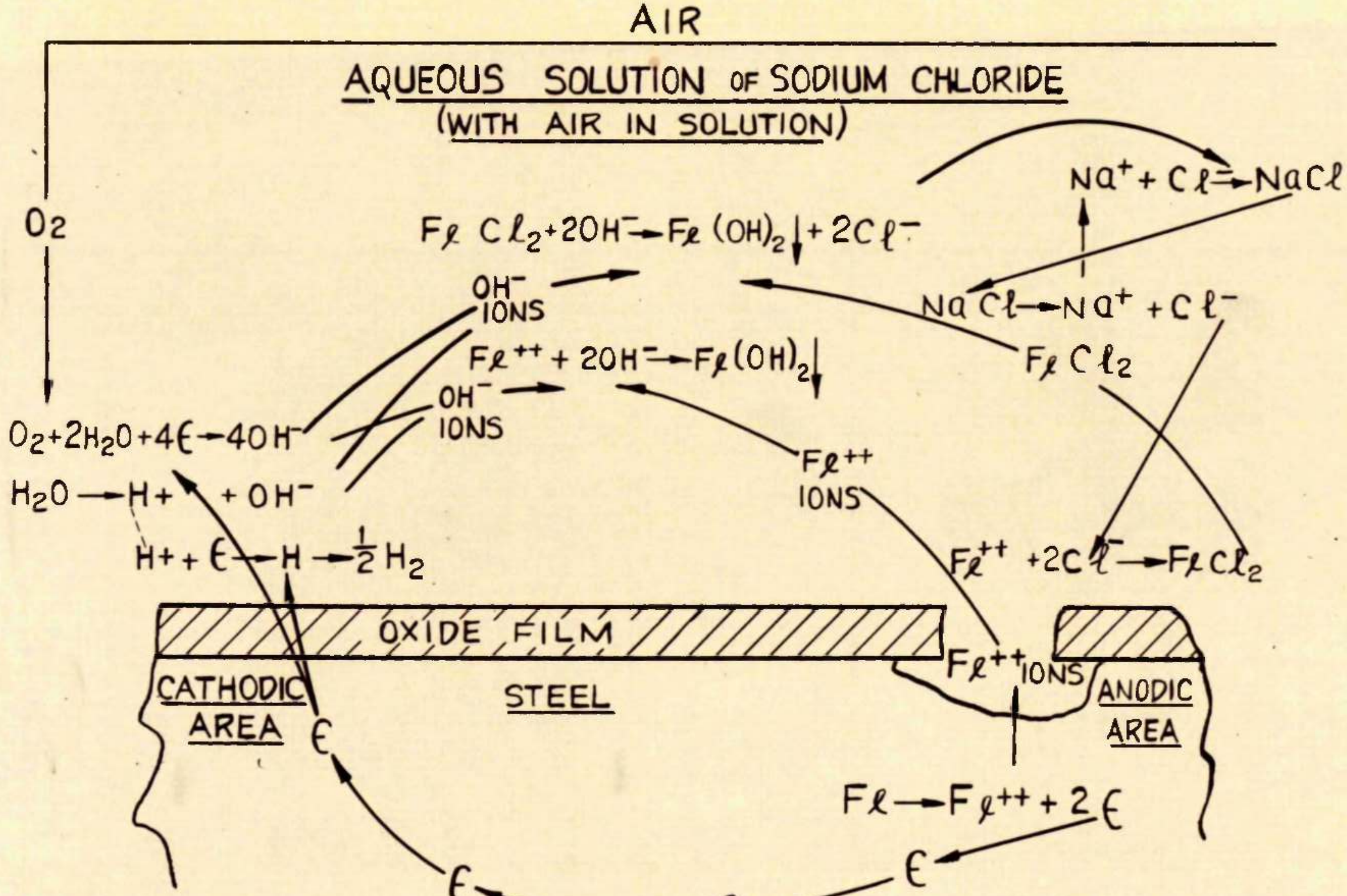
AIR
AQUEOUS SOLUTION OF SODIUM CHLORIDE
(WITH AIR IN SOLUTION)
O_2
$Na^+ + Cl^- \rightarrow NaCl$
$FeCl_2 + 2OH^- \rightarrow Fe(OH)_2 \downarrow + 2Cl^-$
OH^- IONS
$NaCl \rightarrow Na^+ + Cl^-$
$Fe^{++} + 2OH^- \rightarrow Fe(OH)_2 \downarrow$
$FeCl_2$
OH^- IONS
$O_2 + 2H_2O + 4\epsilon \rightarrow 4OH^-$
Fe^{++} IONS
$H_2O \rightarrow H^+ + OH^-$
$H^+ + \epsilon \rightarrow H \rightarrow \frac{1}{2}H_2$
$Fe^{++} + 2Cl^- \rightarrow FeCl_2$
OXIDE FILM
Fe^{++} IONS
CATHODIC AREA
STEEL
ANODIC AREA
ϵ
$Fe \rightarrow Fe^{++} + 2\epsilon$
ϵ
ϵ
ϵ

FIG 47

As in the case of distilled water (with dissolved oxygen), hydroxyl ions for the oxidation of iron, are produced by the dissociation of water and by the adsorption of oxygen from solution. There are also two additional effects which increase the corrosion rate. Firstly, the chloride ions react with ferrous ions at the anodic area, and this ferrous chloride then reacts with hydroxyl ions to form the ferrous hydroxide. This ferrous chloride prevents the accumulation of ferrous hydroxide at the anodic area, and so there is less stifling of corrosion. The sodium ions also react with some hydroxyl ions causing further dissociations of some water molecules. Secondly, the conductivity of the solution is increased due to the addition of sodium chloride, that is the resistance to the movement is decreased, hence the rates of the reactions shown in Fig. 44 are increased and corrosion can take place between cathodic and anodic areas which are further apart. The chloride additions also increase the depolarisation of the cathodic area that is an increase in the rate of the reaction (3). However, the decrease in the endurance limit with added sea water is not so great after about 0.25 per cent sea water (0.0075 per cent chlorides). This is due to a fall in the activity coefficient of the chloride and sodium ions as the concentration of the solution/

solution is increased. This fall in the activity coefficient is based on the theory of Debye and Huckel (58).

It can be seen from Fig. 22 that no safe limit is obtained in aqueous environments. Furthermore, the fatigue strength of the steel deteriorates continuously with an increasing number of reversals of stress in all the aqueous environments used and none of the curves shows signs of a safe range of stress, up to 50 million reversals of stress. These findings are contrary to the statements of Sorensen (59) and McAdam (60) who both believe that if corrosion-fatigue tests are taken to a sufficiently large number of stress reversals, a safe limit would eventually be obtained. However, neither of these workers succeeded in proving the existence of such a safe limit. Certainly up to 50 million cycles of stress, which is further than any of the previous workers have conducted their corrosion-fatigue experiments, no safe limit appears to exist.

Examination of the corrosion-fatigue curves in Fig.22 also shows that there is a change in the slope of the curves for corrosion-fatigue tests in various sea water concentrations, at approximately a stress of 13 tons per square inch and at 2.5 million stress reversals. Although all specimens tested in sea water and distilled water environments show the characteristic/

characteristic corrosion-fatigue fractures it is probable that at stresses above 13 tons per square inch fatigue may account for the greater amount of the damage while at stresses below 13 tons per square inch corrosion may account for an ever increasing amount. That the tests show corrosion-fatigue fractures is probably due to the fact that a newly fractured piece of the material corrodes rapidly in any aqueous environment at 80°C, two minutes being sufficient to produce a brown discoloration. Considering the length of time the crack may take to propagate and the time which elapses between the fracture of the specimen and the removal from the machine, no definite conclusions can be drawn from the appearance of corrosion-fatigue fractures.

2. Effect of Inhibitors

It will be seen from Fig. 24 that in 2.5 per cent sea water, the most efficient inhibitor is sodium chromate although sodium nitrite is only slightly inferior. Indeed, it will be seen from Fig. 25, that the position is reversed in five and ten percent sea water solutions, and concentrations of inhibitor above about 1000 p.p.m. and 1250 p.p.m. respectively. This also emphasises the value of testing to 50 million stress reversals instead of 10 million, because sodium chromate is the better inhibitor at an endurance of 10 million/

million while sodium nitrite is superior at endurances above 10 million.

A striking feature of the results is the poor protection afforded by potassium dichromate compared with sodium chromate, although both confer protection by the formation of a hydrated iron-chromium oxide layer ($Cr_2O_3.3H_2O.2.\gamma.F_2O_3.2H_2O$) on the surface. A possible reason for the difference in behaviour may be in the more acid nature of the dichromate solutions. The pH values of all the solutions used in the present work were measured (See Table 1.) and the results obtained showed that the solutions containing sodium chromate as an inhibitor possessed pH values of about 8 whereas those containing the dichromate possessed pH values of about 5.5. If the form of protection is as stated above the reactions for the dichromate and chromate could be:-

$$Cr_2O_2^{=} + 7H_2O + 6e^{-} \longrightarrow \underset{(Cr_2O_3 \cdot 3H_2O)}{\underline{2\,Cr\,(OH)_3}} + 8\,(OH^{-}) \ldots\ldots(8)$$

$$CrO_4^{=} + 4H_2O + 3e^{-} \longrightarrow \underset{\tfrac{1}{2}\,(Cr_2O_3 \cdot 3H_2O)}{Cr(OH)_3} + 5\,(OH^{-}) \ldots\ldots\ldots\ldots\ldots(9)$$

Using the principle that the free energy of whole reaction is equal to, the sum of the free energies of formation of the components/

TABLE I

THE pH VALUES OF CORROSIVE ENVIRONMENTS

2.5 PER CENT SEA WATER

p.p.m. Inhibitor	$K_2Cr_2O_7$	$C_6H_5COO\,Na$	$NaNO_2$	Na_2CrO_4
0	7.03	7.03	7.03	7.03
500	5.2	6.72	6.7	7.85
1000	4.9	6.73	6.71	8.00
1500	4.7	6.74	6.71	8.09
2000	4.5	6.75	6.77	8.15

10 PER CENT SEA WATER

p.p.m. Inhibitor	$NaNO_2$	Na_2CrO_4
0	6.94	6.94
500	7.16	7.44
1000	7.21	7.63
1500	7.23	7.86
2000	7.27	7.95

components of the reaction on the right hand side of the equation, minus the sum of the free energies of formation of the components of the reaction on the left hand side, then—

$$G^o_4 = G^o_{Cr_2O_7^=} - 7\ G^o_{H_2O} - 3\ G_{e-} + 2\ G^o_{Cr\ (OH)_3} + 8\ G^o_{OH^-}$$

s Substituting the values given in the American Bureau of standards.

$$G^o_4 = -(315.4) - (-7 \times 56.7) - 3\ (0)$$
$$+ \ (-(2 \times 205.5) + (8 \times 37.6)$$
$$= +315.4 + 396.9 - 411 - 300.8$$
$$= +\ 0.5\ \text{K cals.}$$

Since $G^o = -n\,FE^o$

E^o for the reaction (4) $= \dfrac{G^o}{nF}$ volts
(i.e. at a pH of 14 and unit molality of the dichromate ion) $= \dfrac{-0500}{6 \times 23,600}$ volts

$= -\ 0.0036$ volts.

Similarly for reaction (5) $E^o = -\ 0.13$ volts
(i.e. at a pH of 14 and unit molality of dichromate ion)

$$\text{Since } E = E^o - \frac{RT}{nF}\ Ln\ \frac{(\text{oxidised State})}{\text{Reduced State})}$$

the potentials for the reactions can be calculated for various values of the pH and concentrations for example.

Taking/

Taking a pH of 8 and an inhibitor concentration of 500 p.p.m. the potential for reaction (4) will be:-

$$E_4 = E^0 - \frac{RT}{nF} \quad \ln \quad \frac{\left(A_{Cr(OH)_3}{}^2 \times A_{OH^-}{}^8\right)}{\left(A_{(Cr_2O_7{}^=)} \times A_{H_2O}{}^7\right)}$$

For the present work -

$T = 68^\circ C = 261^\circ K$

and $R = 1.98$ cal/deg./mol.

$F = 23{,}060$ cals/ volt. gram. equiv.

$$\therefore E_4 = E^0 - \frac{0.0715}{n} \log \frac{A_{Cr(OH)_3} \times (A_{OH^-})^8}{A_{(Cr_2O_7^=)} \times (A_{H_2O})^7}$$

For reaction (8)

$n = 6$ and $Cr(OH)_3$ is a solid

$\therefore E^0 = 0.13$ volts

$\therefore A_{Cr(OH)_3} = 1$

the pH is 8

$\therefore A_{OH} = 10^{-6}$

the concentration of $K_2Cr_2O_7$ is 500 p.p.m.

$$\therefore A(Cr_2O_7^=) = \frac{500}{1000{,}000} \times \frac{1000}{294}$$

$$= \frac{1}{588}$$

and/

and $A_{H_2O} = 1$ (since the concentration of dissolved salts is very low.

$$\therefore \quad E_4 = -0.0036 - \frac{0.0715}{b} \; \frac{\log (10^{-6})^8}{\frac{1}{500}} \text{ volts}$$

$$\text{i.e.} \quad E_4 = (0.0036 - 0.012 \log. 500 + 0.012 \log 10^{48}) \text{ volts.}$$

$$= (-0.0036 - 0.0324 + 0.576) \text{ volts}$$

$$= 0.540 \text{ volts.}$$

similarly at a pH of 5

$$E_4 = 0.028 \text{ volts}$$

In the same way

$$E_5 \text{ (at a pH of 8)} = + 0.530 \text{ volts.}$$

$$E_5 \text{ (at a pH of 5)} = + 0.09 \text{ volts.}$$

According to the American convention of signs (which is used above), the more negative the potential, the more passivating in the reaction and the greater the inhibition. In the tests carried out with 500 p.p.m. of these inhibitors, the potassium dichromate solution had a pH of 5.2, while that containing 500 p.p.m. sodium chromate 8.3. Thus it would appear that/

that the chromate should be the more efficient inhibitor.

It is possible that equations (8) and (9) may not express the reactions which take place, and it is possible that the following reactions will occur.

$$Cr_2O_7^{=} + 7\,H_2O + 4\,Fe \rightarrow Cr\,(OH)_3 + 4\,Fe\,(OH)_2 + 2\,e^-$$

$$Cr\,O_4^{=} + 4\,H_2O + \frac{5}{2}\,Fe \rightarrow Cr\,(OH)_3 + \frac{5}{2}\,Fe\,(OH)_2 + 2\,e^-$$

or reactions of the type

$$Cr_2\,O_7^{=} + O_2 + Fe + H_2O \rightarrow CrO_4^{=} + Fe\,(OH)$$

The potentials for the above reactions have been calculated and no matter which is the type of reaction, the chromate reaction is the more passivating. In a similar way potentials were calculated for the nitrite reaction

$$NO_2^- + O_2 + H_2O + 2e^- \longrightarrow NO_3^- + 2\,(OH^-) \text{ ....} (10)$$

$$\text{or } NO_2^- + H_2O + e^- \rightarrow NO + 2\,(OH^-) \text{ ....} (11)$$

where E^o_6 + 0.13 volts and $E^o_7 = -\,0.263$ volts.

It is most likely that reaction (10) is the one which takes place under the conditions of the present work, but again no matter which one it is the final result is the same.

Substituting the values in reaction (10)

o/

E^{o}_{B} = − 0.01 volts.

Hence the potentials at pH values of 8, 7 and 5 and a nitrite concentration of 500 p.p.m. can be calculated. The results are

E_6 at pH 8 = + 0.252 volts
--------7 = + 0.324 volts
--------5 + + 0.478 volts

which show that nitrite should be a better inhibitor than the dichromate or chromate. The pH of a 500 p.p.m. nitrite has been measured and is 6.7 which is the result obtained with 5 and 10 per cent sea water concentrations. Fig. 26 shows that although the sodium nitrite confers a lower susceptibility to corrosion, the specimen has not had the endurance of the one tested in sodium chromate. However, it can be observed that after one minute the difference in potential of the specimen being tested in the two different inhibitors is 200 millivolts which is approximately of the same order as the value obtained by calculation.

Results shown in Figs. 24 – 25 and indicated that chromate and nitrite were the two most efficient inhibitors of those tested, hence a further series of tests was carried out to enable S/N diagrams to be constructed for the effects of varying/

varying percentages of these inhibitors in 2.5, 5 and 10 per cent sea water solutions. From Fig. 33 it is shown that in 2.5 per cent sea water 400 p.p.m. of sodium chromate were necessary to combat the addition of these chlorides to distilled water, while 700 p.p.m. sodium nitrite were required. The position however changes with increasing sea water content and 1400 p.p.m. of sodium chromate were required to combat the addition of 5 per cent sea water to distilled water, but only 1050 p.p.m. of sodium nitrite were necessary. Similarly to nullify the effects of a 10 per cent sea water addition, 2750 p.p.m. of sodium chromate or 1300 p.p.m. of sodium nitrite were required.

Fig. 33 also shows that at 5 per cent sea water sodium chromate is the better inhibitor up to 800 p.p.m. of the inhibitor , but at higher concentrations sodium nitrite is superior. Similarly at 10 per cent sea water sodium chromate is better up to 600 p.p.m. and sodium nitrite is better at concentrations above this. Similar findings are obtained when the inhibitors are compared for endurance limits at 10 and 50 million cycles. Further examination of Fig. 33 shows the difference in form between the sodium nitrite and the sodium chromate curves. Taking sodium chromate first, the graphs show that concentrations of inhibitor up to about 500 p.p.m. increase/

increase the protection and hence increases the endurance limit but with concentrations of inhibitor between 500 p.p.m. and 2000 p.p.m. very little further increase is obtained. It is probable that inhibitor concentrations beyond this would show little increase. Sodium nitrite does not show the same tendency of becoming asymptotic to the inhibitor axis as sodium chromate and inhibitor concentrations above 500 p.p.m. still show substantial increases in endurance. The form of the curves in Fig. 33 are the reverse of those in Fig. 23 and show the effect on the endurance limit of chloride additions. They all show that the initial addition has the greatest effect. If the activity coefficient of the chlorides decreases the graph would level off as in Fig. 23, similarly the graphs for sodium nitrite and sodium chromate in Fig. 33 should level off. A possible explanation of this is that the activity coefficients of the ions on solution decrease as indicated the Debye-Hückel theory. The activity coefficient of the nitrite ions is not lowered as much by an increase in concentration, as the activity of the chromate ions and this is a possible explanation for the differences shown in Fig. 33. Figs. 27-29 further show that even with inhibitor concentrations as high as 2000 p.p.m. there is no indication of a safe range of stress as far as 50 million cycles.

Although/

Although Speller, McCorkle and Mumma (47) used a different method of applying their corrosive environment, and a different steel (0.35 per cent carbon normalised) their results using sodium chromate as an inhibitor show good agreement with those in the present work.

Taking the endurance limits at 10 million cycles, their steel showed an endurance limit of 7.5 tons per square inch 3000 p.p.m. NaCl (equivalent to 100 per cent sea water) and 11.5 in the same corrosive environment with 2000 p.p.m. of sodium chromate added. This gives about a 53 per cent improvement in the endurance limit. In the present work, for 10 per cent sea water, without acid with inhibitor, the respective figures were 8.2 tons per square inch and 12.4 tons per square inch which is a 51 per cent improvement.

A comparison was also made of the efficiency of a number of adsorption inhibitors, where the mechanism of inhibition is different from that of the inorganic inhibitors.

These inhibitors form adsorbed films on the surface and protection from corrosive attack is conferred by means of a mechanical film of inhibitor, and not by reaction with the specimen surface.

Fig. 34 shows that the initial addition causes quite a rapid increase in the endurance but further additions give an approximately/

approximately constant increase. Since Oil F. was the most efficient of those oils tested, further tests were carried out using this oil. Fig. 35 shows the effects of sea water per centage on the endurance. The reason that Oil F is best can be probably attributed, to the fact that it is a true 'soluble' oil, where as oils A, B and C are opaque emulsions and Oils D and E are clear emulsions. The breakdown of these emulsions will certainly be enhanced by chloride additions and by a temperature of 80°C. Dorey (61) who found soluble and emulsifying oils very satisfactory in the prevention of corrosion-fatigue stated that 5 per cent NaCl prevented emulsification. On the other hand, Hamer, Powell and Colbeck (62) found that 0.5 per cent of oil added as an emulsion to corrosive water gave considerable protection from normal stressless corrosion in the emulsion at 90°C and the emulsion retained its function for over 72 hours. Figs. 36 - 37 show that although the mode of protection of oils is different, the nature of the S/N curves is similar to those for the anodic inhibitors described previously. The principal feature of these graphs is the proximity of the curves for 0.25 per cent, 0.5 per cent and 0.75 per cent in 5 per cent sea water, but while this does not occur in any of the other two graphs, had tests in 2.5 per cent sea water been carried out at higher concentrations of oil, a similar/

similar result may have been obtained.

Fig. 33 shows that to overcome the added corrosion brought about by the addition of 2.5, 5 or 10 percent sea water to distilled water, 2000 p.p.m., 2500 p.p.m. and 6250 p.p.m. of Oil F are respectively required. In all three chloride solutions the nature of the curves for Oil F is similar to those for sodium nitrite, but the positions are reversed in 10 per cent sea water, showing once again that nitrite is the least affected by the addition of chloride.

As lower concentrations of anodic inhibitors were used it was necessary to use different scales in Fig. 33 to show clearly the nature of all curves.

3. The Effect of Temperature

As the temperature of the environment was increased from 25°C. to 88°C. the endurance limit (at 50 million cycles) fell from 8.4 tons per square inch to 5.2 tons per square inch as shown in Fig. 39.

Speller (48)(1) has indicated four effects associated with a rise in temperature:-

(a) Increase in the rate of chemical and electrochemical reactions.

(b) Lowering of the oxygen solubility in water.

(c) Increase in the solubility product of the corrosion products, which would accelerate corrosion.

(d)/

(d) Decrease in the viscosity and surface tension of the solution.

The first factor will increase corrosion damage, because an increase in the mobility of ions leads to the passage of higher current, and with the increasing rate of reaction, more corrosion will take place.

The second is the most important, since the decrease in oxygen solubility with rise in temperature causes small bubbles to form on all surfaces (including metallic surfaces) immersed in the solution. This has the effect of producing differential aeration which increases the corrosion rate. It has been shown by Heyn and Bauer (63) and later by Friend (64) that the corrosion rate reaches a maximum when the temperature is slightly over 80°C.

Viscosity and surface tension decrease in value with increasing temperature. Decreased viscosity increases the rate at which the oxygen content of the solution comes into equilibrium with the atmosphere. A decrease in surface tension increases the wetting of the surfaces and tends to prevent the formation of oxygen concentration cells, resulting from bubble formation. There is no doubt that this is specially important with adsorption inhibitors and could be a reason for their good performance.

From/

From Fig. 39 it is apparent that the first factor is the most important in a consideration of the effect on corrosion-fatigue of the temperature of the environment, but for any reactions to take place oxygen is necessary, therefore oxygen is the most important single factor and it should be noted the solubility of oxygen falls to only 17.2 ml/litre at 00°C. It might be expected that some change would be shown in the trend of the curves shown in Fig. 40 which is a cross plot endurance limit plotted against temperature of the points in Fig. 39, shows a straight line relationship. This bears no resemblance to the curve for the variation of the solubility of oxygen in water with temperature demonstrating that although oxygen is necessary for corrosion, a small quantity will be sufficient.

Gould (65) has carried out investigations on the effect of variation on corrosion-fatigue and although his tests were only to 45°C. the trend shown by him agrees with that obtained in the present work.

4. Effect of Surface Finish

In fatigue testing one of the most important variables is the surface finish of the specimen, and this effect is accentuated in corrosion-fatigue testing. It was also a possibility/

possibility that variation of the surface finish of specimens tested would provide some information on the initiation of cracks. These are the two reasons, for the undertaking of corrosion-fatigue testing with a variety of surface finishes.

The surface finish of the specimen subjected to tests in the present work were obtained in two different ways. Those finishes over 25 μ (microinches) were obtained using a centre lathe with a variety of speeds and tools, while those under 25 μ were obtained as previously described by varying the grades of emery paper on the specially designed polishing machine.

The results are shown in Figs. 41-43 and the form of the curves indicates the significance of surface finish.

Fig. 41 representing the effect of variations in the surface finish of specimens tested in corrosive environments with various chloride additions, shows that no increase in endurance was notice until the surface finish was finer than 20 micro-inches, when finer finishes produced substantial increases in life. The greatest effect was noticed in the least corrosive environment.

Fig. 42 which shows the effect of introducing an anodic inhibitor (sodium chromate) to the most corrosive solution used for the test results of Fig. 41. This produced increased the endurance/

endurance when the surface finish was finer than 50 micro-inches, and although increasing the inhibitor concentration gives less corrosive solutions, each curve has a similar form.

Oil F. was the adsorption inhibitor used in the results shown on Fig. 43 and these show a most unusual trend. The endurance is affected by the surface finish, but the increase appears to be gradual for all finishes examined.

All results on the effects of surface finish emphasise the importance of standardising finishes before testing, so that the scatter may be reduced to a minimum. The results also demonstrate how the surface is important in the first stage of corrosion-fatigue. The first stage in corrosion- fatigue is dependent on the formation of corrosion pits and the resultant stress concentration round the pit. A particular surface finish may accelerate pit formation depending on the surface contour.

Figs. 48 and 49 show the Taly-surf records of two different specimens before testing. From these, it can be seen, that the 'valleys' in the rougher specimen are much deeper and more angular. This means that there will be a greater stress concentration round these grooves in the rougher specimen. The smaller grooves in the finer finished specimen do not have such a high stress concentration factor and hence deformation and strain/

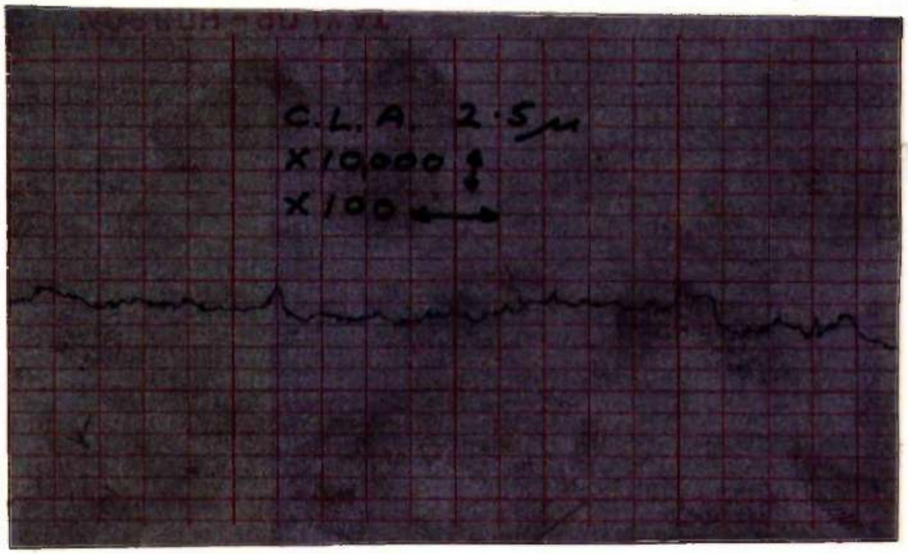
C.L.A. 2·5μ
X10,000 ↕
X100 ↔

FIG 48

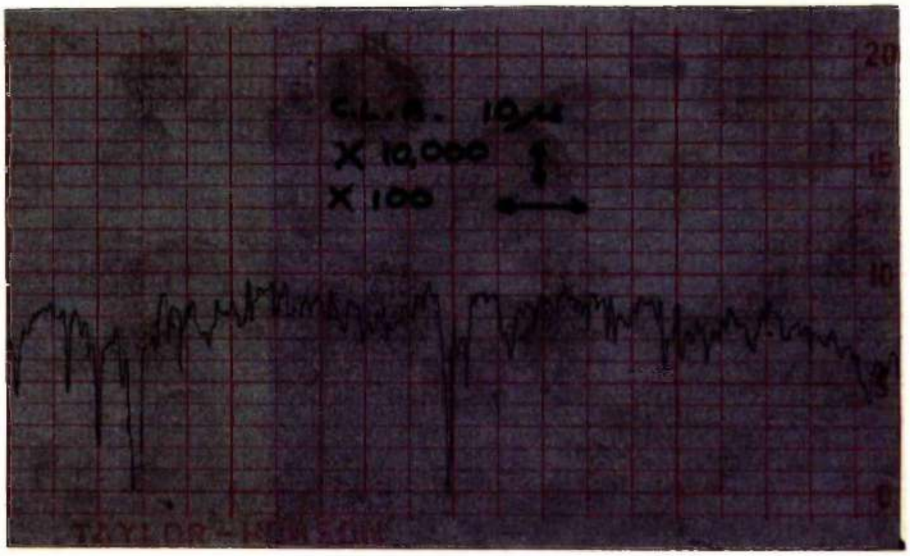
C.L.B. 10μ
X 10,000 ↕
X 100 ↔
20
15
10
5
0
TAYLOR-HOBSON

FIG 49

strain do not take place so quickly. The greater the rate of straining the more readily it will corrode, because strained metal has a higher potential than unstrained metal. This means that the rougher finished specimens will corrode faster than the finer finished specimens, but that the latter will ultimately corrode through time. Even a perfectly smooth specimen would have small notch effects at the surface, where there are grain boundaries, hence the inevitability of corrosion-fatigue attack and the failure to obtain a safe range of stress.

CHAPTER SIX

CONCLUSIONS.

The results of this section of the work can be summarised as follows:-

1. Distilled water at 60°C lowers the fatigue limit of mild steel.
2. Small additions of chlorides to an aqueous environment will rapidly deteriorate the corrosion-fatigue resistance of mild steel.
3. There was no indication of a safe range of stress in corrosion-fatigue.
4. Of the inorganic inhibitors tested, sodium nitrite had the best all-round performance.
5. The lower the surface tension, the better the performance of adsorption inhibitors, and of those tested oil F had the best performance.
6. Increasing the temperature of the aqueous environment lowers the endurance limit of mild steel.
7. The surface finish of specimens subjected to corrosion-fatigue has profound influence on the ultimate endurance.

SECTION TWO

METALLOGRAPHIC EXAMINATION

The objective of the work discussed in Section One was a study of the behaviour of inhibitors under conditions which normally induce corrosion-fatigue. A very full metallographic examination was made of both the fractured and cracked specimens arising from the investigation. It was early realised that this study would be greatly facilitated by the examination of specimen fractured under conditions of 'pure' fatigue by which is meant specimens fractured by fatigue in air, and also of specimens fractured under corrosion-fatigue conditions. Finally it was decided to examine specimens which had been subjected to both fatigue and corrosion-fatigue conditions by subjecting specimens to one form of test for part of its life and to complete the test to destruction under the other form of test.

Firstly a series of specimens was tested in a number of different corrosive environments. The tests were stopped at fractions of the expected life, varying from 0.5 to 0.95. This procedure was expected to produce corrosion-fatigue cracks in various stages of development.

In a second series of tests, a small stress raiser was introduced at the surface of the specimen as near as possible to the critical section. The stress raiser was introduced because it was expected that such a stress raiser would minimise the number of corrosion pits and therefore, the number of cracks. This would facilitate sectioning of the specimen at the exact location of the crack. Furthermore the life would be reduced. The stress raiser was produced using the 'Vickers' hardness testing machine with a five kilogram load, giving a reasonable size of indentation, on the centre of the barrel of the specimen in the position described above. Specimens containing stress raisers were tested to various fractions of a previously determined expected life, the tests being carried out in a variety of corrosive environments, but generally a corrosion inhibitor was present to minimise the general overall corrosion.

After the examination of cracks in this series of tests, a number of specimens were subjected to period of testing in air

in/

in the hope that this might give a 'pure' fatigue crack at the end of a corrosion-fatigue crack. Specimens were taken and indented as previously described and again tested in a corrosive environment to 0.6 - 0.8 of their expected life. The specimens were then removed from the tank and dried in an oven at 160°C. for 24 hours. The specimens were subjected to a period of fatigue in air bringing the expected life cycle to about 100 per cent.

Although these results proved difficult to interpret, as will be described later, nevertheless, it was hoped that yet another period of corrosion-fatigue testing would help to resolve some of the difficulties. Hence a three stage crack was produced and the observations of these are also described later.

Specimens containing cracks were sectioned as shown diagrammatically in Fig. 50. The small section containing the crack was then mounted in 'Diakon' as shown in Fig. 51. Emery paper was used in the initial stages but three different methods were used in the final stages of polishing, namely:-

1. Coarse medium and fine grades of alumina paste.
2. Coarse and fine grades of diamond dust.
3. Electrolytic polishing.

to determine if any of the crack characteristics, particularly the deposits of the corrosion products in the crack, were affected by the final polishing technique.

When/

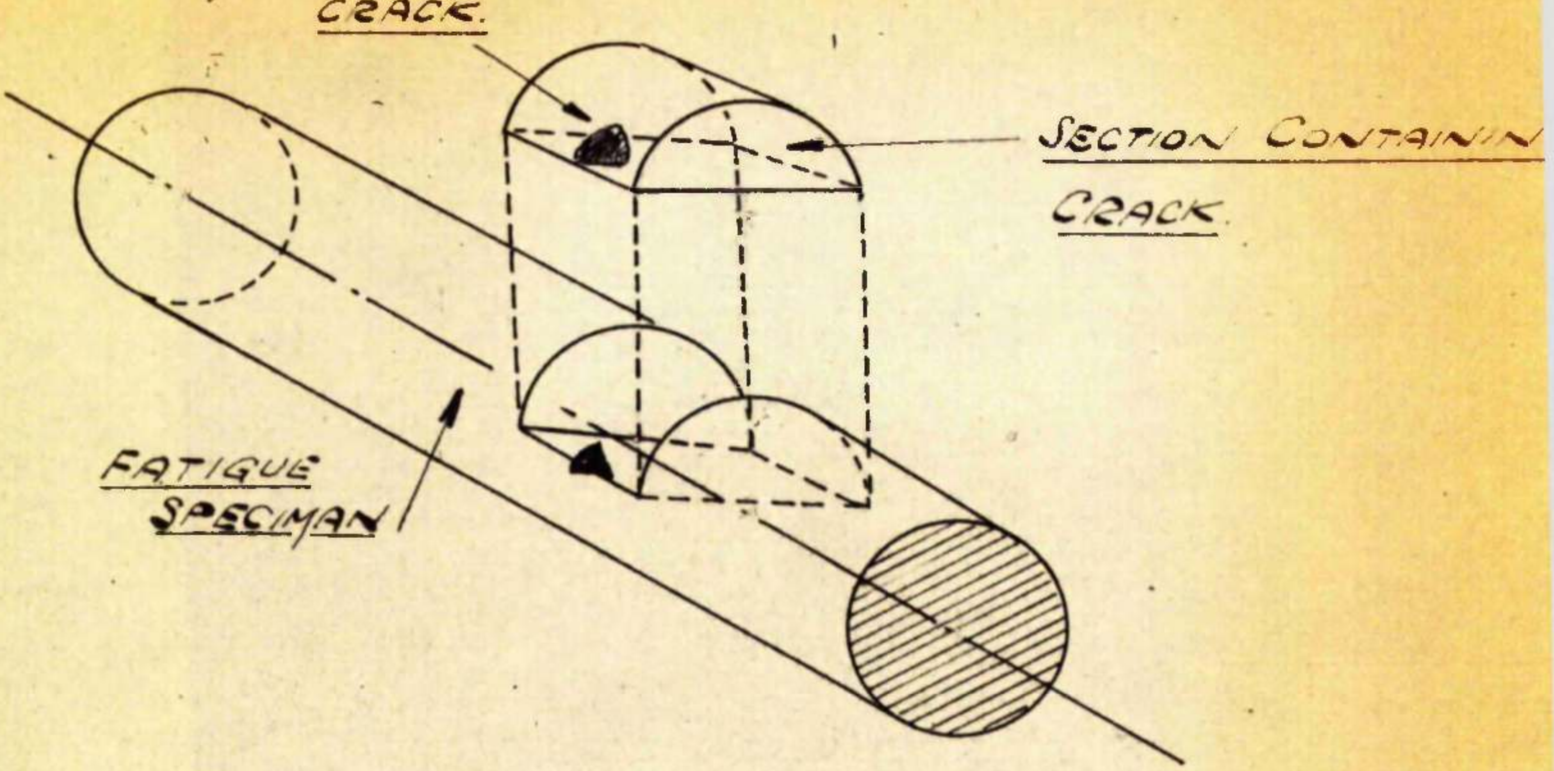
CRACK.
SECTION CONTAININ
CRACK.
FATIGUE
SPECIMAN

FIG. 50

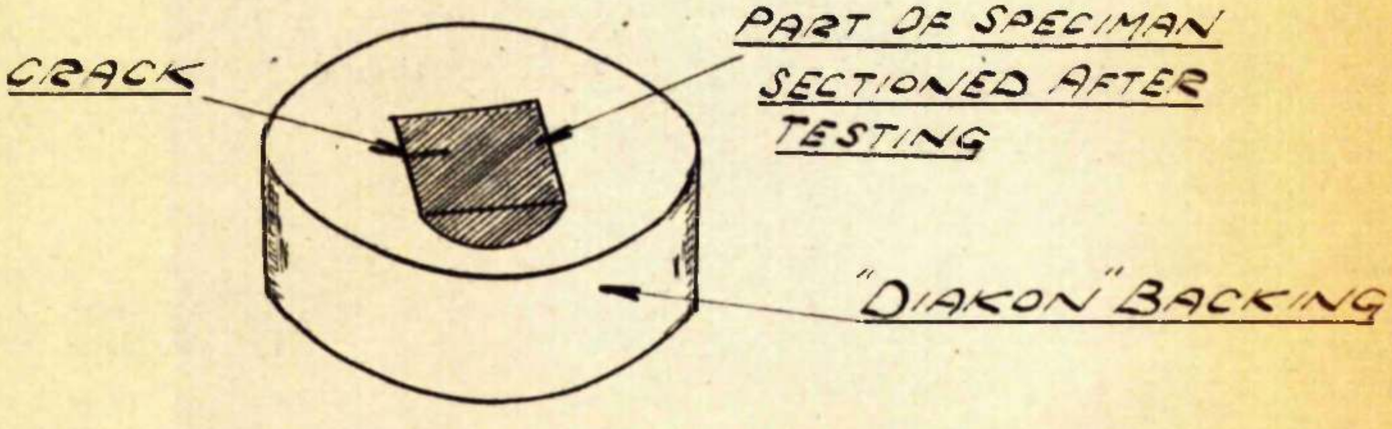
CRACK
PART OF SPECIMAN
SECTIONED AFTER
TESTING
"DIAKON" BACKING

FIG 51.

When sectioning and polishing had been completed, examination of the specimens in the unetched and etched conditions, were conducted using the metallurgical microscope (Vickers projection type). Magnifications up to x 1000 were employed and all interesting regions of the cracks, especially the tip, were photographed. All the photographs were taken by fitting a 35 mm camera, to the eyepiece of the microscope.

The metallurgical microscope has a limited range of resolution even at magnifications of the order of x 1500 did not clearly reveal either the ultimate path of the crack or the essential difference between corrosion-fatigue cracks and cracks caused by fatigue in air. It was therefore decided to use the electron microscope which gives a much higher resolution than the light microscope. The usual methods of making replicas, using formvar or nitro-cellulose, proved unsuitable due to their fragile nature, which always resulted in a tearing of the replica in the region of the crack. Even, such improvements in replica techniques for the electron microscopy of steel as suggested by Modin (66) which uses a reinforced collodian film from an isoamylacetate solution were unsuitable and a new technique had to be developed.

This new technique which has also been described elsewhere (67)/

(67) was a two stage process using PVA (polyvinyl alcohol) and carbon. A 10 per cent solution of PVA was poured over the surface of the specimen and allowed to harden at 40°C for 20 minutes. The PVA replica thus formed was then removed and a layer of carbon deposited on it by evaporation from a carbon arc in high vacuum (10^{-5} m.m. Mercury). The carbon layer was protected with a drop of 0.5 per cent formvar in dioxane. A supporting grid ($\frac{1}{8}$" diameter and 200 mesh) was now placed in position on top of the formvar film and drops of 7 per cent bedacryl in benzene were allowed to drop on the edge of the grid, until the whole grid was covered with a hardened layer. Great care was taken that this solution did not penetrate behind the film. The replica was now inserted in a cap and the PVA dissolved by flow washing for 30 minutes with water at 70°C. The formvar and bedacryl were dissolved, using chloroform delivered form a burette at the rate of $\frac{1}{5}$ c.c. per minute, two or three minutes being sufficient to complete the dissolution; longer washing may damage the carbon film. The film was then shadow cast with 60/40 gold palladium alloy, carried out under the same vacuum conditions as the carbon evaporation. The region of interest was located using the light microscope and the relevant grid square noted before the specimen was inserted in the electron microscope. Fig. 52 shows the stages in the preparation of the replica.

Although/

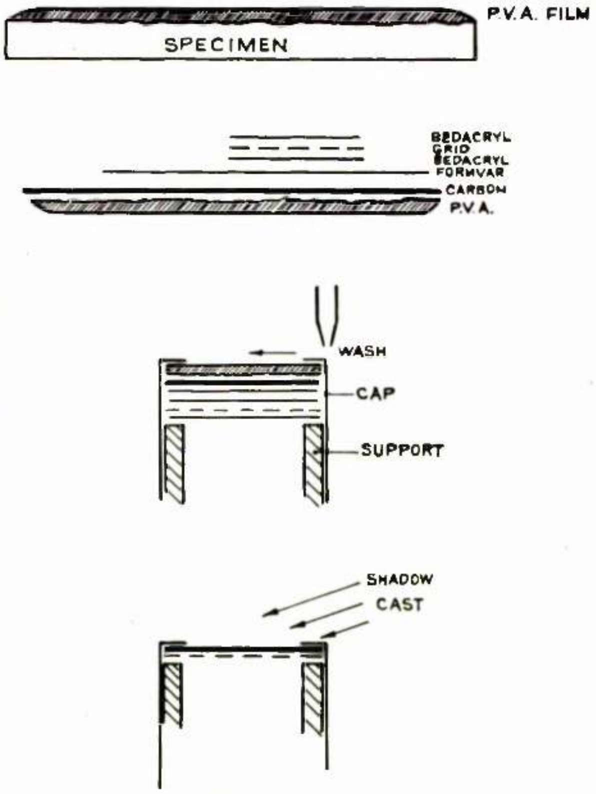
P.V.A. FILM
SPECIMEN
BEDACRYL
GRID
BEDACRYL
FORMVAR
CARBON
P.V.A.
WASH
CAP
SUPPORT
SHADOW CAST

FIG 52

Although this technique gave ideal replicas, great difficulty was experienced in locating very fine cracks, and the following method of location was developed. Using the Vickers Micro-hardness indentor, small pyramidal indentations 2 μ square and $\frac{1}{2}\mu$ deep were made round the crack on the polished surface of the specimen. This was photographed before the replica was made. The photomicrograph served as a key to locate the crack in the finished replica. Figs. 53 and 54 show one of these photographs, and an electron microscope photograph of a region of the crack.

Another method for crack observations was developed during the present work because it was hoped that the observation of the formation and propagation of cracks would enable a sounder idea of the mechanisms of fatigue and corrosion-fatigue to be formulated. Although this method has not been fully developed, the results so far obtained have been very helpful in providing some new information.

The tests were carried out in a 2 ton Amsler Vibrophore fatigue testing machine. A flat specimen, shown in Fig. 55 is used and it has a small hole (0.028 inch diameter) drilled in the centre, to act as a stress raiser and provide the point of initiation of the crack. The specimen was given a 'mirror finish' metallurgical polish (finished electrolytically) and was etched before/

FIG 53 X 430

FIG 54 X3000

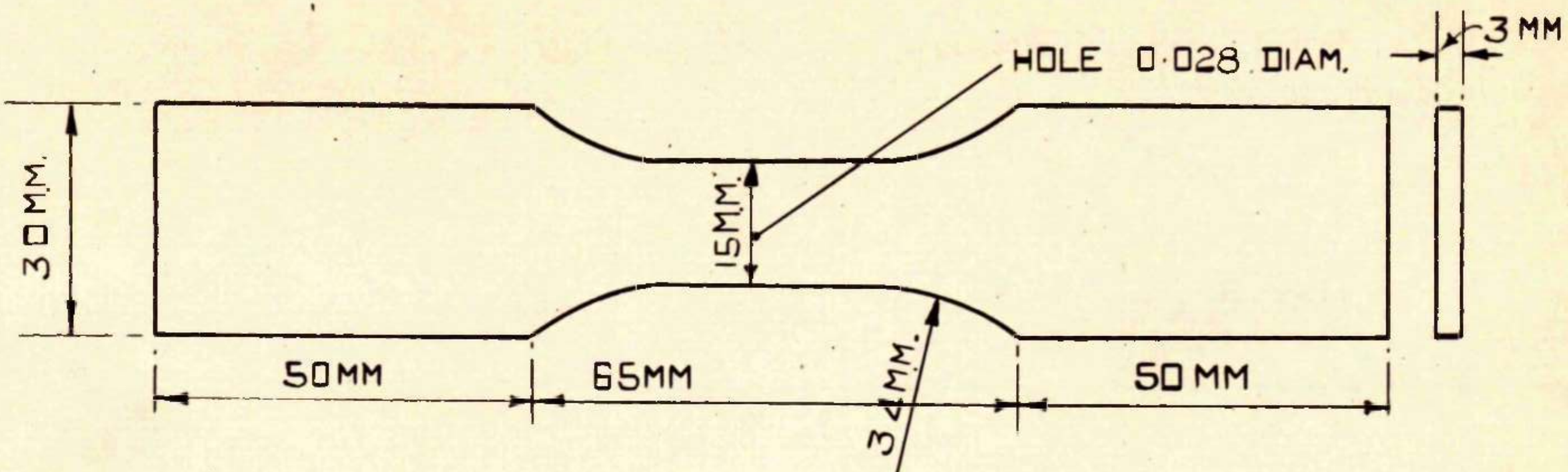

FLAT SPECIMEN FOR AMSLER

FIG 55

before being fitted into the machine.

A schematic representation of the apparatus is shown in Fig. 56. Light from a stroboscope is directed from a convex mirror into the opaque illumination tube of a microscope. This light is directed on to the specimen surface by means of a prism and is reflected from the surface up the tube of the microscope on to the eyepiece. The accompanying Fig. 57 shows the apparatus in use.

When the specimen has been inserted it is subjected to fatigue at 9000 cycles/min. at varying stresses, dependant on the desired rate of propagation. The stroboscope is adjusted to the same frequency, and the specimen surface as viewed through the microscope, appears to be stationary. The microscope is mounted in such a position that it is possible for it to be moved horizontally, to enable the path of the crack to be followed. During testing, a crack is initiated at the stress raiser and propagates through the specimen. The course of the crack and the deformation round it can be viewed with ease through the microscope.

Figs. 58 and 59 respectively show representative fatigue and corrosion-fatigue cracks and the most obvious difference between these two types of crack is in the width. The width of a fatigue crack is about 0.6 μ and is approximately the same size as the grain boundaries in the steel employed in the tests. The corrosion-fatigue cracks, with the exception of the last 25 μ of their length/

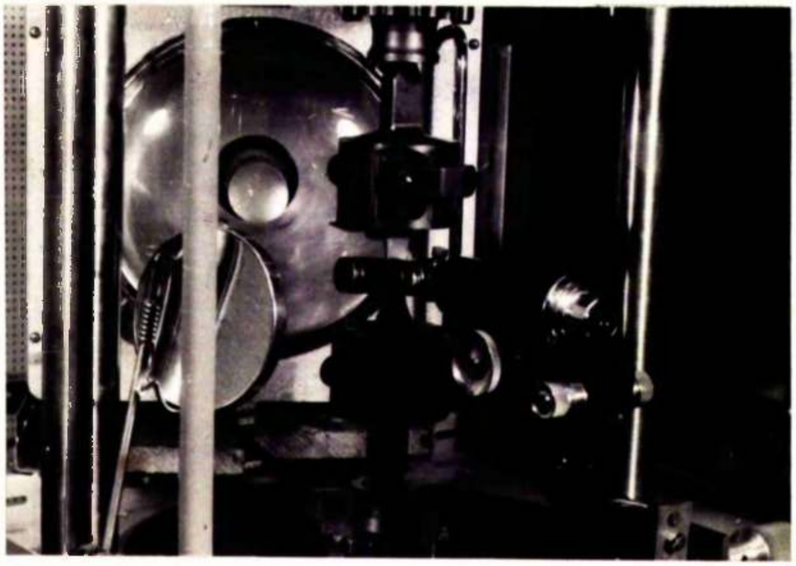

FIG 57

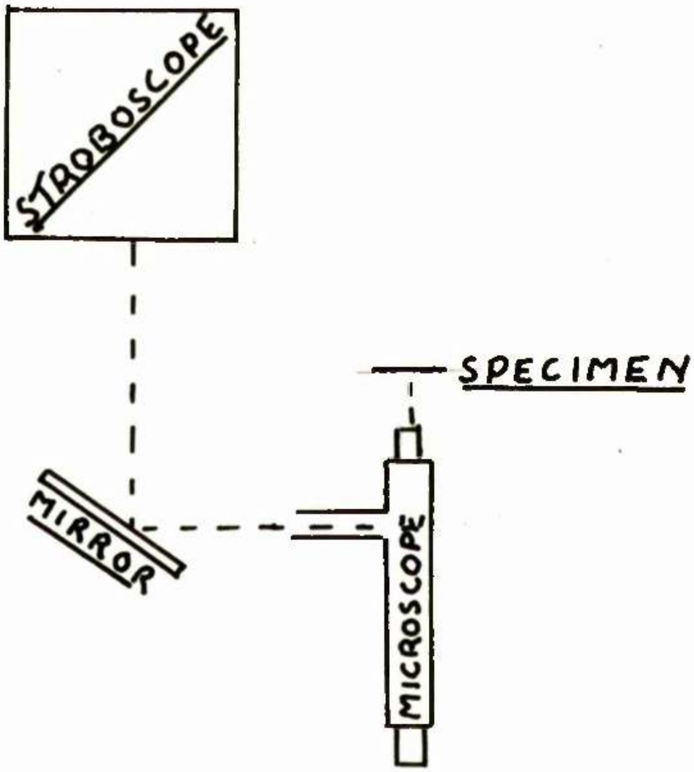

FIG 56

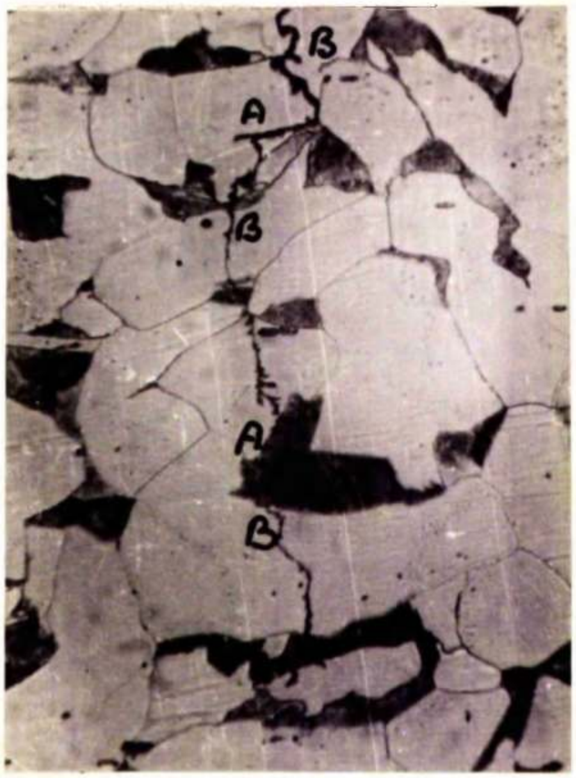

FIG 58 X430

FIG 59 X 430

FIG 60 X250

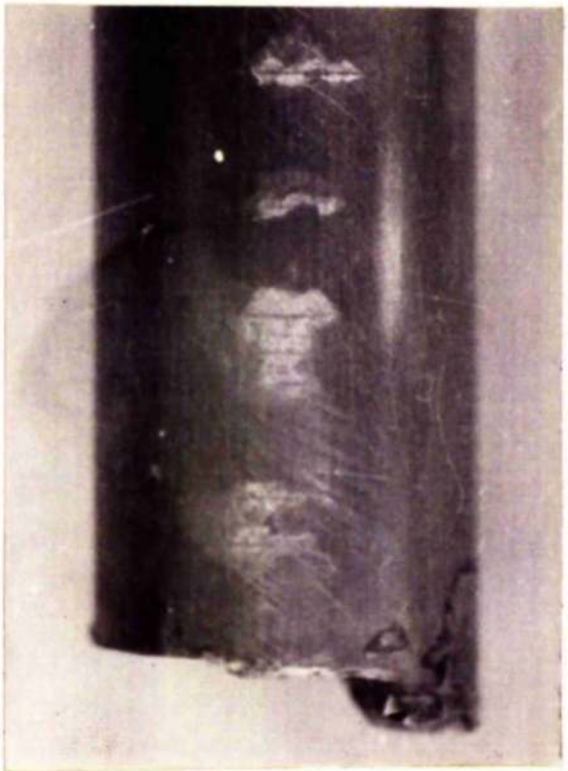

FIG 61 X3

length vary in width from 1-5 μ As far as can be seen under the metallurgical microscope the corrosion-fatigue crack is filled with a deposit while there is no material filling the fatigue crack. This will be further commented on later. The next feature observed is the predominately transcrystalline nature of the both cracks, although an intercrystalline fracture is apparent in certain parts.

These observations are consistent for all cracks observed the width of the corrosion-fatigue crack depending on the corrosive nature of the environment and the range of stress. The observations of Schulz and Buchholtz (35), Inglis and Lake (37), Gough (31) and Karpenko (30) all agree with the author that fatigue and corrosion-fatigue cracks are predominantly transcrystalline, but in a few cases cracks follow the grain boundaries. On the otherhand, McAdam (68) did not state what was the nature of the cracks, he examined although he said "their chief progress is probably along intercrystalline boundaries".

Corrosion-fatigue cracks always develop from corrosion pits, similar to that shown in Fig. 60. The development of this pit can be called the first stage of the crack. The production of this pit has resulted mainly from the action of corrosion, although stressing the material has also been effective because the pit is pointed and not hemi-shperical. This 'pitting' may be attributed to many causes for example local corrosion, removal of inclusions/

inclusions, local strain etc. In the majority of cases it was impossible to determine the exact location of the start of pitting and whether its fokus was transgranular or inter granular. The appearance of these pits on the surface is seen in Fig. 61 where the corrosion products have been removed to show the exact profile of the pits.

After a considerable amount of corrosion has taken place in the pit, a stress concentration is set up at the apex of the pit and a crack is initiated. A typical crack is shown in Fig.62, which illustrates admirably the general mechanism. Fig. 63 shows cracks in various stages of development, at E there is a corrosion pit, and a small portion of crack. E, F, G and H have all increasing lengths of crack coming from their respective corrosion pits. This is a section through the part of the specimen shown in Fig.61.

The approximate dimensions of corrosion-fatigue cracks have already been mentioned, with the exception of the last 25 of the length, when the crack becomes less wide. Fig. 64 shows an electron photomicrograph of the end of a corrosion-fatigue crack. The width at the tip if about $1/3\,\mu$ which is a similar size to the tip of a fatigue crack. Presumably the fatiguing action moved ahead of the corrosive action during crack propagation. The size of the ends of corrosion-fatigue cracks will be further discussed when/

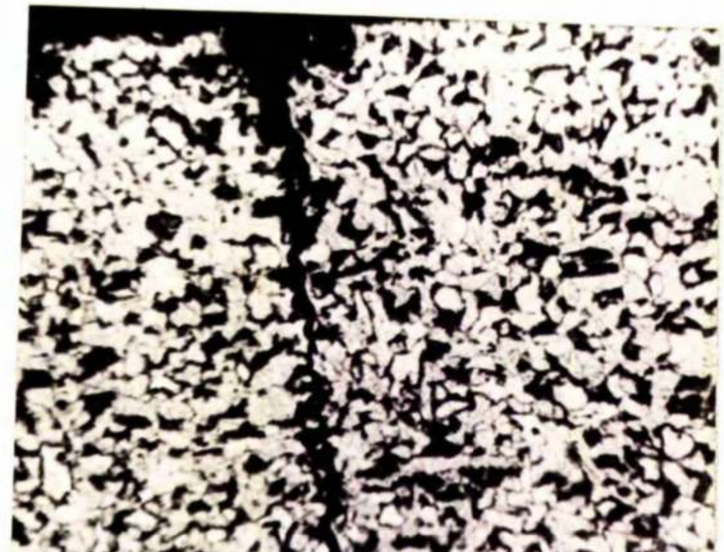

FIG 62 X250

FIG 63 X 250

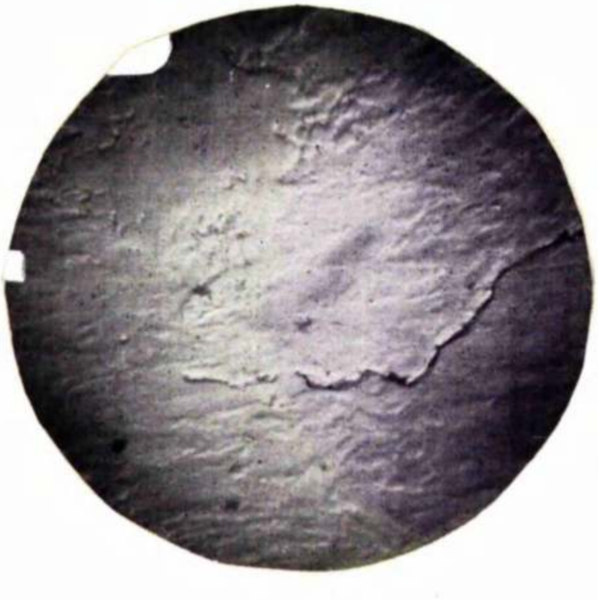

FIG 64 X 4500

when considering the results of the two and three stage tests.

Another prominent feature of both fatigue and corrosion-fatigue cracks is their tendency to avoid traversing pearlite grams. At points A in Figs. 65-66 it is quite obvious that the crack is deliberately avoiding passing through pearlite. This has been a feature of every crack examined, although it is more difficult to distinguish in corrosion-fatigue cracks. At the points A, the crack is running along the grain boundary between the ferrite and pearlite, but it very rarely runs along the grain boundary between two ferrite grains. When the crack does traverse pearlite grains it normally crosses at the narrowest part, as at B in Fig. 58 or passes through the grain in a direction parallel to the lamellae of cementite and ferrite. Although this characteristic has never been reported, close examination of cracks shown by Gough (31), McAdam (68) and many others demonstrate it quite clearly.

The reasons for this phenomenon are not obvious but it is reasonable to assume that it bears some relation to the process of slip. Slip can take place in ferrite grains since they are homogeneous but slip cannot occur in pearlite since it is an heterogeneous solid, composed of two constituents, cementite and ferrite. Pearlite is also stronger than ferrite, as borne out by the different strengths of a 0.01 per cent carbon steel and a 0.83/

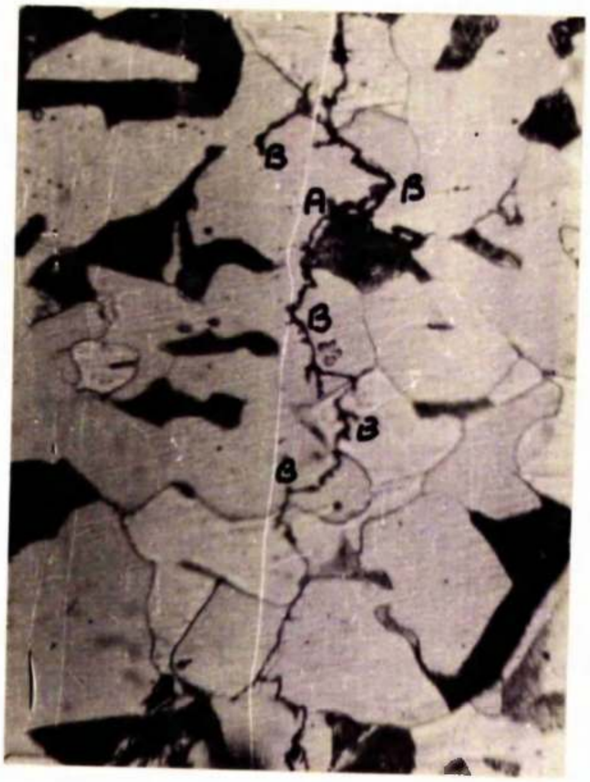

FIG 65 X 430

FIG 66 X 430

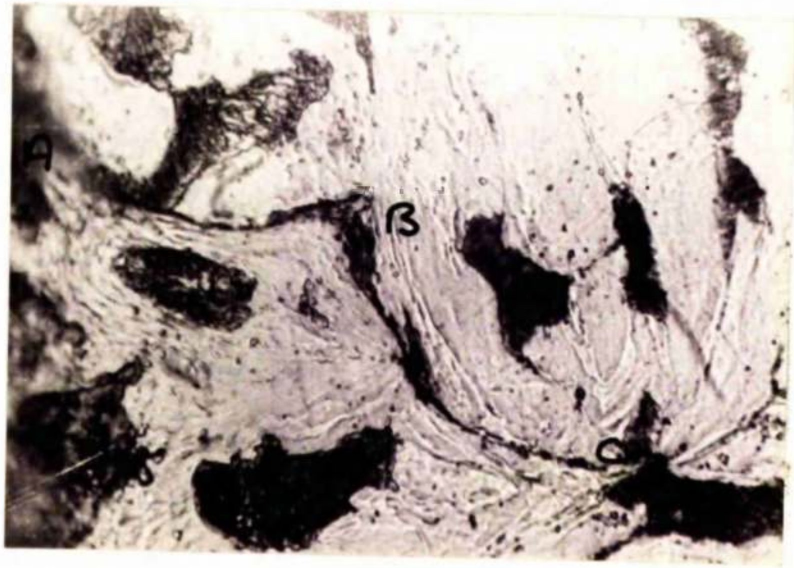

FIG 67 X430

0.83 per cent carbon steel. This means that pearlite will offer more resistance to the path of a crack, because it has no planes of weakness, caused by the occurrence of slip, and because it is inherently stronger. If this is the reason for this characteristic, and it appears to be the only one possible, then this again shows that the fatigue mechanism is the major reason for the propagation of corrosion-fatigue cracks.

From this it follows that it must be possible to have slip bands in the vicinity of corrosion-fatigue cracks. Although Gough and Sopwith(23) and Gould (69) have produced evidence of this nature, no success has been recorded in the present work, which can be attributed to the nature of the material employed. However, during tests carried out at high stresses (i.e. 10 tons per square inch) it is possible to observe flow lines round the crack provided the specimen is electropolished and etched in Fry's reagent. Fig. 67 shows a photomicrograph of one such specimen A being the bottom of the corrosion pit, and the crack following the line ABC. It is clear that the flow lines in the ferrite grains run in the same direction as the crack. This evidence further suggests, the probability of a stress concentration round the bottom of the corrosion pit and the crack propagating along the line of the maximum resolved shear stress. This means that the/

the part played by corrosion has become less, now that the pit has reached sufficient dimensions to cause this stress concentration.

Another observation, which can be associated with slip, is the changes in direction made by both corrosion-fatigue and fatigue cracks. This normally occurs inside ferrite grains and are illustrated at points B in Figs. 65 and 66. It is most likely, that when slip occurs in the one grain, the slip bands will be parallel to one another, as shown in the pure fatigue crack shown in Fig. 69. This crack formed in a flat specimen which was constantly under observation in the microscope using a stroboscopic light as the source of the opaque illumination. From Fig. 69 it can also be observed that the fatigue crack runs parallel to the slip bands, which phenomenon was also noted by Gough and Sopwith (23) and Gould (69). Fig. 68 however, being a photomicrograph of a specimen being tested in a similar way to that shown in Fig. 69 only at a much lower stress, shows slip bands occurring in two different directions in the one grain. The angle between the two planes can vary, for example, in the grain marked I, the angle is about 30°, while in the grain marked II, the angle is about 60°. This is called cross slip. Since this cross slip can occur, as shown in Fig. 68, and since cracks tend to align themselves with existing slip planes, the crack/

FIG 68 X 730

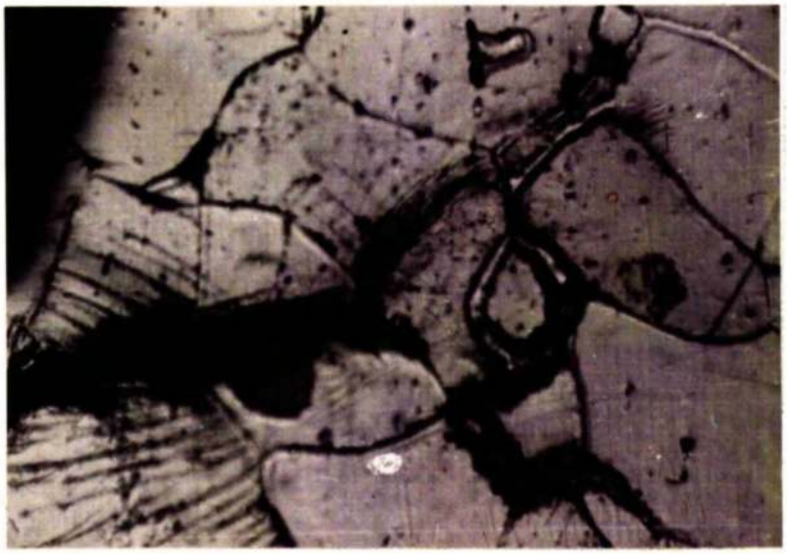

FIG 69 X 125

crack only needs to follow a different slip system to change its direction inside a grain. This change of direction of corrosion-fatigue cracks and its relation to slip is still further evidence in support of fatigue preceding corrosion during propagation.

Small branch cracks are another common feature of corrosion-fatigue and pure fatigue cracks. Fig. 65 illustrates the typical types of branch crack obtained during fatigue testing in air. This characteristic can again be related to slip and cross slip. However, if corrosion attacks a specimen outwith the presence of an alternating or flucuating load, a similar type of crack would be formed, but the crack would be predominantly intercrystalline, as obtained on stress-corrosion and caustic embrittlement (27). The cracks shown in Fig. 65 (Fatigue) and Figs. 70, 71 , 72 and 73 are various stages of corrosion-fatigue and all show the cracks to be transcrystalline. Fig. 70 is of particular interest, having one broad corrosion-fatigue crack and smaller branch cracks. The small branch cracks are similar in size to pure fatigue cracks and do not appear to be filled with corrosion products. If corrosion was the major factor in the propagation of corrosion-fatigue cracks, it is to be expected that all cracks would be the same size and would be intercrystalline. Fig. 71 does show them to be the same size,

but/

FIG 70 X 730

FIG 71 X 230

FIG 72 X 430

FIG 73 X 730

but this is an exception, and the various inclusions present such as at the points X are thought to be responsible for this. Fig. 72 and 73 show the branch cracks present in corrosion-fatigue specimens which were being tested to a percentage of the known endurance. Both photomicrographs show the small cracks which appear to racing ahead of the broader corrosion-fatigue crack. Especially in Fig. 73 at X, Y, and Z do these cracks resemble ordinary fatigue cracks. It is quite evident from the size of these cracks alone, that corrosion has not taken place. However, closer examination shows that although the crack at Y is very narrow, there is a definite portion of a corrosion fatigue crack beyond Y. This corrosive area can be simply explained by the fact that the crack is three dimensional, and the photograph only shows two dimensions. Since the steel used in the present work was a commercial mild steel, it is to be expected that there were some inclusions present in the steel. This was true, and the inclusions which were present, were found to be mainly manganese sulphide. These inclusions influenced the propagation of cracks quite frequently, as shown in Fig. 71 and Fig. 74 which illustrate the degree to which this influence can extend. The crack has been propagating in the direction shown and on reaching the point/

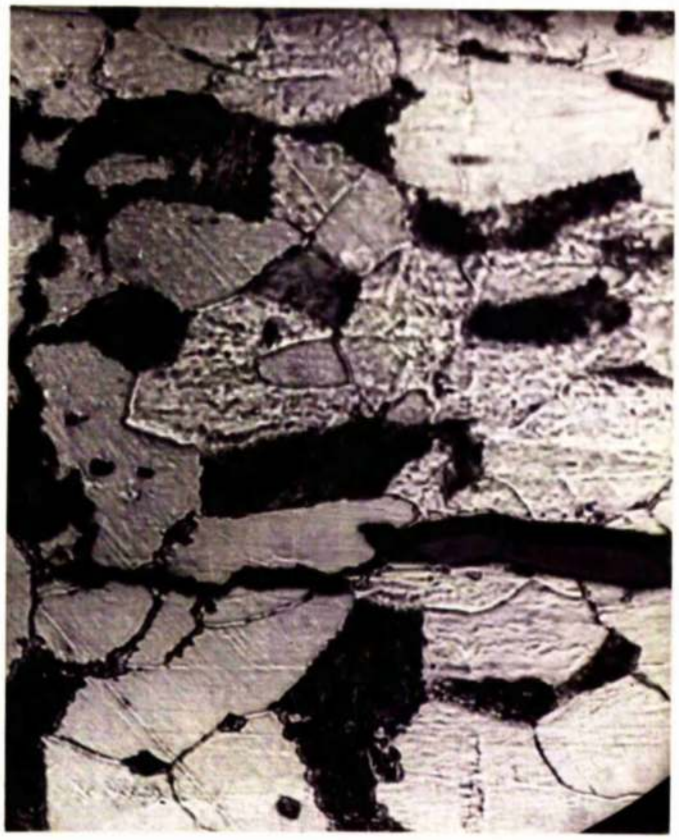

DIRECTION OF PROPAGATION

FIG 74 X 430

point Y has momentarily halted, before changing direction by 90° to pass alongside the inclusion X. This is caused by the stress concentration round the inclusion being greater than that round the end of the crack when it reached Y. Since the crack always propagates in the direction of the maximum stress, the crack changed direction towards the inclusion. The inclusion itself appears to be corrosion resistant, because it has not been attacked, but the surrounding metal has undergone considerable corrosion. That inclusions in metals are stress raisers is generally recognised (70), but the inclusions present in the steel would only influence the direction of propagation of a corrosion-fatigue crack, if stress itself was mainly responsible for the propagation. Thus, the very nature of the change in direction of the crack illustrated by Fig. 74 further suggests that fatigue rather than corrosion is responsible for corrosion-fatigue crack propagation.

A characteristic feature of all corrosion-fatigue cracks was the presence of corrosion-fatigue products in the crack. It is clearly shown in Fig. 70 that the crack is filled with products of corrosion. However, the detection of these corrosion products, was very difficult using reflected light, especially at the tips of the cracks. This was mainly overcome by the use of the electron microscope and by the use of polarised light in the metallurgical microscope./

microscope. Figs. 75 and 76 respectively show a fatigue and corrosion-fatigue cracks, as viewed under the electron microscope. The black areas in Fig. 75 are the corrosion products. The distribution inside the crack is noticeably uneven, and it might be thought that the black areas in the crack may be due to the polishing medium, but this is discarded on the following four counts:-

(a) The polishing medium has a definite crystalline structure, when analysed by electron diffraction, but all the probable corrosion products have a poor crystalline structure. On an electron diffraction pattern of the deposit being taken, it was shown that the crystalline structure was very poor, proving that it definitely was corrosion products.

(b) Under polarized light, ferric oxide appears light red, while all the polishing media used have low interference colours, and these are certainly not red. Fig. 77 is a photomicrograph of a specimen taken under polarized light. The light area in the crack was brownish red in colour and was found to run the whole length of the crack. A replica was also taken of specimen and observed under polarized light in a Vickers projection microscope. Fig. 78 shows the result, a dark colour in the region of the crack indicating that some corrosion deposit has adhered/

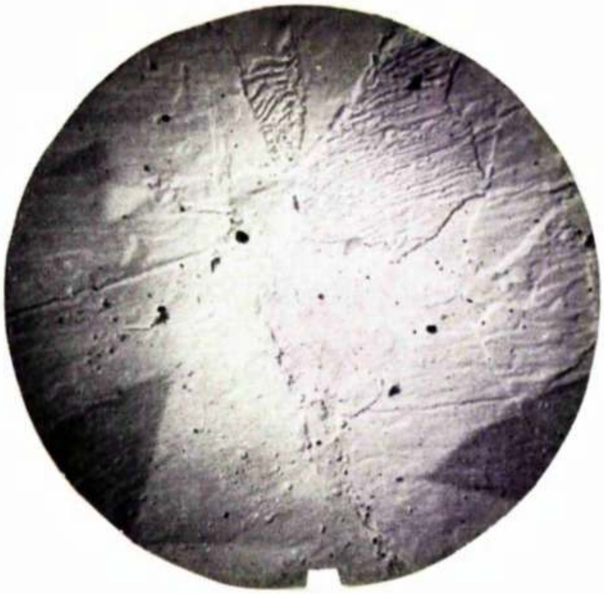

FIG 75 X 3000

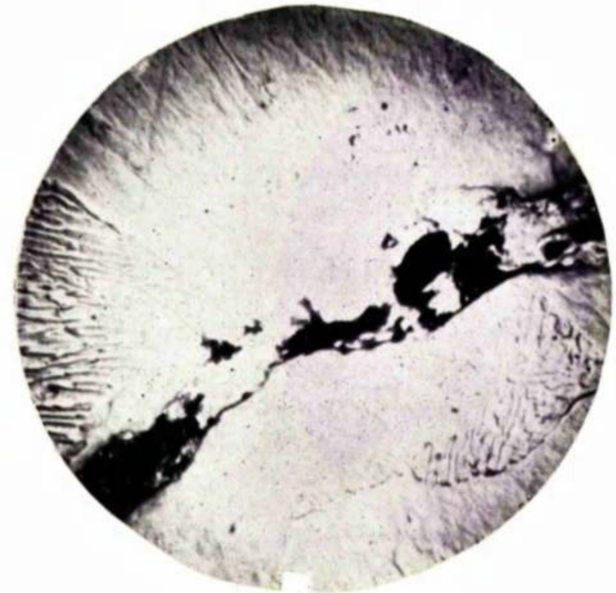

FIG 76 X 3000

FIG 77 X 1500

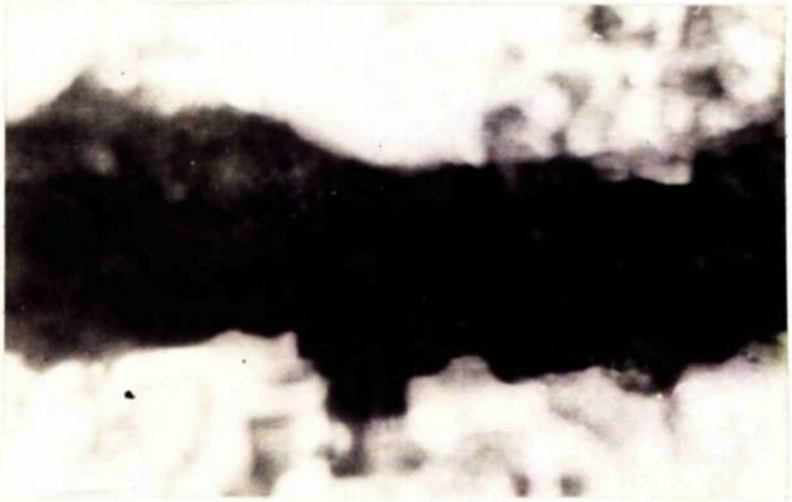

FIG 78 X 1500

FIG 79 X 1500

adhered to the PVA. Fig. 79 is another photomicrograph taken under polarised light, but in this instance the corrosion products are now shown very clearly. The arrows indicate small areas of the corrosive deposit in both figs. 77 and 79.

(c) Three methods of polishing were used previously described, and similar photomicrographs were obtained for all three methods.

(d) No deposits were visible in 'pure' fatigue cracks, similar in size to corrosion-fatigue cracks containing deposits.

A black area on an electron photomicrograph means that whatsoever is present in the crack is impervious to the electron beam and suggest that some of the deposit must be sticking to the replica, as proved in (b) above. It is known that iron products are impervious to the electron beam, but so is iron itself, which would lend support to the Attrition Theory of Ewing and Humfrey (6). However the fact that there are no black areas on photomicrographs of 'pure' fatigue cracks is not in agreement with either the Attrition or the Amorphous layer theory. As explained in (b) various specimens were examined under reflected polarised light, and all were found to have a deposit in the crack which gave a light reddish brown interference colour. On some iron compounds, for example/

example iron chromate, iron carbonate, iron itself, ferric oxide, ferrous hydroxide and ferric hydroxide being tested under crossed nicols, only ferric oxide and ferric hydroxide gave similar interference colours. For this reason and also from a study of the electron diffraction photographs it seems reasonable to assume that the products of corrosion are γ Fe_2O_3 (hydrated).

On account of the fact that it was now possible to recognise corrosion products, many replicas of corrosion-fatigue cracks were studied in the electron microscope to try to discover whether or not the corrosion products did exist at the ends of the crack. Reference back to Fig. 64 shows the end of a corrosion-fatigue crack which has a deposit at the tip of the crack, even although the crack is less than 0.25 μ in width. Some corrosion-fatigue cracks were examined at magnifications up to × 9,000, and all had deposits up to the tip of the crack, as shown in Fig. 80 which shows the end of a corrosion-fatigue crack between a ferrite and pearlite grain. The presence of corrosion deposits at the end of the crack would support alternative mechanisms for crack propagation either that corrosion proceeds fatigue or that both proceed at the same rate. If, however, fatigue precedes corrosion, as suggested by some of the results already described, which is the explanation of the presence of corrosion products at the tip of the crack? The nature of the testing procedure means that the corrosive fluid is forced/

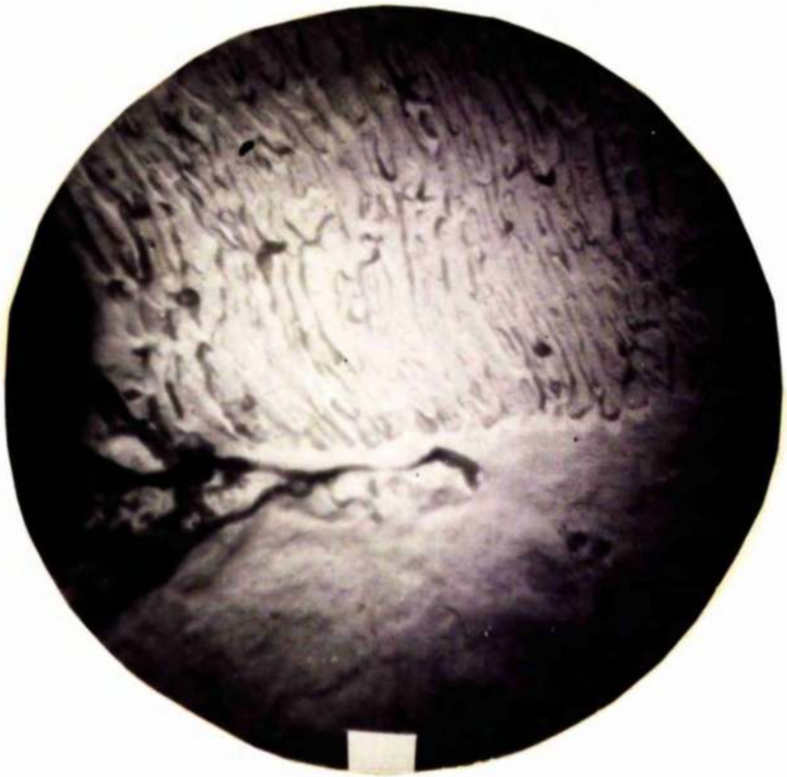

FIG 80 X9000

forced into the crack by a head of 2-3 inches of water, and since the crack is opening and shutting with the bending fatigue, a differential pressure will be set up. This means that there are two possibilities of the corrosion products being in the crack; either being forced in by the corrosive fluid or being drawn in by the flexing of the material.

Generally the results produced by the two and three stage tests were difficult to interpret, and were on the whole inconclusive. On examination of microsections cut from specimens tested in this manner, it was found to be very difficult to differentiate between the different stages. Figs. 81 and 82 show the general pattern of this work; Fig 81 being a corrosion-fatigue crack, while Fig. 82 illustrates a crack obtained in a two stage test (corrosion-fatigue followed by fatigue in air). Both show a broad portion of the crack which is definitely corrosion-fatigue, and another narrower part, whose origin is unknown, but whose size is very similar to pure fatigue cracks.

Figs. 83 and 84 illustrate cracks from other two specimens; Fig. 83 being taken from a specimen stopped at 95 per cent of its expected corrosion-fatigue life, and Fig. 84 from a specimen which was tested under corrosion-fatigue conditions followed by a period of fatigue in air, but during the latter the stress was increased to enable easier indentification of the pure fatigue region. Fig. 83/

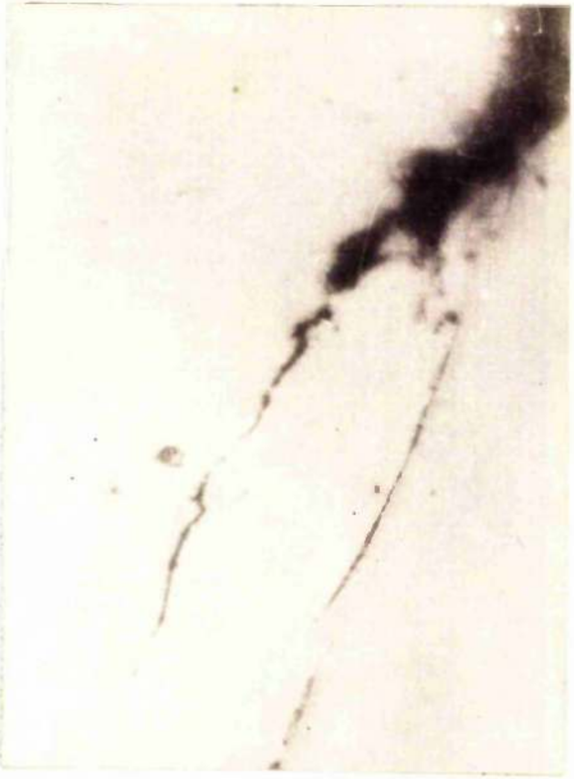

FIG 81 X 730

FIG 82 X 730

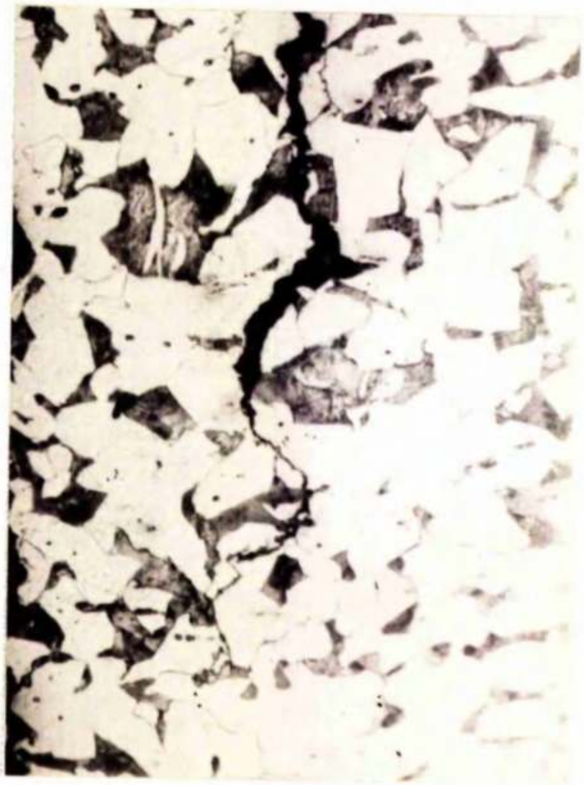

FIG 83 X250

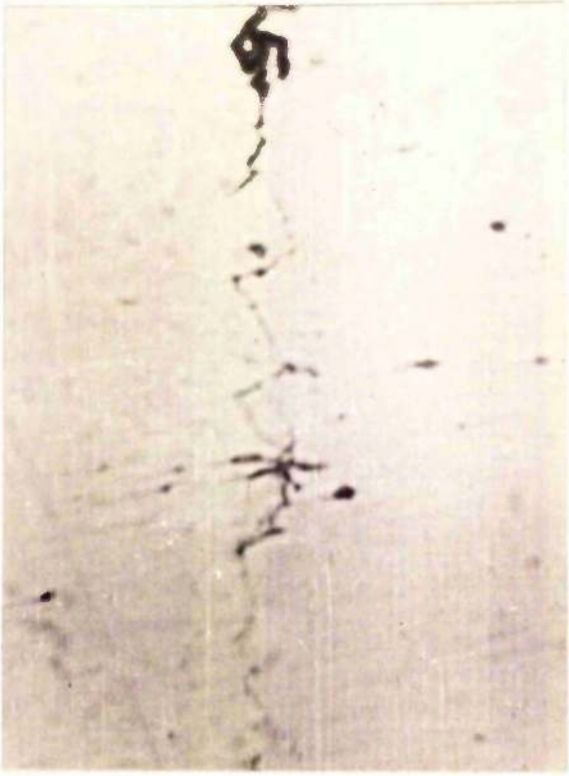

FIG 84 X730

83 shows two different areas of the crack, one resembling corrosion-fatigue and the other resembling pure fatigue. Fig. 84 illustrates two stages, similar to that obtained with corrosion-fatigue alone. In an endeavour to obtain another crack, similar to that shown in Fig. 83 a repeat test was carried out, and again the test was discontinued after 95 per cent of the expected life. This time, the result was entirely different, and Fig. 85 shows the type of crack obtained. The result of the latter experiment was quite a common occurrence, in that it was possible to obtain cracks with two regions but where a repeat test gave only one region. This could be due to the microsection only showing two dimensions of a three dimensional crack.

Fig. 85 is typical of the cracks obtained in the three stage experiments. Again, it was not possible to differentiate between the three different periods of testing, and the whole crack has the appearance of corrosion-fatigue. Since these cracks were similar to many ordinary corrosion-fatigue cracks (e.g. Fig.86) it was concluded that any hair line fatigue crack formed during the second period of testing, was attacked during the subsequent corrosion-fatigue period, and the crack broadened out, until it was too similar to the remainder to allow definite differentiation. Fig. 87 was the only crack obtained in the two stage testing where the crack had a real definite division into corrosion-fatigue and pure fatigue resions (X in Fig. 87) and where the length of the pure/

FIG 86 X 430

FIG 85 X 430

FIG 87 X 230

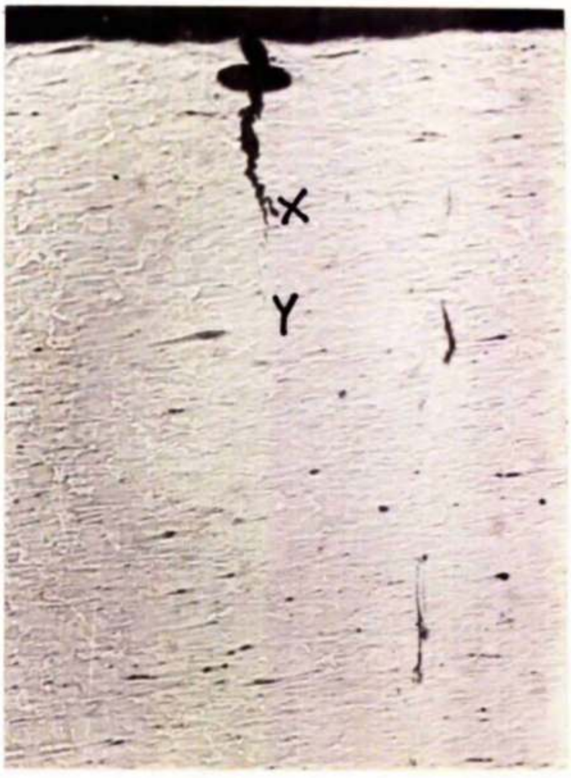

FIG 88 X 230

pure fatigue crack was considerable. However, subsequent examinations showed that cracks of a similar nature were present in specimens subjected to corrosion-fatigue only. Fig 88 illustrates one of these cracks.

The reason for the failure to differentiate between the periods of corrosion-fatigue and pure fatigue is not obvious but it is most likely that the cause is the heterogeneous nature of the steel. Although the results allow no definite conclusion to be arrived at, the evidence produced shows that the most likely mechanism of the propagation of corrosion-fatigue cracks is by the spread of a pure fatigue crack followed by corrosion of the fracture faces.

In the experiments on crack propagation, using the method specially developed for observation during propagation corrosion-fatigue tests could not be carried out for the reason that it is not yet possible to view the corrosion-fatigue specimen. However the following results will show the relation between the process of slip and that of fatigue crack propagation, since the foregoing discussion has already shown that fatigue is likely to precede corrosion during the corrosion-fatigue of ferrous alloys.

The first tests carried out illustrated that slip was obtainable when α iron was fatigued. Figs. 89 and 90 demonstrate this. Fig. 89 shows the extent to which slip takes place in the metal, the/

the broad bands being about 50,000 Augstran units wide. These broad slip bands only occur at loads above the fatigue limit. Fig. 89 also illustrates that slip bands cross grain bounderies. There is a slight change in direction on crossing the grain boundery, indicating that the slip systems in grain A did not concede with those of grain B.

Fig. 90 shows a region of the iron, where the grains are showing slip in more than one direction. This phenomenon was obtained at a loading, well below the fatigue limit. Wavy slip bands in α iron were noted by Gough (72). Their occurrence can be attributed to the fact that iron has 48 slip systems and that the waviness was merely the result of more than one slip system operating at the same time. Fig. 91 shows a crack propagating through an area of metal, where slip has already taken place. The crack follows the direction of slip as was shown previously by Thompson (12) and Hempel (14). However, as shown earlier it is possible for a crack to change direction inside a grain, by changing from one slip system to another. Although Hempel also obtained this type of crack, he was only able to show slip in one direction inside the grain.

To facilitate the explanation of the electron photomicrographs showing slip bands, it is necessary to explain briefly the technique of shadow-casting the replicas for electron microscope study. When dealing with fine metal structures, although/

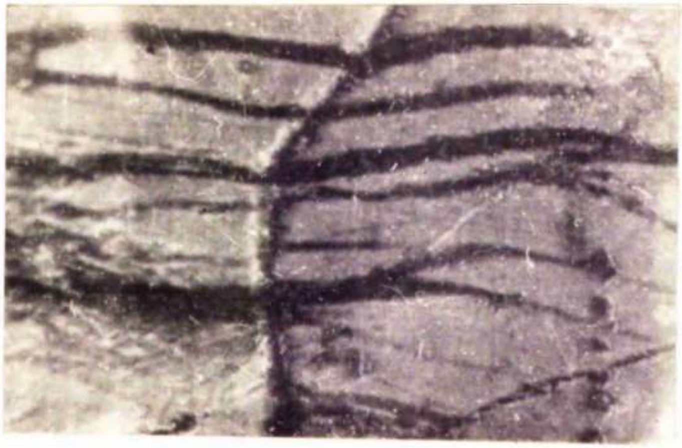

FIG 89 X 450

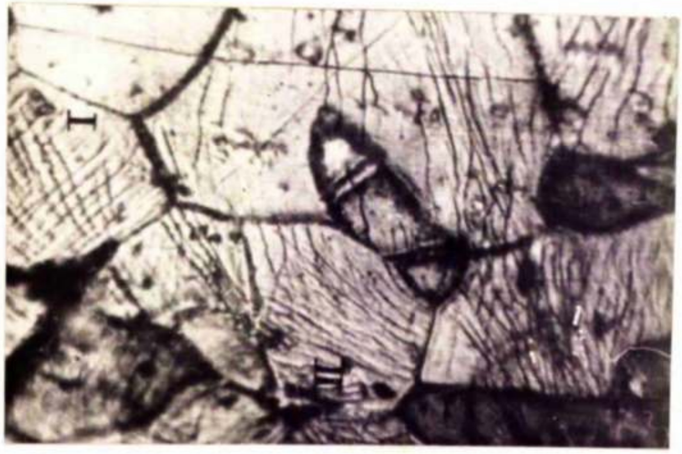

FIG 90 X 450

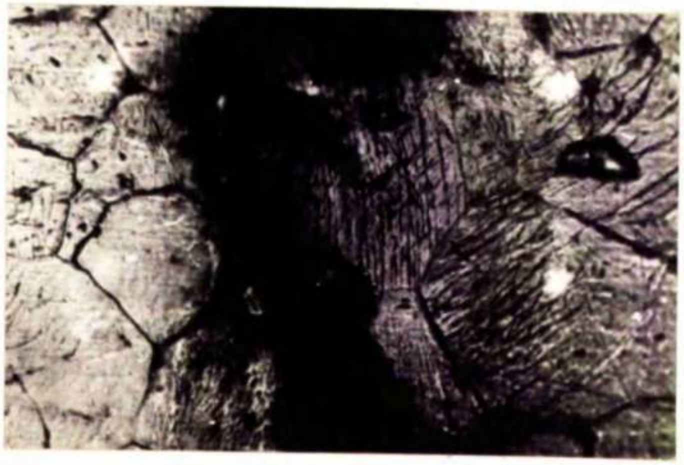

FIG 91 X 250

although well within the limit of resolution of the electron microscope, the transmission microscope may reveal little of the structure present. The shadowing technique, in addition to other advantages, coats the replica with a highly scattering layer of heavy metal atoms and greatly enhances the contrast properties of the specimen. In a specimen already possessing fairly good contrast properties for transmission microscope, a very thin coating of metal is sufficient to show up details in the surface structure, without the danger of obscuring the fine structure with metal atoms.

Fig. 92 (a) shows a section of an unshadowed replica, and 92 (b) shows this as viewed through the microscope. Fig. 93 shows the result of shadowing with a 60/40 gold/palladium alloy. It illustrates how extrusions on the surface are shown up darker, due to the shadow metal piling up against the side S. It also shows how intrusions show up white or practically white depending on the width), which means that cracks would show up white. The area behind the extrusion also shows up white. If the direction of shadowing is changed to that shown in Fig. 94 then a different result is obtained. Both the extrusions and the intrusions show up black, and a crack would show up particularly black, due to the alloy piling up on the side. Hence, it would be difficult to distinguish between an intrusion and an extrusion. This would only/

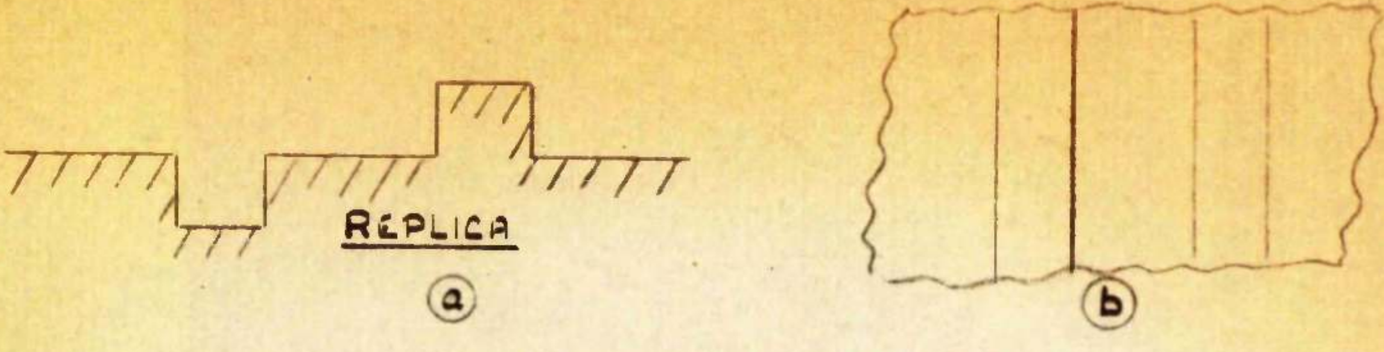

FIG 92.

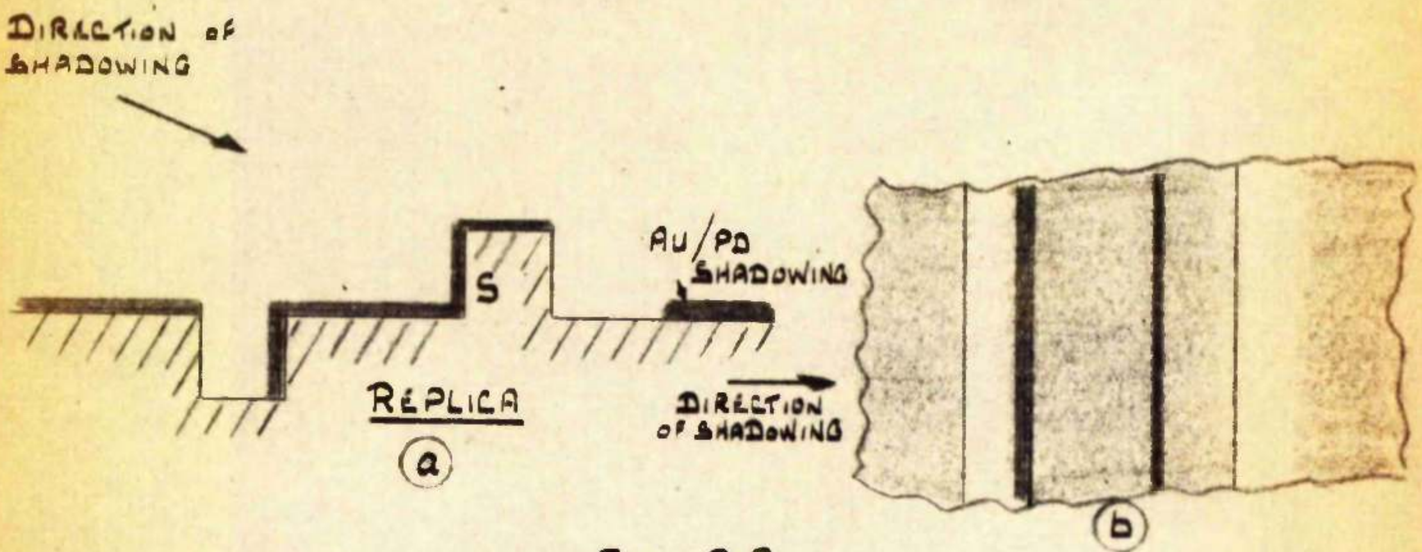

FIG 93.

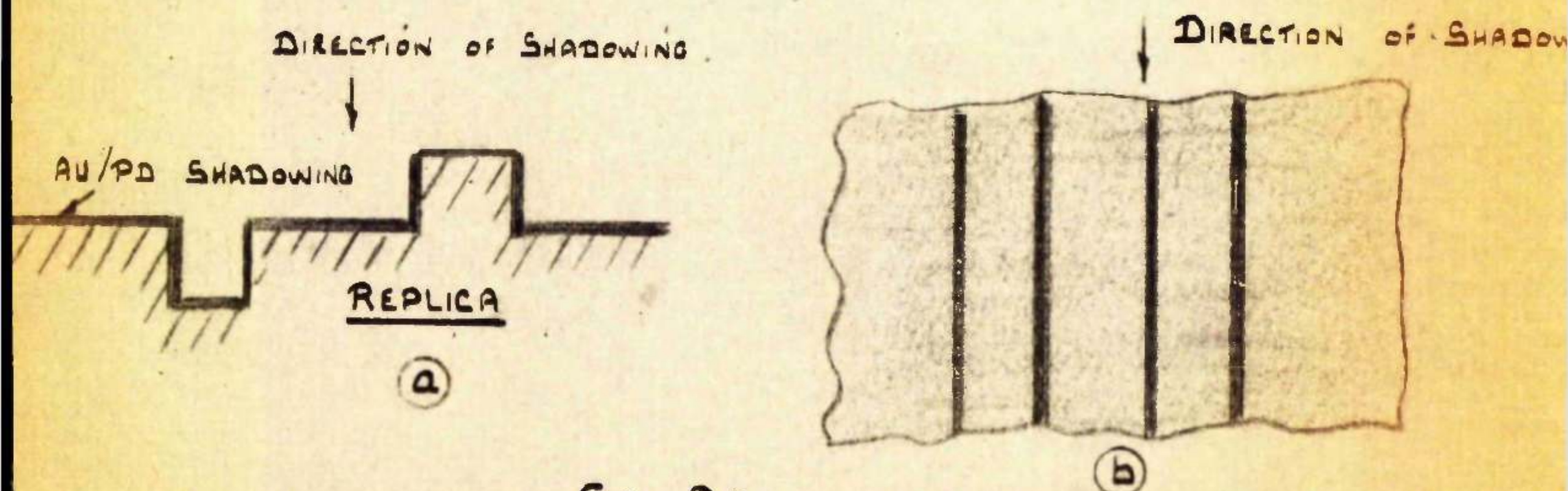

FIG 94

only hold if the intrusions and extrusions were parallel to the direction of shadowing, and since this rarely occurs a small shadow is sufficient to determine the nature of the structure.

A further advantage of the technique is that from a measurement of the length of 'shadows' cast an estimate of the height of particles may be obtained as shown in Fig. 95.

Fig. 96 is a high magnification photograph of cross slip. The broad slip bands have occurred first, because they have been slightly displaced, when the fine slip has taken place. Measurement of this displacement clearly shown in Fig. 97 gives an indication of the distance the metal has moved during slip, and from Fig. 96 this movement amounts to 100 Angstrom units (or about 28 atomic diameters). From the direction of shadowing, it is obvious that these bands are intrusions into the metal, whose depth is 100A^{o} (or about 28 atomic diameters).

The fine slip is 220A^{o} wide (or about 70 atomic diameters) and the coarse slip is about 2,500A^{o} wide (about 800 atomic diameters).

Fig. 98 shows broad slip in α iron, and the direction of shadowing shows these to be extrusions. Figs. 99 and 100 are higher magnification photographs of the areas marked in Fig.98. Examination of these shows fine microcracks present in the slipband/

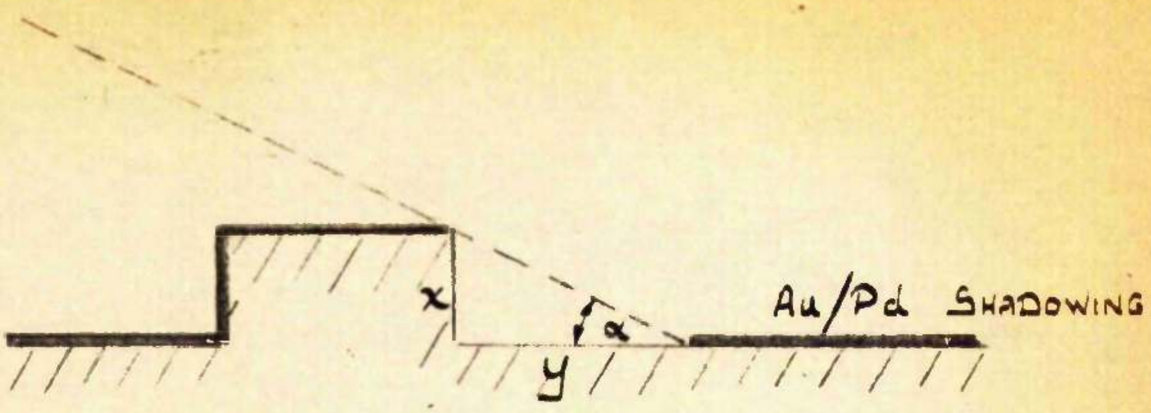

REPLICA

For the present work $\tan \alpha = \frac{x}{y} = \frac{1}{2}$ (y can be measured hence x

FIG 95

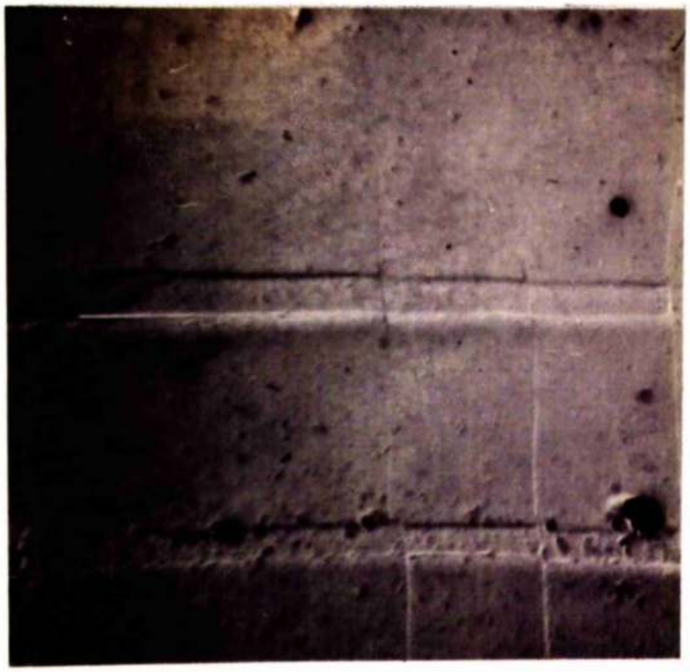

FIG 96 X18,000

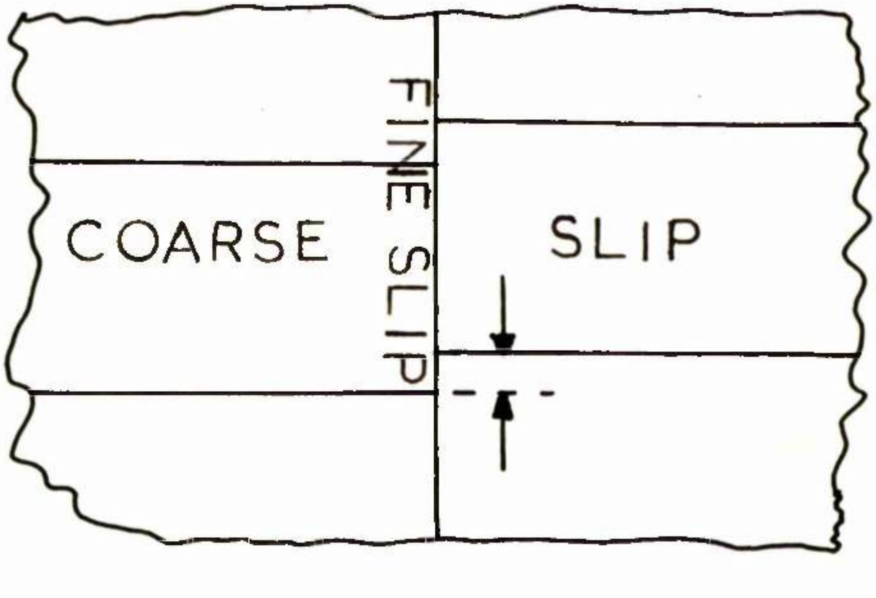

FIG 97

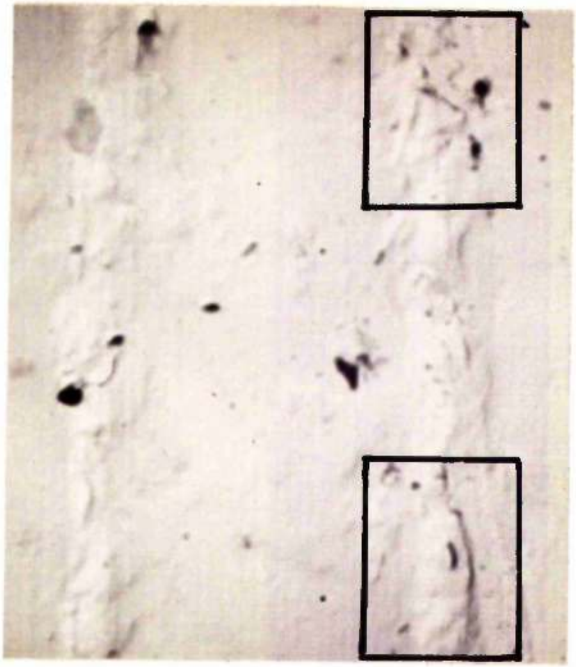

FIG 98 X 8,000

FIG 100 X24,000

FIG 99 X 24,000

slipband, (black because they have been nearly parallel to the direction of shadowing. Hempel (14) has also found these sub-microscopic fissures in high magnification electron photomicrographs of mild steel. From Fig. 99 the slip band is 10,000 x A^o broad and 2,5000 A^o high. The microcracks in Fig. 99 is 380A^o wide and in Fig. 100 200 A^{o}wide. These widths approximate to the size of fine slip, as shown in Fig. 96.

It is most likely that these microcracks will grow, because they have stress concentrations at their ends. When growth takes place a fatigue crack will be formed, or a fatigue crack may propagate due to these microcracks joining up.

From this work, the following conclusions can be made:-

1. That corrosion-fatigue cracks are wider than pure fatigue cracks.
2. That both corrosion-fatigue and pure fatigue cracks are predominantly transcrystalline.
3. That both types of crack avoid, if possible, traversing pearlite grains.
4. That inclusions in ferrous metals are stress raisers, and they have an effect on the crack direction.
5. That the corrosion product in corrosion-fatigue cracks is most probably γ Fe_2O_3 (hydrated) and that even in the presence of inhibitors this condition still prevails.

6/

6. That cracks propagate quicker through grains, than across grain boundaries.
7. That the corrosion alone is responsible for the initiation of corrosion-fatigue cracks by the production of corrosion pits.
8. That fatigue preceeds corrosion in the propagation of corrosion-fatigue cracks.

It is now possible to draw final conclusions from both sections, correlating the work on inhibition with that on crack propagation. From the results of the experiments in section two, it is apparent that during propagation fatigue precedes any corrosive action, but, from section one, the effects of added inhibitors have been shown to prolong the endurance of corrosion-fatigue specimens tested in aqueous environments. This means that the action of the inhibitor is to prevent corrosion pits forming on the surface and thus prevent the initiation of corrosion-fatigue cracks. This was further demonstrated by the experiments with specimens of varying surface finish, where the inhibitors had very little effect on a roughly turned specimens, due to the stress raisers already present on the surface. Many workers (72, 73, 74) have noted that fatigue cracks are not initiated until between 65 - 85 per cent of/

of the life of a specimen or component. Since the corrosive action gives rise to pits early in the life, this is the period when the inhibitors are required to be most active and fortunately this was found to be the case. It was further observed that whether or not any inhibitors were added to the corrosive environment the corrosion-fatigue cracks still contained products of corrosion although the widths of the cracks were slightly reduced when inhibitors were present. However, the foregoing does not necessarily mean that corrosion-fatigue cracks will propagate at the same rate as pure fatigue cracks. It has been shown that their dimensions are greater than pure fatigue cracks, and this difference in width will allow the specimen more movement in the region of the crack. This increased movement means that the strain at the end of the corrosion-fatigue cracks will rise, and therefore these cracks will propagate faster.

BIBLIOGRAPHY

1. FAIRBAIRN W. Phil. Trans. Roy. Soc. 1864. Vol. 154 P. 311
2. WÖHLER A. Z. F. Baurvesen, 1860, P. 583. Also Z. f. Bau. 1863 p. 233. 1866, p. 67, 1870, p. 73 Abs. Engineering 1871, p. 199.
3. BATTELLE MEMORIAL INSTITUTE, 1956 "Prevention of the Failure of Metals under Repeated Stresses" (John Wiley Sons, New York)
4. MOORE H. F. and KOMMERS, J. B. 1927 "The Fatigue of Metals" (McGraw-Hill Book Co., New York).
5. GOUGH H. J. 1924, "The Fatigue of Metals" (Scott, Greenwood Son, London)
6. EWING J. A. and HUMFREY, J.C.W. Phil. Trans. Roy, Soc., Series A. 1903, Vol. 200, P.241.
7. BEILBY G. T. "Proc. Roy. Soc. Series A, 1907, Vol. 79 P.403; Jour. Inst. Metals, 1911. Vol 6. P. 5.
8. ROSENHAIN W. and EWEN D. Jour. Inst. Metals, 1912, Vol. 8 P. 149.
9. GOUGH H. J. and HANSON D.Proc. Roy. Soc. A. 1923 Vol. 104. P. 538.
10. GOUGH H. J. and WOOD W. A. Proc. Roy - Soc. A, 1936 of Vol. 154 P. 510.
11. OROWAN E. Proc. Roy. Soc. A. 1939, Vol. 116, P. 576
12. THOMPSON N. Proc. Internat. Conf. Fatigue of Metals, 1956 P.527. Inst. Mech. Eng. and Amer. Soc. Mech. Eng. LONDON.
13. WOOD W.A. ibid P.531
14. HEMPEL M. ibid P.543
15. MOTT N.F. Acta Metallurgica, 1958, Vol. 6, P.195
16. HULL D. Jour. Inst. Metals 1958, Vol. 86, P.417.
17. MOORE H.F. Metals and Alloys 1936, Vol. 7.

18. FORSYTH P.J.E. Proc. Internat. Conf. Fatigue. Fatigue of Metals. 1956, P. 527, Inst. Mech. Eng. and Amer. Soc. Mech. Eng. London.

19. HAIGH B. P. Engineering 1930, Vol. 130 P. 55.

20. EVANS U. R. and WHITWHAM O. Jub. Iron & Steel Inst, 1950, Vol. 165. P. 72

21. GOUGH H. J. Jour. Inst. Metals, 1932. Vol. 49 P. 17

22. GOUGH H. J. and SOPWITH D. G Proc. Roy. Soc. A. 1932 Vol. 135, P. 392.

23. GOUGH H. J. and SOPWITH D. G. Jour Inst. Metals 1932 Vol.49 P. 93.

24. McADAM D.J. and GEIL, C. W. Bur. Stand. J. Res. 1940 Vol. 24 P. 685, 1941, Vol, 26 P. 135

25. McADAM D. J. Jr. Congress Internat. Essai. Mat. Amsterdam 1927 (1). P. 305 - 358.

26. ASTON J. C. Trans. Amer. Electrochem. Soc. 1919. Vol.29 449-464.

27. EVANS U. R. Metallic Corrosion - Passivity and Protection (Edward Arnold & Co. London) 1946.

28. BENGOUGH G. D., LEE A. R. and WORMWELL F. Proc. Roy. Soc. A. 1931. Vol. 131 P. 516.

29. EVANS U. R. and SIMNAD Proc. Roy. Roc. A.1946 - 47 Vol. 188 P. 372.

30. KARPENKO G. V. Doklady Akademii Nauk. SSSR, 1951, Vol.77 No. 5, Pages 827 - 830.

31. REBINDER P.A. "Zhurnal" Tekhnicheskoi Fiziki 1932, Vol 2, No. 7-8 726, Jubilee Symposium USSR Academy of Sciences 1947 P. 533.

32./

32. GOUGH H. J. and SOPWITH D.G. Jour. Iron and Steel Inst. 1933, Vol. 127 P. 301

33. McADAM D. J. Jr. Trans. Amer. Soc. Steel Treat., 1927, Vol. 11, P. 365.

34. McADAM D. J. Jr. Trans. Amer. Soc. Steel, Treat. 1926

35. SCHULZ E. H. and BUCHHOLTZ H. New Internat. Assoc. Test. Mat. 1931 P. 1-26.

36. GOULD A.J. and EVANS U.R. Jour. Iron and Steel Inst. 1948 Vol. 160 P. 164.

37. INGLIS W. P. and LAKE G. F. Trans. Farad. Soc. 1931, Vol. 27, P. 803

38. RYABCHENKOV, A. V. and ABRAMOVA V. F. Vestnik Mashin Vol. 35, 1955, P. 54-57.

39. SOPWITH D.G. and GOUGH H.J. Jour. Iron and Steel Inst. 1937, Vol. 135 P. 315.

40. GOULD A. J. and EVANS U.R. 1939 Iron and Steel Inst. Second Report, Alloy Steels Research Committee, P. 325.

41. KARPENKO G.V. "On the Corrosion-Fatigue Limit" Doklady Akademii Nauk SSSR. 1952, Vol. 87, No. 4, P. 617.

42. GOUGH H.J. and SOPWITH D.G. Jour. Iron and Steel Inst. 1937 Vol. 135, P. 293.

43. GOULD A.J. Jour. Iron and Steel Inst. 1949, Vol. 161 P. 11

44. McADAM D.J. Jr. Proc. Inst. Metals. Div. Amer. Inst. Min. Mech. Engrs. 1928, P. 571.

45. McADAM D.J. Jr. Proc. Amer. Soc. Test. Met. 1928, Vol.28 P. 117.

46. KARPENKO G.V. Doklady Akademii Nauk SSSR. Vol. 92, 1953 No. 3 P. 603 .

47/

47. SPELLER F.N. McCORKLE I.B., and MUMMA P.F. Proc. Amer. Soc. Test. Mat. 1928, Vol, 28, P. 159
1929, Vol. 29, P. 238.

48. SPELLER F.N. "Corrosion-Causes and Prevention" (McGraw - Hill Book Co. New York) 1951

49. WATCHER A. Jour. Ind. Eng. Chem. 1945 Vol. 37 P.749

50. COHEN M. Trans. Electrochem Soc. 1948 Vol. 93, P. 26.

51. WYLLIE D and CHEESEMAN G.C.N., Jour. Soc. Chem. Ind. London, 1949, Vol. 68 P. 165.

52. MAYNE J.E.O. MENTOR J.W. and PRYOR M.J. Jour. Chem. Soc. 1950. Vol 4 P. 3229.

53. COHEN M. and PALMER W.G. Jour. Iron and Steel Inst. 1949, Vol. 163, P. 421.

54. CAIRNEY J.M. Ph. D. Thesis, Glasgow University 1958.

55. LEHMANN G.D. Aero. Res. Comm. Reports & Memoranda No. 1054. 1927.

56. UHLIG, H.H. Corrosion Handbook (John Wiley & Sons, New York), 1948.

57. BINNIE A.M. Aero Res. Comm. Reports and Memoranda No. 1244, 1929.

58. DEBYE P. and HUCKEL E. See Glasstone (S. Elements of Physical Chemistry (MacMillan & Co.Ltd. London) 1950, P. 487.

59. SORENSEN S.V., Strength of Metals and Computation of Machine Elements 1937 Moscow.

60. McADAM D.J. Trans. Amer. Soc. Steel Treat. 1927 Vol.11 No. 3, P. 335.

61. DOREY S.F. Trans. Inst. Nav. Arch. 1933 Vol. 75 P.140.

62. HAMER P.,POWELL L, and COLBECK E.W. Jour. Iron and Steel Inst. 1945 Vol. P. 151.

63/

63. HEYN E. and BAUER O. Mitt. Kyl. Material Prüfungsamt, 1910, Vol. 28 P. 62.

64. FRIEND J.N., Iron and Steel, Carnegie Schol. Memoirs, 1922, Vol. 11, P. 122

65. GOULD A.J. Engineering 1936, Vol. 141 P.495.

66. MODIN H. Jernkontorets Annaler Arg. 139 H.S. 1955 P. 521.

67. MacFARLANE W. Jour. Met. Club. Royal Coll. of Science and Tech. 1958, Vol. 10 P. 31.

68. McADAM D.J. Proc. Amer. Soc. Test. Mater. 1926, 26 (II) P. 224-254.

69. GOULD A.J. Proc. Internat. Conf. Fatigue of Metals, 1956, P. 527, Inst. Mech. Eng. - and Amer. Soc. Mech. Eng. London.

70. STULEN F.B., CUMMINGS H.N. and SCHULTE W.C. Ibid. P. 439

71. GOUGH H.J. Proc. Amer. Soc. Test. Mater 1933 Vol. 33 Part 2 P. 3.

72. HEMPEL M. Mitt. K. Wilh. Inst. Eisenforsch, 1939 Vol. 21 P. 147.

73. HEAD A.K. Jour. Mech. Phys. Solids, 1953 Vol. 1 P. 134.

74. MacFARLANE W. Jour. West of Scot. Iron and Steel Inst. 1959 Paper No. 518.

possibility of cracks of finite length being present in the metal before stressing began.

Inherent weaknesses of the above work in resolving this question are that crack lengths were measured round the circumference of a rod-shaped specimen—this may not give a true measure of the depth

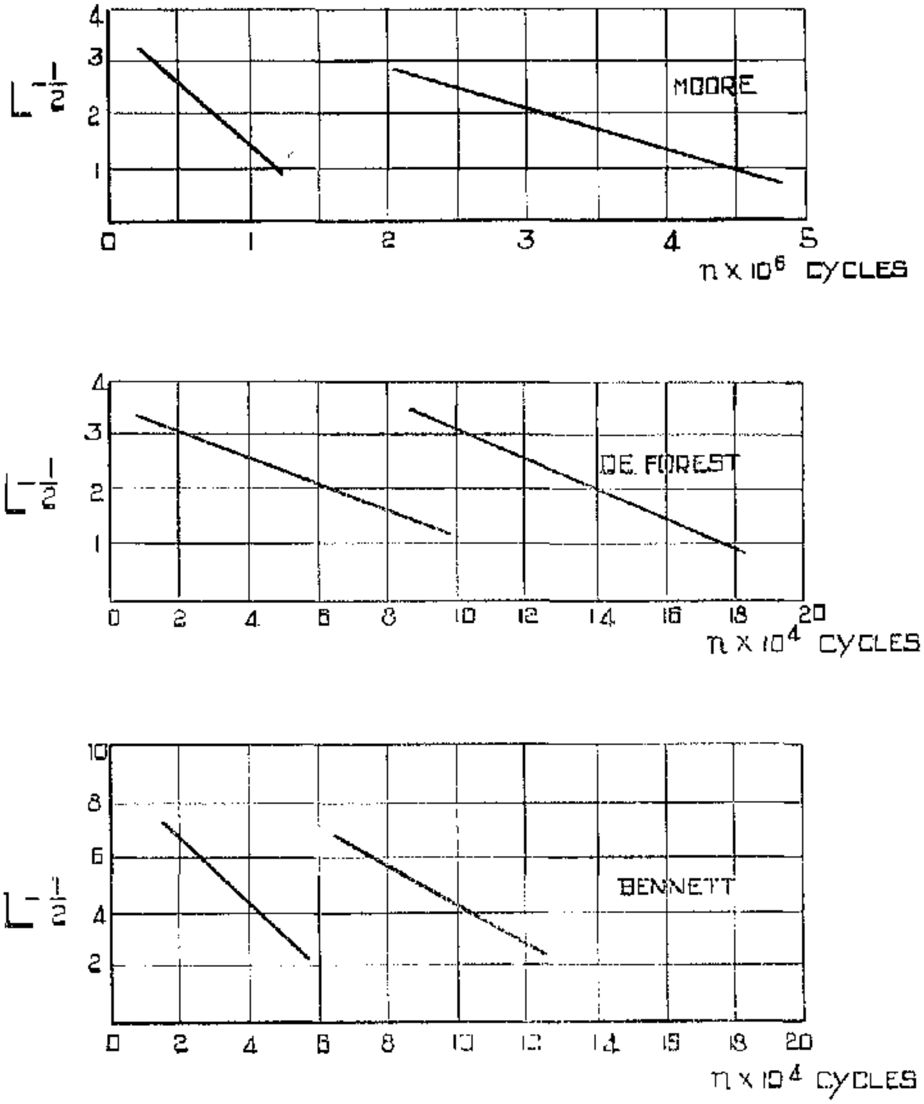

Fig. 2—Results of Moore de Forest and Bennett as plotted by Head.

of penetration of the crack—and that the *initial* rate of propagation of the crack could not be measured as all the above investigators started with a finite length of crack. In the present work two methods were used to obtain and measure fatigue cracks and their rate of propagation. This made it possible to determine whether the type of machine or the procedure used affected the results ob-

obtained, Bacon postulated that each successive crack front was the arc of one of a system of ellipses centred on the circumference at the mid-point of the beam section.

In a similar investigation using magnetic iron powder (magnaflux) to indicate the position of the crack along the cirumference and an initial peripheral crack length of 0·05 in. de Forest[3] obtained the results shown in Fig. 1(b). Crack lengths were measured to within 0·001 in. using a low-power microscope and a graticule eyepiece. Bennett[4] measured the circumferential arc of the crack, after removing the specimen from the fatigue machine, with a low-power microscope having a hairline on the eyepiece. A rotating drum with a vernier scale was attached to the specimen. The time of initiation of the crack was determined by measuring the deflection of the specimen in the fatigue machine. The results of Bennett are reproduced in Fig. 1(c).

The work of Frost and Phillips[5] differs from the above in that fatigue tests were carried out entirely under tensile conditions, and cracks were not present at the commencement of the tests, but were initiated from suitable stress raisers. The curves showing the rate of crack propagation were similar to those of the earlier workers, and are shown in Fig. 1(d). The results of an experiment in which an initial fine saw cut 1 in. in length was present, are also shown.

A theoretical approach to the problem of the rate of crack propagation during fatigue was made by Head[6], who from a mathematical model of a metal under fatigue, arrived at the formula:

$$L^{-\frac{1}{2}}=(F/24\sqrt{2}E)a_0^{\frac{1}{2}}\Sigma^3/[(\Sigma_1-\Sigma_0)(\Sigma_0-\Sigma)^2](N_\infty-n)$$

where L=length of crack

n=number of cycles

N_∞=value of n for which crack is infinitely long, that is fracture

F=work hardening modulus

E=Young's modulus

a_0=critical length of tensile element in the model

$\pm\Sigma$=applied stress (less than the yield point of the material)

Σ_0=yield stress

Σ_1=fracture stress

The formula shows $L^{-\frac{1}{2}}$ to be a linear function of n, the number of stress cycles undergone and the results of Moore, De Forest and Bennett appear to be in agreement with this conclusion as shown by Fig. 2. Extrapolation to $n=0$ should indicate the original crack length before fatigue stressing was applied. Although this represented a lower limit to the possible length of the crack when formed Head did not believe that fatigue was the growth of cracks present in the unstressed metal. However, Machlin[7] and Shanley[8] had previously made this assumption and Bennett had also suggested the

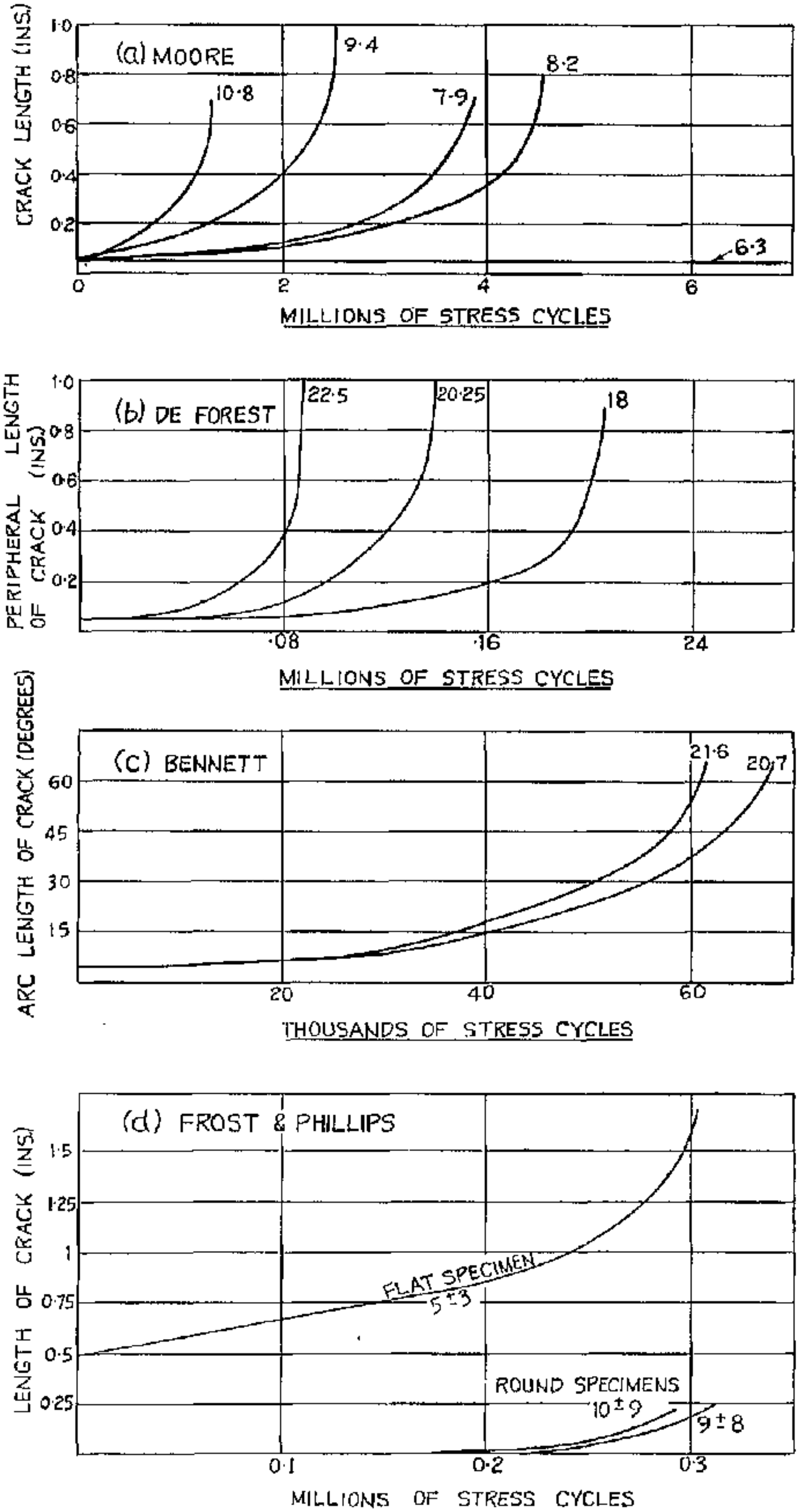

Fig. 1—Rates of crack propagation as found by Moore de Forest, Bennett, and Frost and Phillips. (All stresses in tons per sq. in.)

THE WEST OF SCOTLAND IRON AND STEEL INSTITUTE
39 ELMBANK CRESCENT, GLASGOW.

This paper will be read at a meeting of the Institute on Friday, 16th January, at 6.45 p.m. You are invited to attend and to take part in the discussion. Written contributions should be sent to the Secretary before 26th January. This proof is subject to correction.

Paper No. 518

Crack Propagation

By W. MACFARLANE,* B.SC.

16TH JANUARY, 1959

SYNOPSIS

The previous work is summarized and collated with the Author's experiments and a fairly good correlation is observed when Stanton and Amsler type test pieces were used. A bibliography is included.

Although numerous investigations have been made on various aspects of the fatigue of metals, most of these have been concerned with factors affecting the expected life of the metal during fatigue, and comparatively little has been published on the subject of the rate at which the fatigue cracks, leading to ultimate failure, propagate. In 1927 Moore[1] investigated the rate of propagation of fatigue cracks in axles. Cracks were initiated by applying a sufficiently heavy load. When the cracks had reached measurable length (0·05 in.), the load was reduced and the rate of propagation determined by visual measurement of the crack length appearing on the circumference of the axle after varying intervals of fatigue. Oil and whiting were used to render the crack visible for measurement. The results obtained are reproduced in Fig. 1(a). It will be observed that the crack did not propagate if the applied load was 6 tons per sq. in. or less, that is, about 50 per cent. of the endurance limit of the incracked specimen. Similar results were obtained by Bacon,[2] who used a heat tinting technique to measure the rate of progress of the crack. Contour lines were formed by removing the specimen from the machine at intervals, and heating to temperatures varying between 400° and 250°C. The temperature was successively lowered, so that when the crack was examined after failure, the temper colour contours were usually clearly defined. No data on the rate of propagation of the fatigue crack were given but from the results

---

*Of the Royal College of Science & Technology, Glasgow.

[1] See bibliography, p. 19.

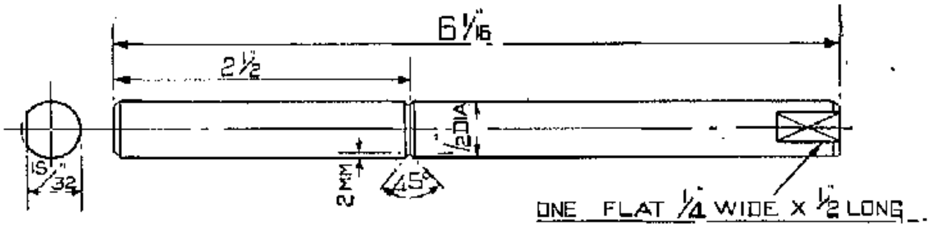

(a) STANTON SPECIMEN

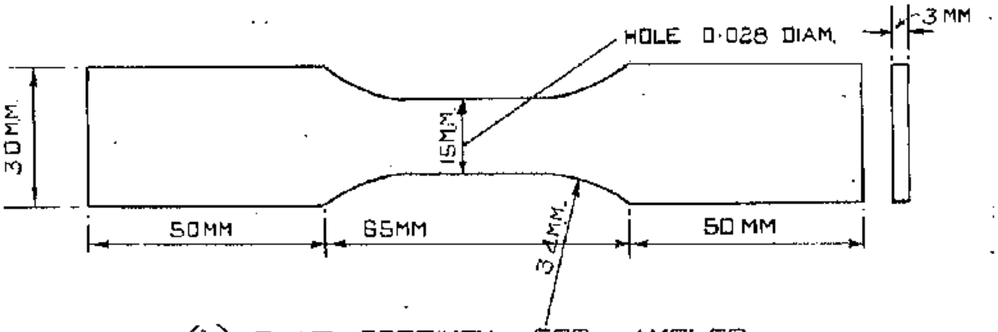

(b) FLAT SPECIMEN FOR AMSLER

Fig. 3.

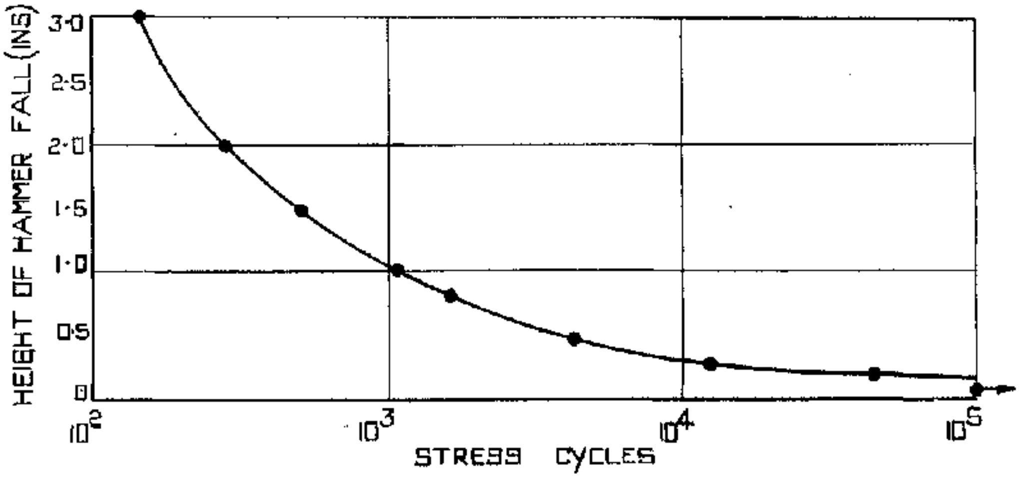

Fig. 4—Fatigue curve for mild steel tested on the Stanton machine.

tained. A Stanton fatigue machine (or, more correctly, repeated impact machine) was used in the first method, the dimensions of the mild-steel test-piece being shown in Fig. 3(a). The composition and properties of the mild steel were as follows:

	per cent.		
C	0·21	Ultimate tensile strength	28·8 tons per sq. in.
Si	0·32	Elongation	40 per cent.
S	0·054	Reduction of area	60 per cent.
P	0·02	Yield stress	17·95 tons per sq. in.
Mn	0·55		

Five hundred ft. of this steel, which had been rolled from a single ingot, were used to ensure maximum uniformity of composition and properties. The fatigue life for various hammer falls (equivalent to a variation in stress) was first determined, the mean of the results of four specimens being plotted for each point on the fatigue curve shown in Fig. 4. The reproducibility of the results obtained is shown in Table I, from which it will be seen that the scatter is much lower than that obtained from conventional fatigue-testing machines.

TABLE I

Height of fall, in.	Max. stress at root of notch, ± tons per sq. in	Endurance, No. of cycles	Max. deviation from mean, per cent.
0·8	49	1,753, 1,790, 1,712, 1,777	2·9
0·5	39	4,320, 4,343, 4,219, 4,391	2·3
0·3	30	11,807, 11,560, 11,670, 11,780	1·2
0·2	24	46,438, 46,826, 46,675, 46,657	<0·5

The four heights of fall chosen for the experiments to determine the rate of crack propagation were low, but above the fatigue limit. Specimens were fatigued to percentages of the expected life varying from 10 to 90 per cent. for each of these four stress levels. After each test the specimen was broken in a Charpy impact machine. This gave two fatigue fracture faces as shown in Fig. 5, where the sharp distinction between the fatigue fracture and the brittle fracture is obvious. The maximum penetration of the fatigue fracture was measured using a microscope with a graticule in the eyepiece. The length could be measured to within 0·001 mm. Four specimens were used in every instance and the mean of the eight measured lengths plotted against the percentage life. A typical example of the scatter obtained is given in Table II.

TABLE II

Crack Length after 70 per cent. Expected Life (8,092 cycles)
Hammer fall=0·3 in.

Specimen	R.71	R.72	R.73	R.74
Crack length, mm.	0·996	0·999	0·987	0·986
	0·989	1·003	0·985	0·993

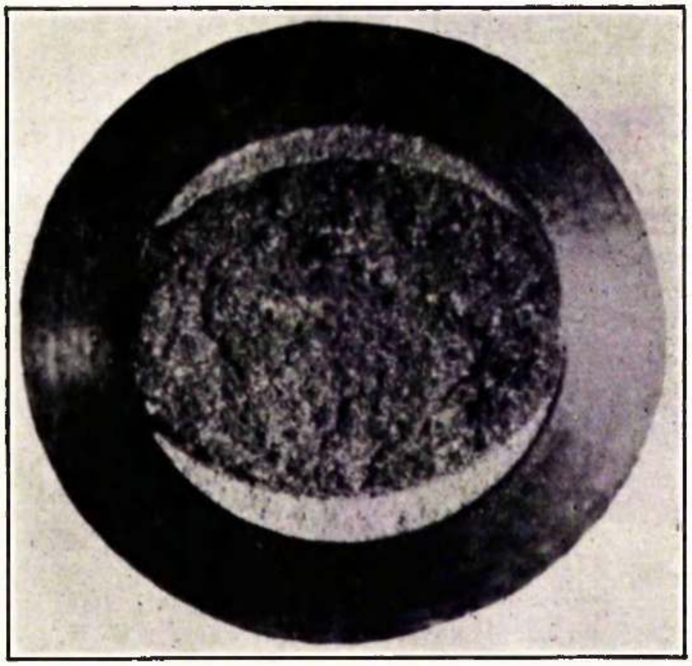

Fig. 5—Fracture fall of Stanton specimen. (0·3 in. fall, 50 per cent. expected life.) ×5

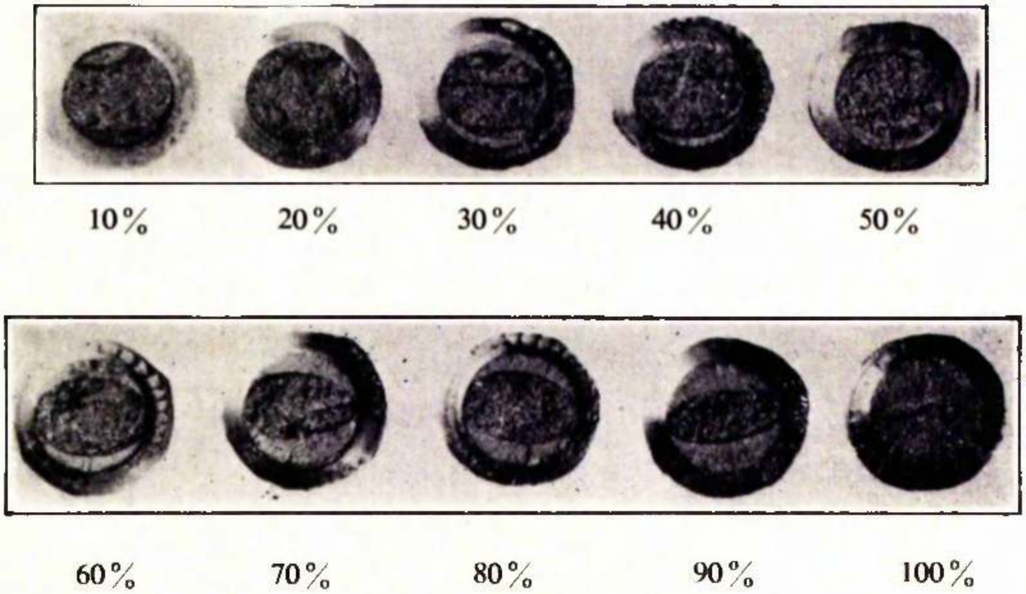

10% 20% 30% 40% 50%

60% 70% 80% 90% 100%

Fig. 6—Fractures faces of a series of Stanton tests. (0·3 in. fall.) ×1

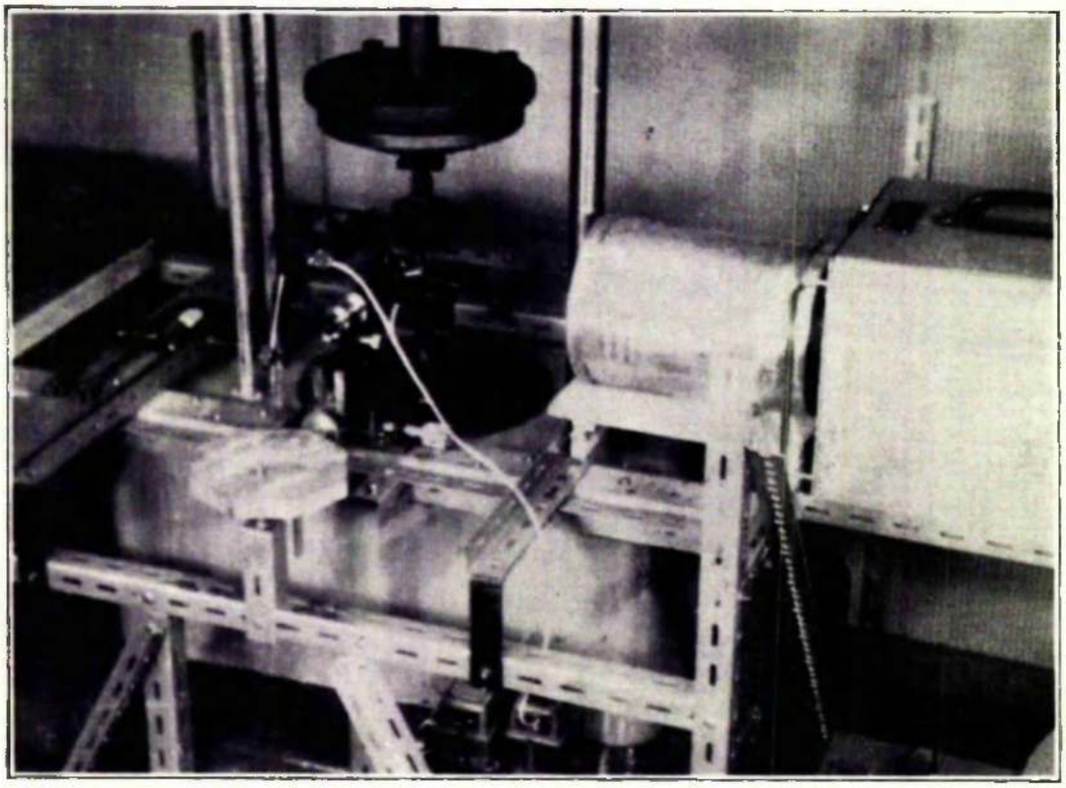

Fig. 7—Apparatus for examining progress of crack in Amsler Vibrophore.

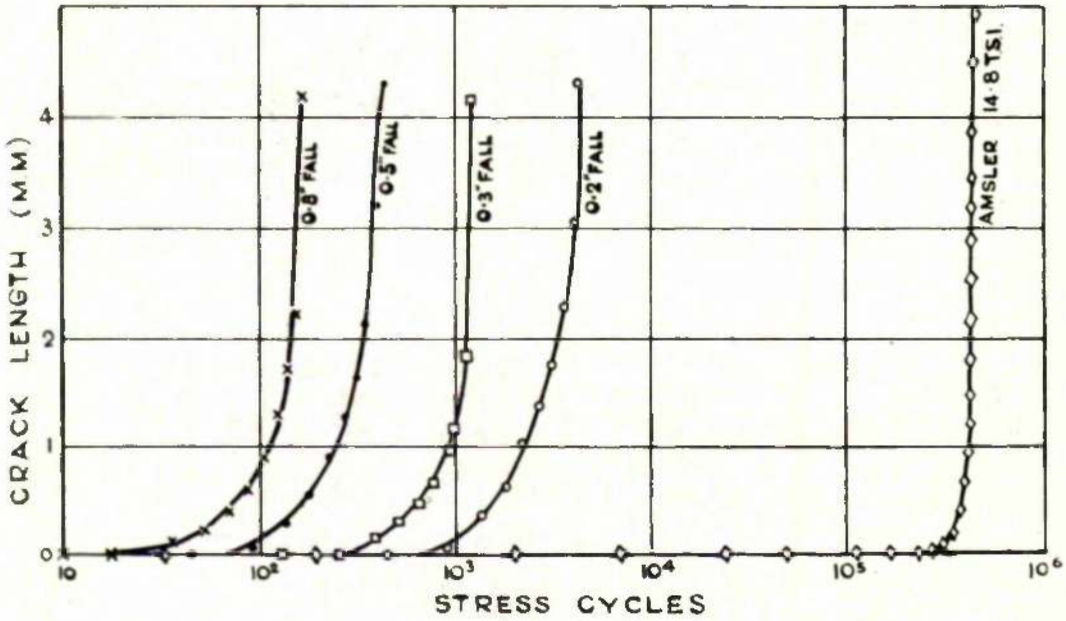

Fig. 8—Test results for rates of crack propagation.

The maximum deviation from the mean value is only 0·009 mm. and in all the tests performed never exceeded 1·6 per cent. of the mean crack length. A complete set of Stanton fractures is illustrated in Fig. 6, which shows the cracks at various stages of specimen life.

In the second method of investigation of crack propagation, a 2-ton Amsler Vibrophore fatigue-testing machine was used. The flat specimen shown in Fig. 3(b) had a small hole, 0·028 in. in diam., drilled in the centre to act as a stress raiser and provide the point of initiation of the crack. The specimen was given a "mirror finish" metallurgical polish (electrolytic finish) and was etched before being fitted into the machine. Light from a stroboscope was passed through a condenser into the opaque illuminator of a microscope and directed onto the specimen surface by means of a prism. The light was thence reflected to the eyepiece. After insertion of the specimen, it was subjected to fatigue at 9,000 cycles per min. at varying stresses, and the stroboscope synchronized with the rate of vibration of the specimen, so that the specimen surface as viewed through the microscope appeared to be stationary. The microscope was so mounted that it was possible to move it horizontally to enable the path of the crack to be followed. The course and rate of pro-

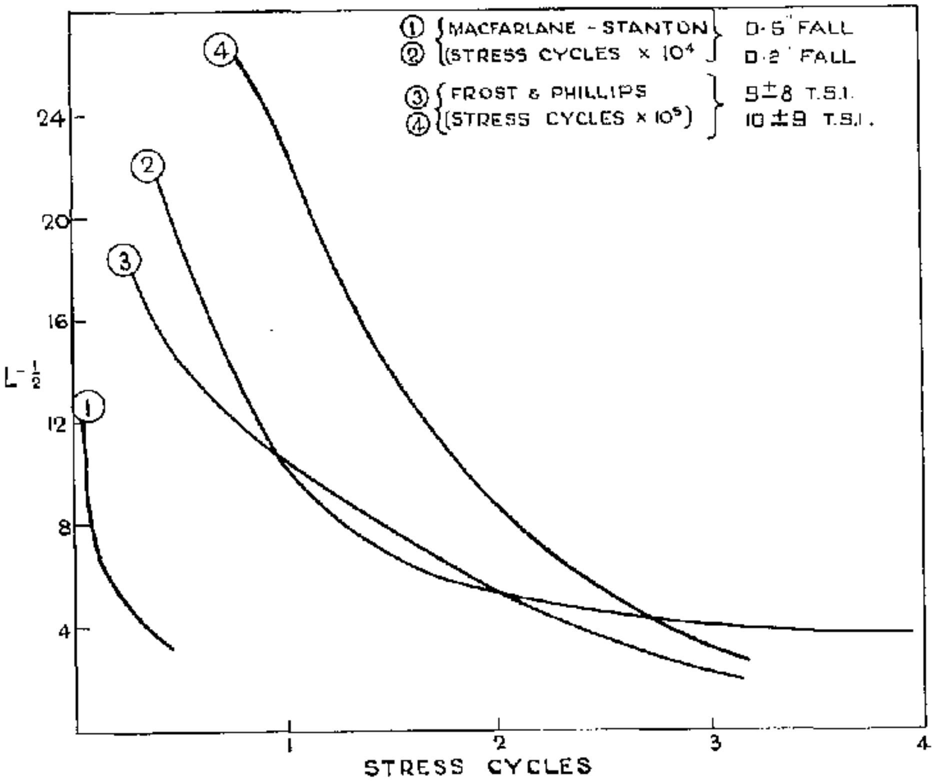

Fig. 9—Comparison of results of Frost and Phillips, and Author with equation of head.

pagation of the crack could be viewed with ease through the microscope at magnifications up to ×500. At suitable intervals photomicrographs were taken using a Watson microscope camera fitted to the eyepiece. Fig. 7 shows the apparatus in operation.

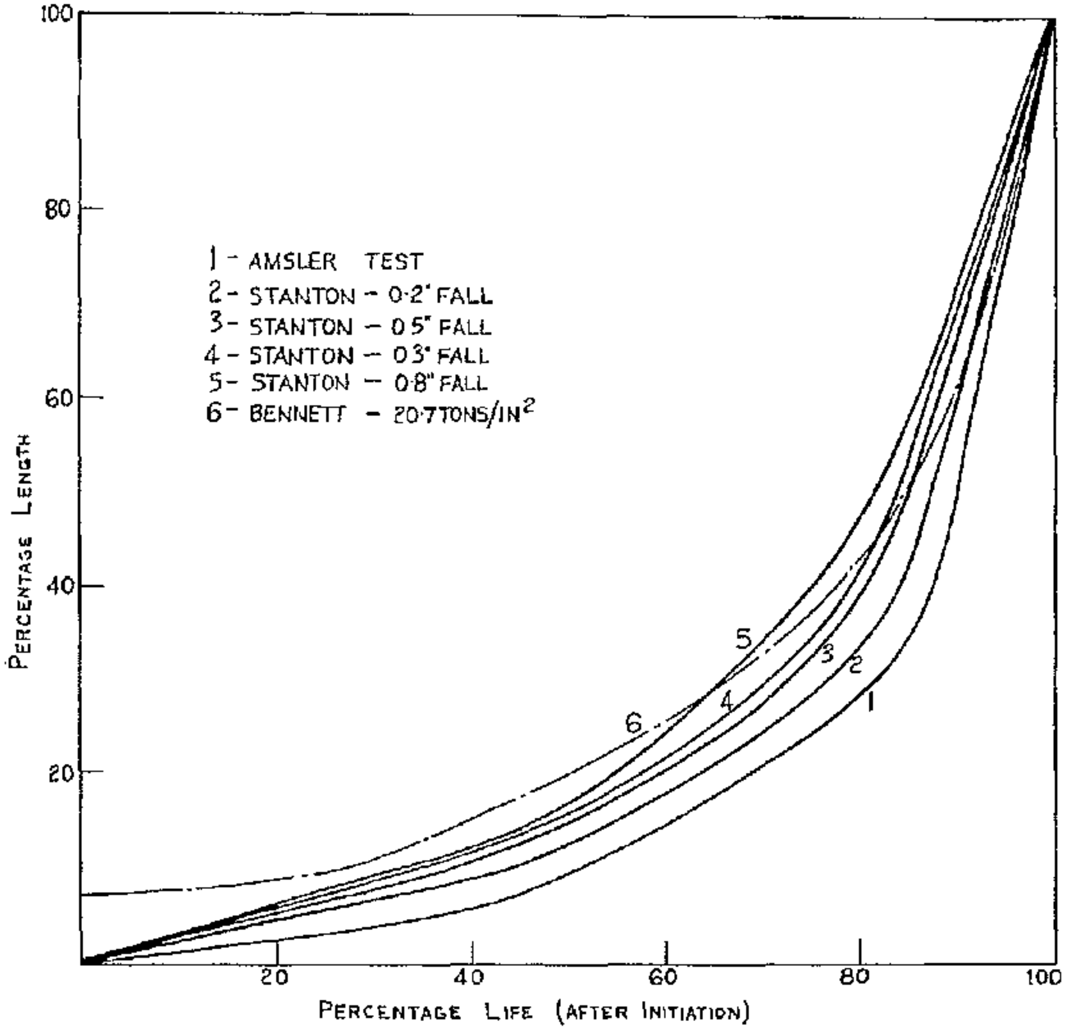

Fig. 10—Variation of the percentage length of crack with the percentage life (after initiation has occurred).

Results and Discussion

Fig. 8 shows the results of crack propagation experiments on both the Stanton and Amsler machines. It will be noted that the crack does not start to propagate immediately but only after about 15 per cent. of the expected life in the case of Stanton specimens, and about 60 per cent. for Amsler specimens. The difference is probably due to the large difference in stress concentration factors of the stress-raisers in the two machines. Crack propagation is slow at first but increases rapidly near the point of failure.

The present results and those of Frost and Phillips are compared with the findings of the equation of Head in Fig. 9. It will be observed that the linear relationship between $L^{-\frac{1}{2}}$ and n is only valid when a crack length of the order of 0·03 in. is exceeded. As might be expected, at smaller crack lengths the curve is asymptotic to the ordinate. It would also be expected that a linear relationship between $L^{-\frac{1}{2}}$ and n could not exist if an initial "incubation period" existed in which cracks could not be detected as was observed in both the Stanton and Amsler fatigue tests. A similar phenomenon has been noted by other workers[9, 10] in normal notchless fatigue in which cracks did not form until 60 to 85 per cent. of the expected life. These values are somewhat higher than that obtained in Amsler fatigue tests, in which the central hole would act as a stress raiser. The much lower percentage obtained in Stanton fatigue tests can be attributed to the effect of the much greater stress concentration factor of the notch.

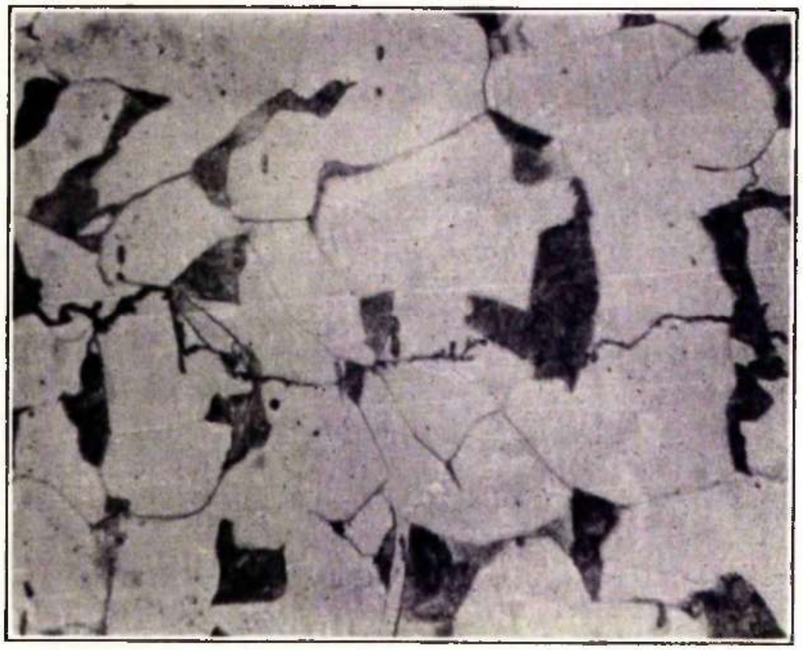

Fig. 11—Fatigue crack. ×425

The difference in the relative position of the curves shown in Fig. 8 is largely due to the difference in incubation period required for the initiation of a crack. A better comparison of the progress of crack formation in different types of test may be obtained by plotting the percentage of life after crack initiation has occurred against the percentage of the final crack length at various stages of crack propagation. This has been done for the Stanton and Amsler fatigue test results in Fig. 10; a comparison has also been made on the same basis with the results of Bennett.[4] It will be observed that similar curves are obtained, the concavity of the curves increasing with decreasing applied stress. It may be concluded that the progress of the crack follows a similar pattern irrespective of the manner in which the fatigue test is carried out.

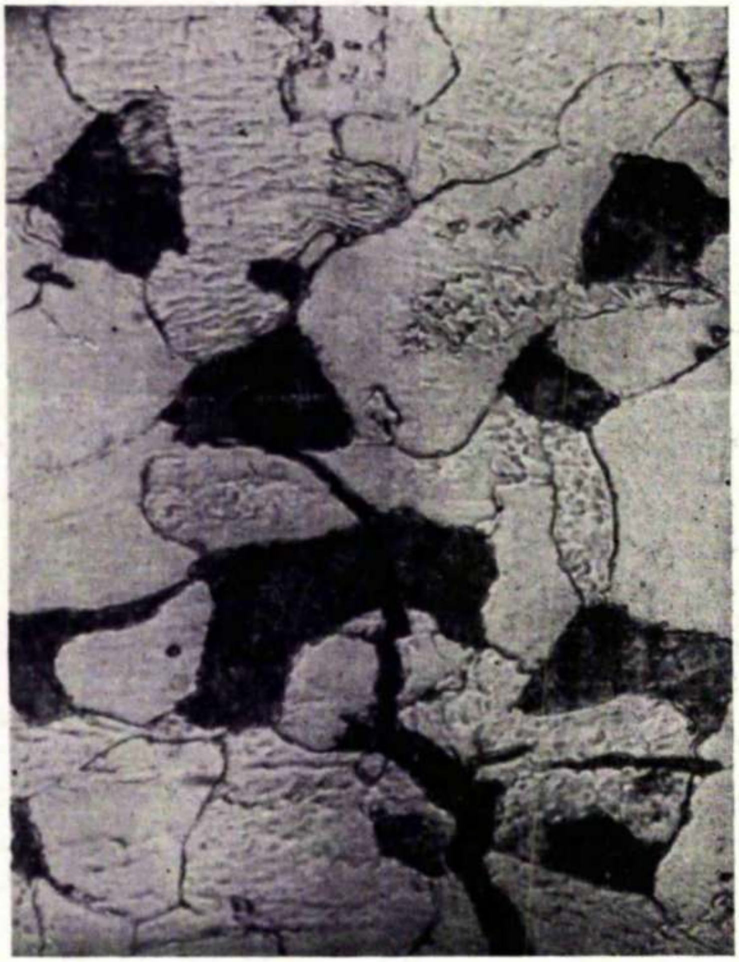

Fig. 12—Corrosion-fatigue crack. ×430

METALLOGRAPHIC FEATURES OF FATIGUE CRACKS

In the course of the above work and in related work on the corrosion fatigue of the same mild steel in dilute brine solutions, using the British Non-Ferrous Metals Research Association rotating load-type of fatigue machine, a number of specimens were examined microscopically in order to relate the observed structural changes to the progress of the fatigue process. Figs. 11 and 12 show typical fatigue and corrosion fatigue cracks, the main differences lying in the width of the crack over the first 95 per cent. of the length (measured

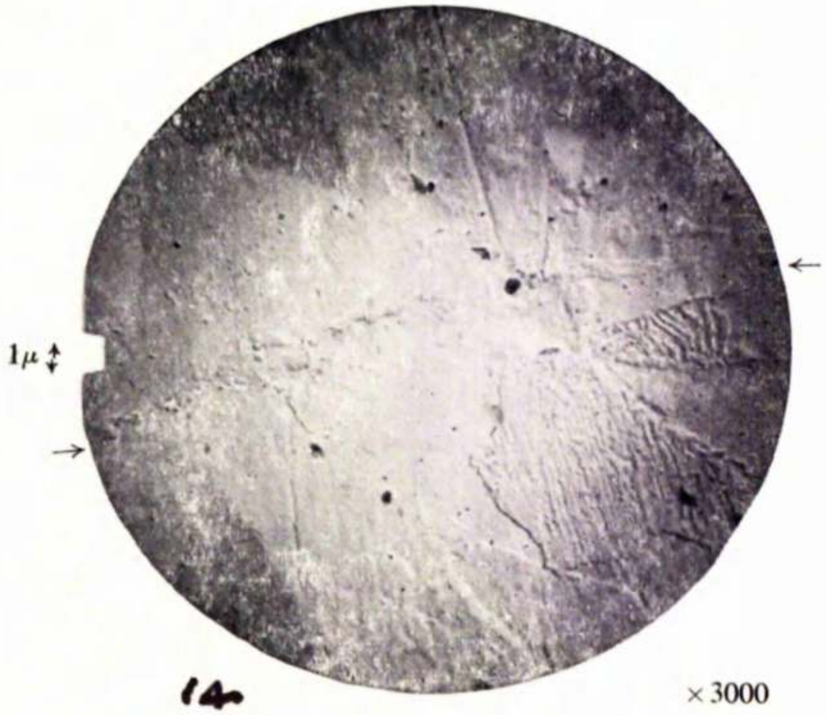

14

Fig ~~15~~.—*Pure fatigue crack showing locating indentations. (Electron photomicrograph.)*

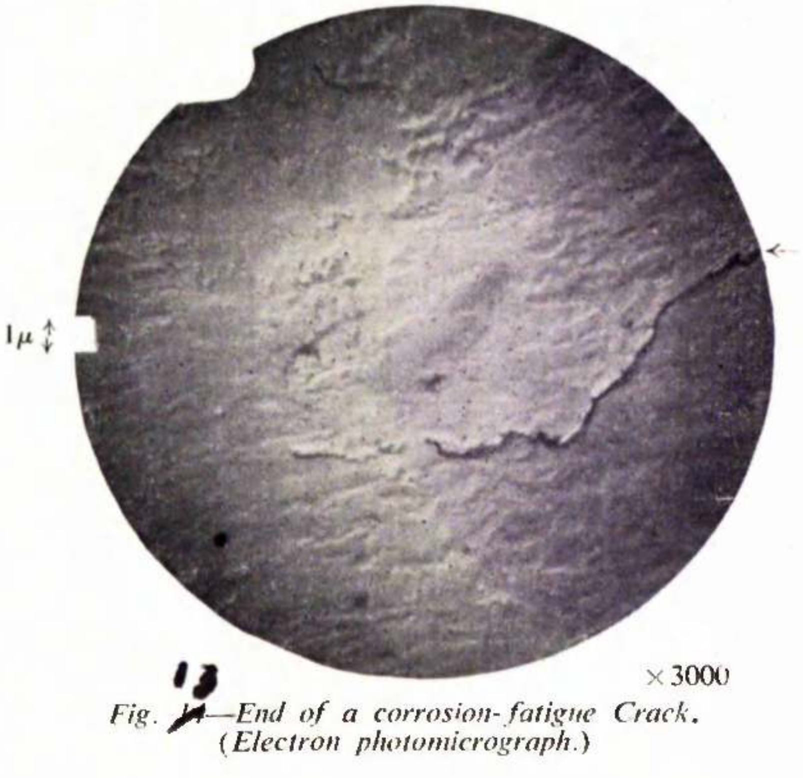

13

Fig. ~~14~~—*End of a corrosion-fatigue Crack. (Electron photomicrograph.)*

from the point of initiation) and the presence of corrosion products in the corrosion fatigue crack. In corrosion fatigue the crack widens rapidly and widths of 10μ are quite common. The width of a pure fatigue crack is about 0·6μ, and of the same order as that of grain boundaries in the steel employed in the tests. Over the last 25μ of corrosion fatigue cracks, the crack narrows as shown in Fig. 13, which is an electron photomicrograph (produced by a technique described elsewhere[11]) of the tip of a corrosion fatigue crack. The width at the tip is about 0·3μ, which is of the same order as that at the end of a fatigue crack. It would appear that in corrosion fatigue the action of fatigue alone moves ahead of the corrosion process during the propagation of the crack, although even at the tip of the crack, corrosion products can be identified under the electron microscope. In the main part of a corrosion fatigue crack, corrosion products are evident even under the light microscope. The appearance of a typical fatigue crack as seen under the electron microscope is shown in Fig. 14. There is no indication of any abraded material within the crack, as might have been expected from some of the older theories of fatigue.[12, 13]

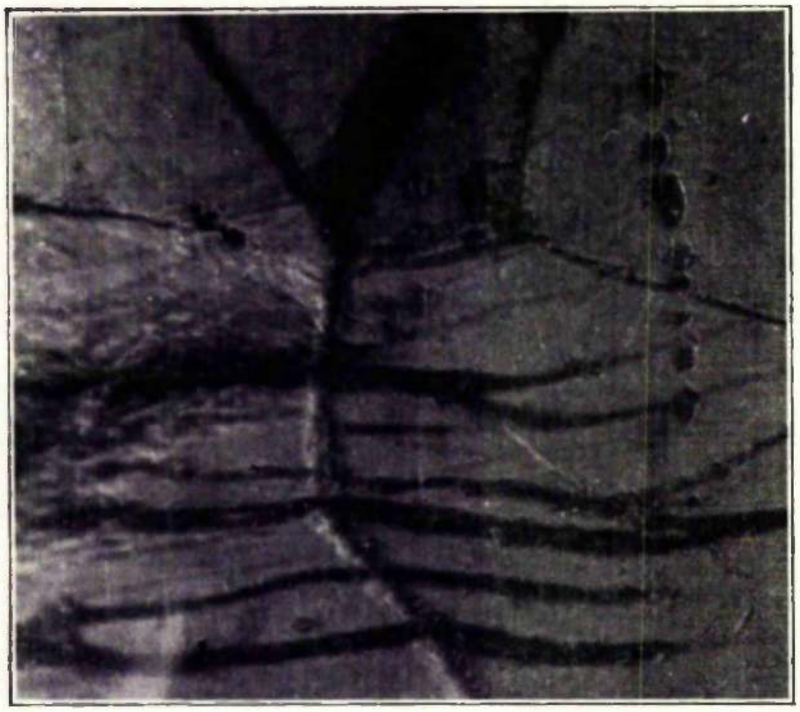

Fig. 15—Slip band crossing a grain boundary. × 425

All cracks examined were predominantly transcrystalline in character, as can be seen from Figs. 11 and 12. The cracks may occasionally run along the boundary between ferrite and pearlite, but rarely along the boundary between two ferrite grains. Another feature of both fatigue and corrosion fatigue cracks is their tendency to avoid traversing grains of pearlite. Figs. 11 and 12 show typical examples of this, although it is more difficult to distinguish in corrosion fatigue cracks at their broadest parts. When the crack does traverse pearlite grains, it normally does so at the narrowest part, as can be observed in Fig. 11, or passes through the pearlite in a direction parallel to the lamellae of ferrite and cementite. This characteristic of fatigue cracks has not been reported previously, but close examination of photomicrographs of cracks reproduced by Gough[14] and McAdam[15] show similar occurrences. The reason for this mode of propagation of fatigue cracks probably lies in the fact

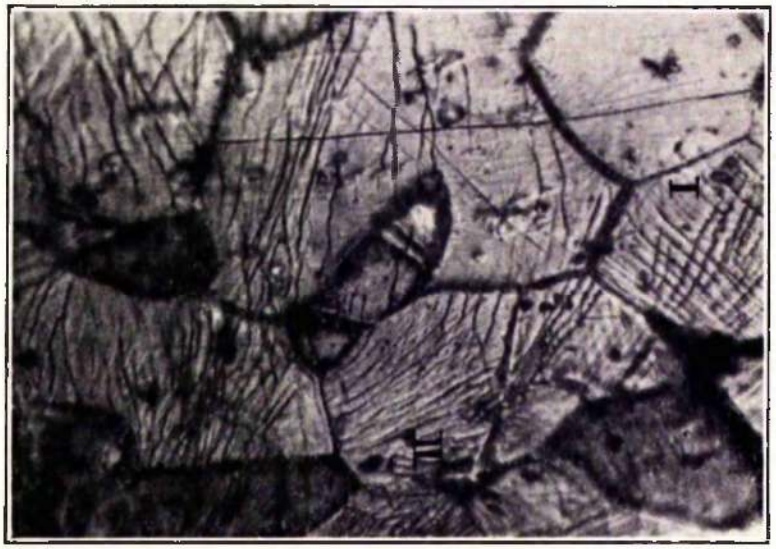

Fig. 16—Cross slip in ferrite grains. ×425

that pearlite is inherently stronger than ferrite and will offer greater resistance to slip and the progress of a crack which follows the slip process, due to its heterogeneous character and its lack of planes of weakness as compared with ferrite. This again suggests that the fatigue mechanism is the major influence in the propagation of corrosion fatigue cracks.

Fig. 15 shows that slip bands formed during fatigue can cross grain boundaries, although Barrett[16] did not believe this possible. There is a slight change in direction on crossing the boundary, indicating that the direction of the favoured slip system in grain A did not coincide with that of grain B.

It may be further observed from Figs. 11 and 12 that both fatigue and corrosion fatigue cracks can change direction within a ferrite grain. This appears to occur during the propagation of all fatigue cracks, and is probably associated with a change in the slip direction caused by a change in the stress distribution resulting from the crack propagation process. It has been shown by Gough and Sopwith[17] and Gould,[18] and further verified during the present work, that fatigue cracks tend to run parallel to slip bands. During the present work it was often observed that during fatigue, slip bands could be formed in two different directions within the one grain, as shown in Fig. 16, which was obtained during a test carried out at a stress well below the fatigue limit on the Amsler machine. The angle between the two sets of slip planes can vary, for example, in grain I the angle is about 30°, whereas in grain II, the angle is 60°. As cracks tend to align themselves with existing slip planes, as shown in Fig. 17, the crack only needs to follow an alternative slip system as provided by such cross slip to change its direction within a grain. Similar changes of direction observed in corrosion fatigue cracks again support the supposition that fatigue precedes corrosion during the propagation of the crack. Fig. 18 shows an electron photomicrograph of cross slip. The broad slip bands occurred first, because they have been slightly displaced by the subsequent fine slip.

Fig. 17—Fatigue crack aligned with slip bands. × 425

Measurement of the displacement indicates that the movement of the metal during fine slip amounted to 100 Å (or about 28 atomic diameters). From the direction of shadowing, it can be seen that the broad slip bands are intrusions into the metal whose depth is about 100 Å. The fine slip lines are about 220 Å wide.

Broad slip bands which are extrusions are shown in Fig. 19. The area delineated is shown at a higher magnification in Fig. 20. Fine micro-cracks can be seen within the slip band (black because they are nearly parallel to the direction of shadowing). Hempel[19] found similar submicroscopic fissures in high magnification electron photomicrographs of mild steel. The slip band shown in Fig. 20 is about 10,000 Å wide and 2,500 Å high. The microcracks are about 380 Å wide, these widths approximating to those of fine slip lines. It seems probable that these microcracks will grow during further fatigue, because of the stress concentration at their ends. This may result in the ultimate formation of a fatigue crack, or a fatigue crack may form due to two or more of these microcracks joining together. The incubation period which was observed in the present work before a crack became visible is probably related to the time required for the formation of slip bands and microcracks, and the subsequent development of these microcracks into a visible fatigue crack.

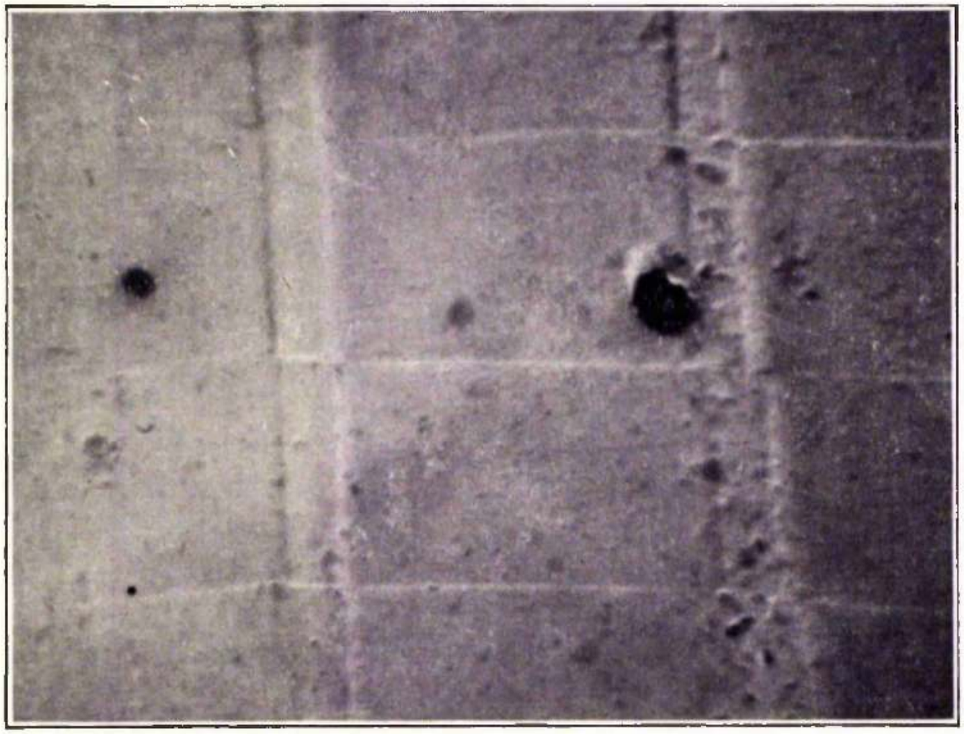

Fig. 18—Cross slip (electron photomicrograph). × 18000

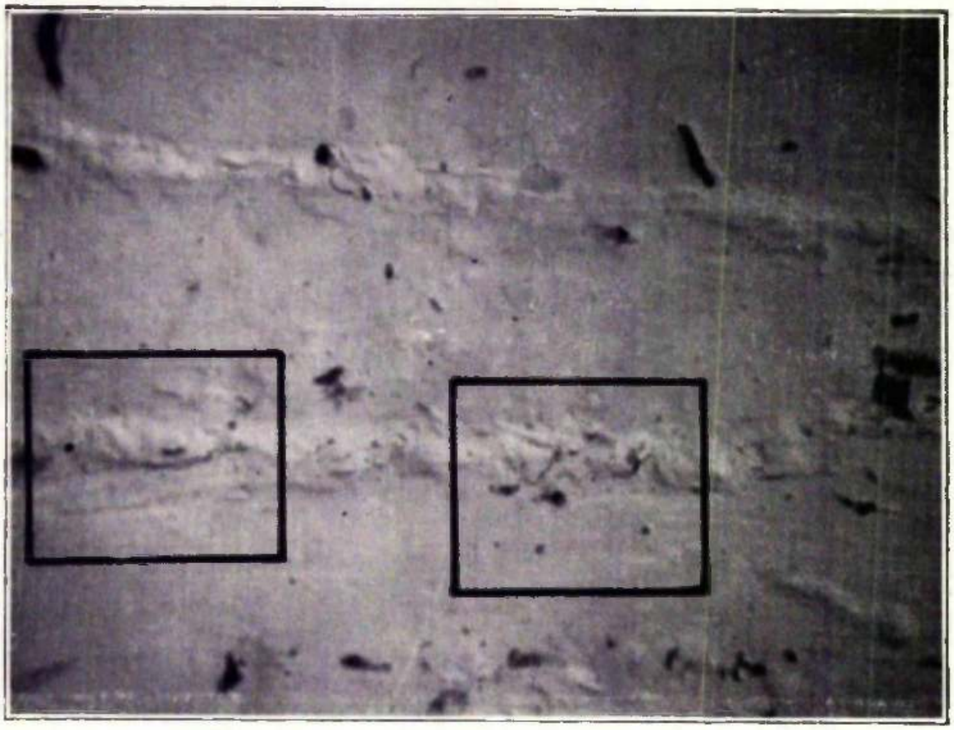

Fig. 19. ×5600

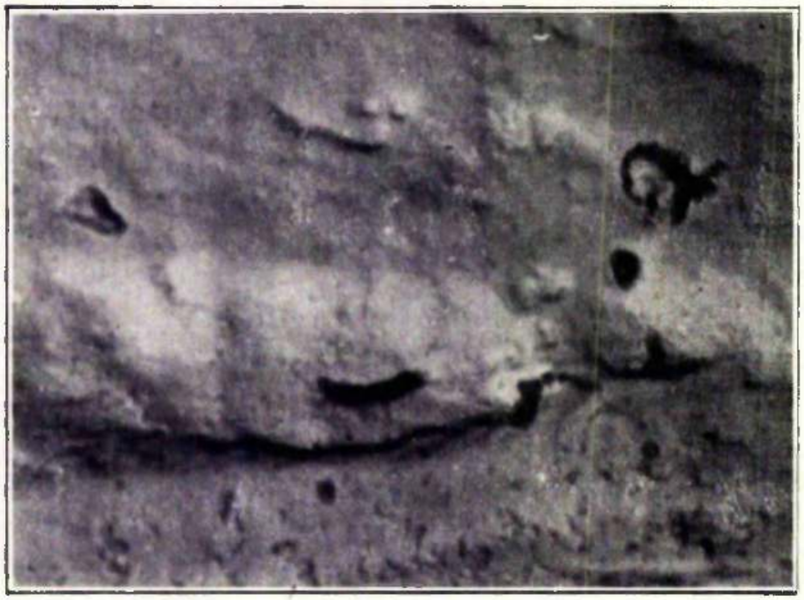

Fig. 20—Enlarged view of sub-microscopic cracks shown in Fig. 19.

Acknowledgments.—The Author wishes to express thanks to Prof. R. Hay of the Metallurgy Department for the assistance and facilities provided and to Prof. A. S. T. Thomson and Prof. A. W. Scott of the Engineering Department for helpful advice and permission to publish the paper. He would also like to thank Dr P. T. Carter for his valuable assistance during the preparation of the paper, Mr J. W. Sharpe for the Electron Microscope photomicrographs, and Mr I. Stevens for his help with some of the experimental work.

BIBLIOGRAPHY

(1) " A Study of Fatigue Cracks in Car Axles," by H. F. Moore. 1927. Bulletin No. 165. University of Illinois, Engineering Experiment Station, Urbana, Ill.

(2) " The Rupture of Shafts by Fatigue," by F. Bacon. *Engineering*, 1933, vol. 135, p. 685.

(3) " The Rate of Growth of Fatigue Cracks," by A. V. de Forest. Trans. Amer. Soc. Mech. Eng., 1936, vol. 58, p. A.23.

(4) " A Study of the Damaging Effect of Fatigue Stressing on X4130 Steels," by J. A. Bennett. Proc. Amer. Soc. Test. Matls., 1946, vol. 46, p. 693.

(5) " Studies in the Formation and Propagation of Cracks in Fatigue Specimens," by N. E. Frost and C. E. Phillips. Proc. Internat. Conf. Fatigue of Metals, 1956, p. 520. Inst. Mech. Eng. and Amer. Soc. Mech. Eng., London.

(6) " The Growth of Fatigue Cracks," by A. K. Head. *Phil. Mag.*, 1953, 7th series, vol. 44, p. 925.

(7) " Dislocation Theory for Fatigue of Metals," by E. S. Machlin. 1948. Tech. Note No. 1489. Nat. Adv. Ctte. Aero., U.S.A.

(8) " A Theory of Fatigue based on Unbonding during Reversed Slip," by F. R. Shanley. 1952. Rand Corp., Santa Monica, Cal.

(9) " Experiments Relating to the Basic Mechanism of Fatigue," by N. Thompson. Proc. Internat. Conf. Fatigue of Metals, 1956, p. 527. Inst. Mech. Eng. and Amer. Soc. Mech. Eng., London.

(10) " The Mechanism of Fatigue of Metals," by A. K. Head. *Journ. Mech. Phys. Solids*, 1953, vol. 1, p. 134.

(11) " The Electron Microscope as a Metallurgical Tool," by W. MacFarlane. Journ. Metallurg. Club, Roy. Coll. Sci. Tech., Glasgow, 1957-58, No. 10, p. 31.

(12) " The Hard and Soft States in Metals," by G. T. Beilby. Proc. Roy. Soc., series A, 1907, vol. 79, p. 403; Journ. Inst. Metals, 1911, vol. 6, p. 5.

(13) " The Fracture of Metals under Repeated Alterations of Stress," by J. A. Ewing and J. C. W. Humfrey. Phil. Trans. Roy. Soc., series A, 1903, vol. 200, p. 241.

(14) " Corrosion-Fatigue of Metals," by H. J. Gough. Journ. Inst. Metals, 1932, vol. 49, p. 17.

(15) " Stress-Strain-Cycle Relationship and Corrosion-Fatigue of Metals," by D. J. McAdam, Jr. Proc. Amer. Soc. Test. Matls., 1926, vol. 26, II, p. 224.

(16) " Structure of Metals," by C. S. Barrett. 1952. McGraw-Hill Book Co.

(17) " The Behaviour of a Single Crystal of Aluminium under Alternating Torsional Stresses while Immersed in a Slow Stream of Tap Water," by H. J. Gough and D. G. Sopwith. Proc. Roy. Soc., series A, 1932, vol. 135, p. 392.

(18) " Corrosion Fatigue," by A. J. Gould. Proc. Internat. Conf. Fatigue of Metals, 1956, p. 341. Inst. Mech. Eng. and Amer. Soc. Mech. Eng., London.

(19) " Metallographic Observations on the Fatigue of Steels," by M. Hempel. *ibid*, p. 543.

NAME	ADDRESS AND AFFILIATION	DATE
M. NEMMOUR	62, Great George St. G12.	11/08/80
"	" " "	12/08/80
N. NEmmour	" " "	14/08/80
"	" "	30/8/80

CORROSION-FATIGUE IN FERROUS ALLOYS

by William MacFarlane, D.Sc., A.R.C.S.T.

The object of the research programme undertaken was to assess the effect of some of the many variables which influence corrosion-fatigue in ferrous alloy The main factors chosen were the composition of the corrosive environment, the temperature of the environment, and the surface finish of the metal undergoing t

The fatigue of metals and the theories associated with the phenomenon are reviewed. This is followed by a critical summary of the previous work on corro fatigue in the light of the present work.

The results of the investigation show that additions of chlorides to distil water environments drastically reduce the endurance of all specimens, even a sma addition of the order of 0.1 per cent synthetic sea water lowering the endurance limit (at fifty million cycles) from 11 tons per square inch to 7.9 tons per squa inch. The effects of the environment were further investigated by the addition a variety of anodic and adsorption inhibitors. The results of these experiment are correlated with the available electrochemical data for the inhibitors. All S/N curves obtained from tests on specimens in aqueous media failed to show the existence of a safe range of stress.

The temperature of the tests was varied from 25°C to 88°C and from the resu it is concluded that an increase in the temperature of the corrosive environment moderately increase the corrosion-fatigue attack. The influence of the surfac topography was also shown by experiments with different surface finishes to have noteworthy effect on the susceptibility to corrosion-fatigue. Hence it is dedu that/

that the initiation of corrosion-fatigue cracks is primarily associated with corrosion while that of crack propagation is mainly associated with the fatigue mechanism.

These deductions were substantiated by the extensive metallographic examination on the many cracks which were produced during testing. These crack were compared with cracks produced by fatigue in air, and any differences in the characteristics were carefully noted. Studies of the various types of cracks revealed many new features concerning the nature and dimensions of the mass movement which takes place when slip occurs. It was further concluded that the appearance of sub-microscopic fissures in the slip bands is the beginning of fatigue cracks.